Soil water management: Evaluation of infiltration in furrow irrigation systems, assessing water and salt content spatially and temporally in the Parc Agrari del Baix Llobregat area

Basem Aljoumani

Nomber 2012

UNIVERSITAT POLITÉCNICA
DE CATALUNYA
BARCELONA **TECH**

Soil water management: Evaluation of infiltration in furrow irrigation systems, assessing water and salt content spatially and temporally in the Parc Agrari del Baix Llobregat area.

PhD Disertation:

BASEM ALJOUMANI

UNIVERSITAT POLITÈCNICA DE CATALUNYA

Campus Tecnològic de la Mediterranea

Thesis Director: Dr. Ramón Josa March (UPC, DEAB)

Thesis Co-Directors: Dra. Nuria Cañameras (UPC, DEAB)

Dr. Joaquim Monserrat (UdL, DEA)

Doctoral Program: "AGRIBUSINESS TECHNOLOGY AND BIOTECHNOLOGY"

Department of Agri-Food Engineering and Biotechnology (DEAB)

Escola Superior d'Agricultura de Barcelona

PhD thesis presented to obtain the title of Doctor by the Universitat Politècnica de Catalunya

Casteldefells, November 2012

Thesis presented by Agricultural Engineer ***BASEM ALJOUMANI*** as a partial requirement to obtain the title of Doctor (Ph.D) by the UNIVERSITAT POLITÈCNICA DE CATALUNYA (Doctoral Program: "Agribusiness Technology and Biotechnology")

This thesis has been carried out under the direction of **Dr. Ramon Josa** and co-directed by **Dra**. **Nuria Cañameras** and **Dr**. **Joaquim Monserrat**.

Director	**Co-Director**	**Co-Director**
Dr. Ramón Josa	Dra. Nuria Cañameras	Dr. Joaquim Monserrat

Acta de qualificació de tesi doctoral	**Curs acadèmic:2012/2013**

Nom i cognoms **BASEM ALJOUMANI**

DNI / NIE / Passaport 000117180/004900233

Programa de doctorat Agribusiness Technology and Biotechnology

Unitat estructural responsable del programa Department of Agri-Food Engineering and Biotechnology

Resolució del Tribunal

Reunit el Tribunal designat a l'efecte, el doctorand / la doctoranda exposa el tema de la seva tesi doctoral titulada

_____

_____

_____

_____.

Acabada la lectura i després de donar resposta a les qüestions formulades pels membres titulars del tribunal, aquest atorga la qualificació:

☐ APTA/E ☐ NO APTA/E

(Nom, cognoms i signatura) President/a		(Nom, cognoms i signatura) Secretari/ària
(Nom, cognoms i signatura) Vocal	(Nom, cognoms i signatura) Vocal	(Nom, cognoms i signatura) Vocal

_____, _____ d'/de _____ de _____

El resultat de l'escrutini dels vots emesos pels membres titulars del tribunal, efectuat per l'Escola de Doctorat, a instància de la Comissió de Doctorat de la UPC, atorga la MENCIÓ CUM LAUDE: ☐ ☐

SI NO

(Nom, cognoms i signatura) Presidenta de la Comissió de Doctorat	(Nom, cognoms i signatura) Secretària de la Comissió de Doctorat

Barcelona, _____ d'/de _____ de _____

To Majd, my wife, your love and support has taught me so much about sacrifice.

To Ammar, my son, who was born before this dissertation was completed and who had to go Syria with Majd to allow me to focus. It was very difficult decision to let you go. I am deeply sorry for each moment when we were not together.

To my family, who have always supported, encouraged and believed in me, there are no words could express how your effort makes me strong.

Acknowledgments

I owe sincere thankfulness to my principal supervisor, Prof. Ramon Josa March, who made me believe in my qualification, gave me the liberty of discussion the data of my experiments with other professors and investigation centers, and guided me through the whole process of dissertation writing. I am sure that this dissertation would not have been possible without his support.

My utmost gratitude to my second supervisor, Prof. Nuria Cañameras, her good advice, support, and her patience during our discussion when we were facing a problem, has been invaluable on both an academic and a personal level.

I wish to acknowledge my third supervisor, Prof. Joaquin for receiving me many times in his office in the Universitat de Lleida to discuss and analysis our data related to irrigation system. He was generous in teach me his model in evaluating furrow irrigation system.

I very thankful to Josep A. Sanchez, professor at the Universitat Politènica de Catalunya, Department of Applied Statistic. I attended his course in time series analysis technique during two academic years. Almost every week I visited him in his office to discus my experimental data, he teach me how to use time series in modeling soil water and soil salinity, whose sincerity and willing to teach me I will never forget.

I would like to acknowledge the financial technical support of Parc Agrari del Baix Llobregat, who provided all the equipments and facilities to achieve my field and laboratory experiments. And a special thanks to Elena Isla, Borja Camí, Núria Cuch, Andreu Vila, Anaa Casanovas, Crsitian Pin, Xavier Pla, Francesc Sgura, and Albert Lacunza for their good advices, support and friendship.

I thankful very much to Miguel Ferrer , Sebastian Saladrigas and Luis Sisas for their collaboration by giving us the opportunity to realize the field experiments in their farms.

I would like also to acknowledge the financial academic support of Agencia Española de Cooperación Internacional para el Desarrollo (AECID) during four years.

Special thanks should also go to Prof. Gerad Arbat from the Universitat de Girona, Department of Chemical and Agricultural Engineering, who received me many times in his office, to discuss and analysis my data in Hydrus program, looking to publish our work soon.

I thankful to Prof. Ramon Aragüés, from Agrifood Research and Technology Center of Aragón, for the time he spent with me when I visited him to discuss my experimental data.

I am very grateful to Dr. Carles Rubio for the time that he spent with me to discuss my ideas related to my work, and for sending me a valuable collection of scientific papers.

Discussions with many people led to get improvements in this thesis. I am very grateful for their patience and stimulating suggestions, especially to Prof. Gaylon S. Campbell (USA), Prof. Laosheng Wu (USA), Prof. Magnus Persson (Sweden), Prof. Teruhito Miyamoto (Japan), Prof. Sebastia Olivella (Spain), Prof. Jean Vaunat (France), Prof. Axel Ritter (Spain), Prof. Carlos M. Regalado (Spain), Prof. David Moret (Spain), Prof. Carles Aliaw (Spain), Prof. Francesc Ferrer (Spain), Prof. Marc van Iersel (USA) and many others for answering my emails related to modeling soil water and salinity. And I strongly acknowledge to Prof. Gaylon S. Campbell and Prof. Laosheng Wu for reviewing my first publication.

I would like to thank Raghad Shwiekh, Alfred Kwame Bedi and Dra. Fatima Lambarraa for their support and spending their time in discussion my ideas, and reviewing the English of my work.

I would like to thankful Montserrat Mariné, for her patience in answering all my questions related to the administrative documents for my registration and stay in the university.

In my office in this College, I was surrounded by knowledgeable and friendly people who helped me daily. My office mates, Graciela Marando, Mohammad el Moctar and Jordi Llop have been a great source of practical information, as well as being happy to be the first to hear my outrage or glee at the day's current events.

The road to my graduate degree has been long and winding, so I would also like to thank some people from the early days, Prof. Carlos Cafiero, Prof. Jose M. G. Alvarez Coque, Antonio del Valle, and especial thankful for Ricardo Martín Borlaff, who helped me to solve my problems with foreign police and housing, Maite Agusti Sierra, who taught me the Spanish language when I came to Spain, and till now she calls to support me.

Table of Contents

Chapter 4 Soi salinity

Summary

Sustainability of irrigated agriculture is a growing concern in the Baix Llobregat area. Although irrigated land accounts for a substantial proportion of food supply to the local market, it has been, and still is increasingly degraded by poor agricultural management. This dissertation focuses on ways to evaluate furrow irrigation and to assess soil water content and soil salinity (temporally and spatially) under usual farmers' management practices. This dissertation meets these goals through an extensive study of relevant literature and the implementation of practical research. The latter was carried out with a case study on representative fields of the area. Empirical and stochastic models were applied to evaluate furrow irrigation as well as to monitor water flow and solute transport in the root zone. An empirical model was used to evaluate infiltration in furrow irrigation in two fields irrigated with water of different qualities. Performance indicators for each field were calculated. The volumetric water content of the study area was measured in situ for a horticultural crop during its growing vegetative stage, using capacitance soil moisture sensors at five depths within the root zone. Time series analysis techniques were applied to evaluate soil water content in the root zone in order to predict soil water content at the depth of interest by measuring one shallow depth, and a methodology was suggested to determine the next irrigation time and its effect on soil water content at the depth of interest.

Hilhorst (2000) presented a theoretical model describing a linear relationship between soil bulk electrical conductivity (σ_b), and soil dielectric constant (ε_b) in moist soils, to estimate pore water electrical conductivity (σ_p). With linear relationship, Hilhorst (2000) found that measurements of σ_p can be made in a wide range of soil types without soil-specific calibrations. When applying the linear relationship $\varepsilon_b - \sigma_b$ to the field data in our study, we observed that the residuals of the estimated linear relationship displayed extremely strong positive autocorrelations. We improved this linear relationship by adding a stochastic component to it. After estimating σ_p, two studies have been performed: a) prediction of soil salinity at shallow depth and in the upper soil profile (0.60 m depth) by measuring soil water content and soil temperature at shallow depth; b) comparison between the fields of the study area to evaluate the

effects of irrigation frequency according to the farmer's usual management practice on soil salinity behaviour, depending on soil depth and position (furrow or ridge).

A volume balance model was used to evaluate the furrow irrigation system in the study area. Field data were collected to evaluate the advance-recession time for stream flow along the furrow, field infiltration and soil moisture distribution after irrigation. A sensitivity analysis was made on the response of the model to changes in specific parameters.

The time series consisted of hourly measurements of soil water content and was transformed to a stationary situation. Subsequently, the transformed data were used to conduct analyses in the time domain in order to obtain parameters for a seasonal autoregressive integrated moving average (ARIMA) model. In the case of variable interval irrigation, predicting the soil water content time series cannot be properly explained by the ARIMA model and its underlying normality assumption. By completing the ARIMA model with intervention analysis and outlier detection, the prediction of soil water content with variable interval irrigation could be made. The transfer function models were then used to predict water contents at depths of interest (0.20, 0.35, 0.50 and 0.60 m) as well as the average water content (W_{AVG}) in the top soil profile by measuring water content at 0.10 m depth.

We rearranged the Hilhorst (2000) model to a stochastic model called time- varying Dynamic Linear Model (DLM) to obtain an accurate offset $\varepsilon_{\sigma b=0}$ of the relationship between ε_b and σ_b. When DLM is completely specified, i.e., there are no unknown parameters in its definitions, we can use the well known Kalman filtering and smoothing algorithms to obtain means and variances of the conditional distributions of the unobservable system state ($\varepsilon_{\sigma b=0}$ and σ_p).

Studying the cross-correlaiton function between soil salinity, soil water content and soil temperatue and using a (multiple input-one output) transfer function model, we were able to predict soil salinity at 0.10 m depth and in the top 0.60 m of the soil profile by measuring soil water content and soil temperature at 0.10 m depth.

This research produced a number of key findings: first, evaluating furrow irrigation confirmed that 30-43 % of the applied water would have been saved in the study fields if irrigation was stopped as soon as soil water deficit was fully recharge taking the amount of water needed for salt leaching into account, and that the application efficiency (AE) would increase from 52% to 84% and from 41% to 68% (Field 1 and Field 2, respectively). Second, the predictions of soil water content using ARIMA models were logical, and the next irrigation time and its effect on soil water content at the depth of interest were correctly estimated. Third, considering the linear relationship $\varepsilon_b - \sigma_b$, by transforming the Hilhorst (2000) model, which is based on the deterministic linear relationship ε_b-σ_b, into a time- varying Dynamic Linear Model (DLM) enabled us to validate this relationship under field conditions. An offset $\varepsilon_{\sigma b=0}$ value was derived that would ensure the accurate prediction of σ_p from measurements of σ_b. It was shown that the offset $\varepsilon_{\sigma b=0}$ varied for each depth in the same soil profile. A reason for this might be changes in soil temperature along the soil profile. The σ_p was then calculated for each depth in the root zone. Fourth, by using a (multiple input–single output) transfer function model, the results showed that soil water content and soil temperature had a significant impact on soil salinity. Moreover, soil salinity was predicted as a function of soil water and soil temperature, was correctly estimated. Finally, applying the analysis of variance (ANOVA), the results showed that the irrigation frequency, according to the farmer's usual management practice, had statistically significant effects on soil salinity behaviour, depending on soil depth and position (furrow, ridge). Moreover, it was shown that at the end of the crop's cycle the farmers left the field with less soil salinity, for each depth, than at the beginning of the crop's agricultural cycle.

Resumen

La sostenibilidad de la agricultura de regadío es una preocupación creciente en la zona del Baix Llobregat. A pesar de que las tierra irrigadas abastecen de alimentos en una proporción sustancial al mercado local, estas tierras han sido y siguen siendo degradadas por una gestión agrícola no adecuada. Esta tesis doctoral tiene como objetivo evaluar el riego por surcos realizado conforme a las prácticas de gestión habitual de los agricultores de la zona, del contenido de agua y de la salinidad del suelo (de forma temporal y espacial) en dos campos ubicados cultivados con lechuga y alcachofa y regados con aguas de diferente calidad. Se aplicaron modelos empíricos y estocásticos para evaluar la irrigación por surco, así como para monitorear el flujo de agua y el transporte de solutos en la zona radicular del cultivo. Se utilizó un modelo empírico para evaluar la infiltración en el riego por surcos en los dos campos regados y para calcular los indicadores de calidad de riego. El contenido volumétrico de agua de la zona estudiada se midió in situ con sensores de capacitancia de humedad a cinco profundidades dentro de la zona radicular del cultivo durante su ciclo productivo vegetativo. Las técnicas de análisis de series temporales se aplicaron para predecir el contenido de agua del suelo a profundidades determinadas teniendo en cuenta el contenido de agua en la capa superficial. Ello permitió predicer el momento más adecuado para el próximo riego.

Para estimar la conductividad eléctrica del agua capilar (σ_p) se utilizó el modelo propuesto por Hilhorst (2000), el cual describe una relación lineal en suelos húmedos entre la conductividad eléctrica aparente del suelo (σ_b) y la constante dieléctrica del mismo (ε_b). Mediante el uso de esta relación lineal, Hilhorst (2000) encontró a través de sus experimentos de laboratorio que las mediciones de σ_p se pueden hacer en una amplia gama de tipos de suelo sin calibraciones específicas. Al aplicar la relación lineal $\varepsilon_b - \sigma_b$ a los datos de campo de nuestro estudio se observó que los residuales estimados de la relación lineal mostraban una fuerte autocorrelación positiva. Se ha mejorado esta relación lineal mediante la inclusión de un componente estocástico. Después de estimar σ_p se realizaron dos estudios: a) la estimación de la salinidad a 0,10 m de profundidad, así como el contenido medio de la salinidad del suelo en la parte superior del perfil (profudnidad 0,60 m) midiendo el contenido de agua y la temperatura del mismo a 0,10 m de profundidad; b) la estimación de σ_p permitió comparar los datos de los campos

estudiados y mostrar el efecto de la frecuencia de riego sobre la salinidad del suelo, en función de la profundidad del mismo y la posición (surco o caballón).

Para evaluar el sistema de riego por surco en el área de estudio se utilizó el modelo de balances en volumen. Los datos de campo fueron recogidos para evaluar el tiempo de avance-recesión para el flujo de la corriente de agua a lo largo de la longitud del surco, la infiltración y la distribución de la humedad del suelo después de riego. El análisis de sensibilidad se realizó sobre la respuesta del modelo a los cambios en los parámetros específicos.

La serie de tiempo consistió en mediciones horarias del contenido de agua del suelo y se transformó a una situación estacionaria. Posteriormente, los datos transformados se utilizaron para realizar los análisis temporales con el fin de obtener los parámetros de un modelo estacional autorregresivo integrado de media móvil (ARIMA).

En el caso de riegos a intervalo variable, predecir las series temporales del contenido de agua del suelo no es adecuadamente explicada por el modelo ARIMA y su supuesto de normalidad subyacente. Al completar el modelo ARIMA con análisis de intervención y detección de los atípicos, se puede hacer la predicción del contenido de agua del suelo para riegos de intervalo variable. Se utilizaron posteriormente modelos de función de transferencia para predecir el contenido de agua a las profundidades de interés (0,20, 0,35, 0,50 y 0,60 m), así como el contenido medio de agua (W_{AVG}) en la parte superior del perfil del suelo midiendo el contenido de agua a 0,10 m de profundidad.

Para obtener una intercepción $\varepsilon_{\sigma b=0}$ exacta de la relación lineal entre ε_b y σ_b se ha transformado el modelo de Hilhorst (2000) a un modelo estocástico llamado Modelo Dinámico Lineal variable en el tiempo (DLM). Cuando el DLM se especifica completamente, es decir, que no hay parámetros desconocidos en sus definiciones, entonces se pueden usar los conocidos algoritmos de filtrado y suavizado de Kalman para obtener medias y varianzas de las distribuciones condicionales del estado no observable ($\varepsilon_{\sigma b=0}$ y σ_p).

El uso del modelo de función de la transferencia permitió predecir la salinidad del suelo a 0,10 m, así como el contenido medio de la salinidad del mismo en la parte

superior del perfil del suelo midiendo el contenido de agua y la temperatura del suelo a 0,10 m de profundidad.

Los resultados obtenidos fueron: a) la evaluación del riego por surco confirmó que se podría haber utilizado un 30-43% menos de agua en los suelos estudiados, teniendo en cuenta la recarga completa de agua del suelo y el agua necesaria para la lixiviación de las sales. De este modo, la eficiencia de aplicación (AE) aumentaría del 52% al 84% y del 41% al 68% en los campos de estudio (Campo 1 y Campo 2, respectivamente); b) las predicciones del contenido de agua del suelo mediante modelos ARIMA eran lógicas, y el tiempo del próximo riego y su efecto sobre el contenido de agua del suelo a la profundidad de interés se había calculadoó correctamente; c) teniendo en cuenta la relación lineal $\varepsilon_b - \sigma_{b,}$ la reorganización del modelo de Hilhorst (2000), desde una relación lineal determinista ε_b-σ_b, a un Modelo Dinámico Lineal (DLM) variable en el tiempo permitió validar esta relación en condiciones de campo y obtener un valor $\varepsilon_{\sigma b = 0}$ que garantice la predicción exacta de σ_p a partir de mediciones de σ_b. Se demostró que la $\varepsilon_{\sigma b = 0}$ varía para cada profundidad en un mismo perfil del suelo, posiblemente debido a los cambios de temperatura a lo largo del perfil.

Mediante el uso del modelo de la función de transferencia, los resultados mostraron que el contenido de agua y temperatura del suelo tenian un impacto significativo en la salinidad del suelo, y que la predicción de la salinidad del suelo como una función de la humedad y temperatura del mismo se había estimado correctamente. Finalmente, al aplicar el análisis de la varianza (ANOVA), los valores de σ_p calculados a distintas profundidades permitieron demostrar que la frecuencia de riego, practicada normalmente por el agricultor, tenía efectos estadísticamente significativos sobre la salinidad del suelo dependiendo de la profundidad y posición (surco o caballón). Sin embargo, la gestión del riego no afectó a la salinidad del suelo durante el ciclo productivo del del cultivo.

1. Introduction

1. Introduction

Table of contents

1. Introduction

1.1 Genearal context

Irrigated agriculture and efficient irrigation techniques are fundamental for crop production and world food security. The poor agricultural management in irrigated land (such as water-logging resulting from over-irrigation) leads to land degradation due to salinization and contaminated groundwater (Ghassemi et al., 1995). The sustainability irrigated agriculture requires increasing the irrigation efficiency to conserve water and maintain the root zone in good conditions for plant growth, this mean keeping the soil water content at its field capacity and the soil salinity at adequate level for plant growth. Moreover, increasing the irrigation efficiency alleviates groundwater pollution associated with irrigated agriculture. Because of increasing water needs in industrial, agricultural and human activities and the limitation of water resources, reusing of saline drainage water and treated wastewater for irrigation have been increased (Rhoades et al., 1997). With less leaching and drainage discharge and greater use of saline water for irrigation, soil salinity may increase in some areas. Thus, to achieve adequate level of soil salinity at root zone and to reach the efficient irrigation, functional methodology is required for the timely evaluation of soil salinity and soil water content in irrigated areas.

Our study area is located near a coastal zone. For decades, some of its parts started facing emerging of soil salinization and noted pollution in its some aquifers because of some typical reasons of costal area problems (such as excessive exploitation of aquifers, sea water intrusion, and high infiltration by irrigation). Therefore, it is important to start with giving detailed description of water resources and how the responsible water authority in the area manage and distribute it to meet industrial, human and irrigation needs. After that, a general outlines for our research will be described related to the water resources and environmental situation in the Llobregat Delta from the agricultural point of view, focusing on the most common irrigation techniques that farmers usually use in this area, which accounts one of the most agricultural operation could affect on the sustainability of irrigated agriculture. In the end a general objective of the research will be presented.

1.2 Description of the study area

Site: the study area is located in the Parc Agrari del Baix LLobregt (delta of the Llobregat river), in the south of Barcelona, Spain. It covers about 100 square kilometers and forms a valuable natural habitat. Its wetlands are of international importance for wildlife and form a significant wintering ground for many migratory birds, its classified as "Special Protected Areas" (SPA) in accordance with the purpose of the EU Bird Protection Directive (according to Article 4 of the Council Directive 79/409/EEC). The delta aquifer is one of the most important freshwater resources for Barcelona region, with a groundwater capacity of 100 Mm^3 yr^{-1}, used by numerous industries, agriculture and the cities. The fertile delta farmland supports intensive agriculture making it an important agricultural productive supplying the local market. Three representative fields of the area were chosen for our study (Fig. 1.1). Sites were selected as representative of the soils, water quality (electrical conductivity, EC: 1 dS m^{-1} in Field 1 and 2 dS m^{-1} in Fields 2 and 3), irrigation design, area and agricultural management practices of the region.

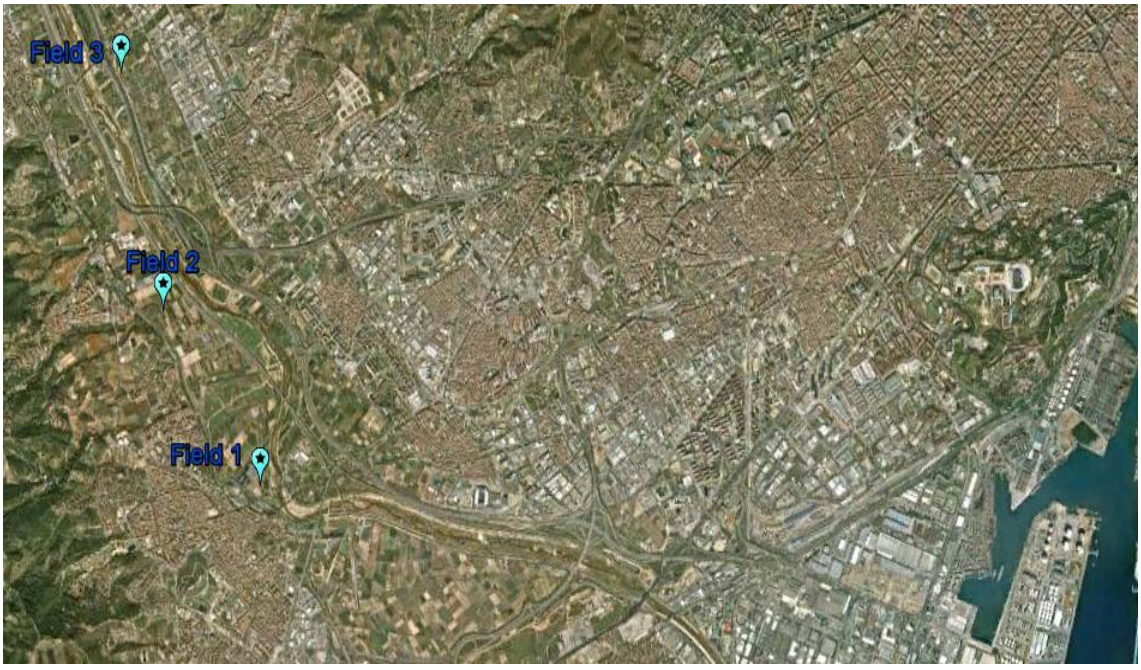

Fig. 1.1. The study area in the Llobregat Delta site (sites of representative Fields 1, 2 and 3).

1.2.1 Environmental problems face the area

Since 1960s, the delta´s land has been exposed to constant pressure from Barcelona´s urban and industrial expansion. The most factors affect on the water resources and environmental sustainability are:

1. Using delta area to develop Catalonia´s infrastructure: most of logistics and transports services was built in this area (railways, port, airport and motorway network). Less than 5% of the original wetlands in the area now remain after the recent port extension (FAO, 2010).
2. Salinization of the aquifer due to seawater intrusion as a result of the overexploitation of the underground water, rendering 30% unusable of deltaic aquifer (FAO, 2010).
3. By the end of the 1980s, the Llobregat River was considered one of the most polluted in Western Europe due to:
    a. Potash-mining activities in the upstream Manresa (one of the main Llobregat River tributaries).
    b. Sewage treatment plants and industrial effluents (estimated at 137 hm^3 yr^{-1} or 4.3 m^3 s^{-1} as average)
    c. The river in its lower part receives large inputs from industrial and human activities (paper mills, tannery and textile industries), this lower part of river flows through one of the most densely populated areas of the Mediterranean region (Metropolitan area of Barcelona, over 3 million people).
    d. Aquifer extractions are also affected by the water quality of Llobregat River (Catalan Water Agency, 2008).
4. Intrinsic variability of the Mediterranean climate, especially in precipitation. Drought makes the flow from the Llobregat River insufficient to meet industrial, agricultural and human needs.

1.2.2 Procedures to face environmental problems in the Delta area

The most important practices that the public responsible authorities were adapted to manage environmental problems are:

1. The infrastructure: it prevents excessive pollution of the river by intercepting specific effluents, such as the channels that receiving treated urban wastewater from Rubí and those collecting brines from the salt-mine sites (Fig. 1.2). Apart from that, there are two major channels which are located on two sides:
    a. On the right side of the river, Canal de la Dreta provides water extracted from the middle course of the river to horticulture.
    b. On the left side of the river, Canal de la Infanta, was also built for irrigation purposes, but now its main role is diverting treated wastewater from industries and towns away from the river, hence improving the latter´s water quality.
2. Wastewater treatment plants: public responsible authority built a lot of wastewater plants in the area, there are two main wastewater treatment plants (WWTPs): *El Prat de Llobregat* and *Sant Feliu de Llobregat*, both with tertiary treatment. For *Prat de Llobregat* WWTP, the concept is to pump effluent upstream to a regulatory pond from which water will flow into the Canal de la Dreta. Currently, freshwater with an average conductivity of 1.5 dS m^{-1} from the Llobregat River is conveyed via this channel to irrigate farm lands. The use of effluent in irrigation would need the desalination of the WWTP effluent by EDR (electrodyalisis reversal) unit and facilities to pump it to the Canal de la Dreta and a storage pond. The average salinity of the irrigation water would be reduced from 2.9 to 1.2 dS m^{-1} (Sabater et al., 2012). Effluent from the Sant Feliu de Llobregat WWTP is fully treated to tertiary levels and accessible to be used in irrigated agriculture. The effluent volume around 19 Mm^3 yr^{-1} can be transferred to the Canal de la Infanta to be used for irrigation purposes. The effluent is usually mixed with well water in order to reach an acceptable water quality for irrigation purposes (its average electrical conductivity is around 2.3 dS m^{-1}).

Moreover, an important part of the reclaimed flow of *El Prat de Llobregat* WWTP will also be used to create a hydraulic barrier to seawater intrusion in the Llobregat lower delta aquifer (Sabater et al., 2012).

3. Three large dams were built in upstream sections of the Cardener and Llobregat River to ensure water supply during low flow periods.
4. When the flow of the Llobregat River is insufficient to face the demand for indusial, human and agricultural needs, additional water has to be conveyed from the Ter River to the Llobregat watershed. Aquifer extractions are also affected by water quality of the Llobregat River. If water quality is poor, the surface water has to be mixed with more groundwater in order to be treated for domestic use (Sabater et al., 2012).

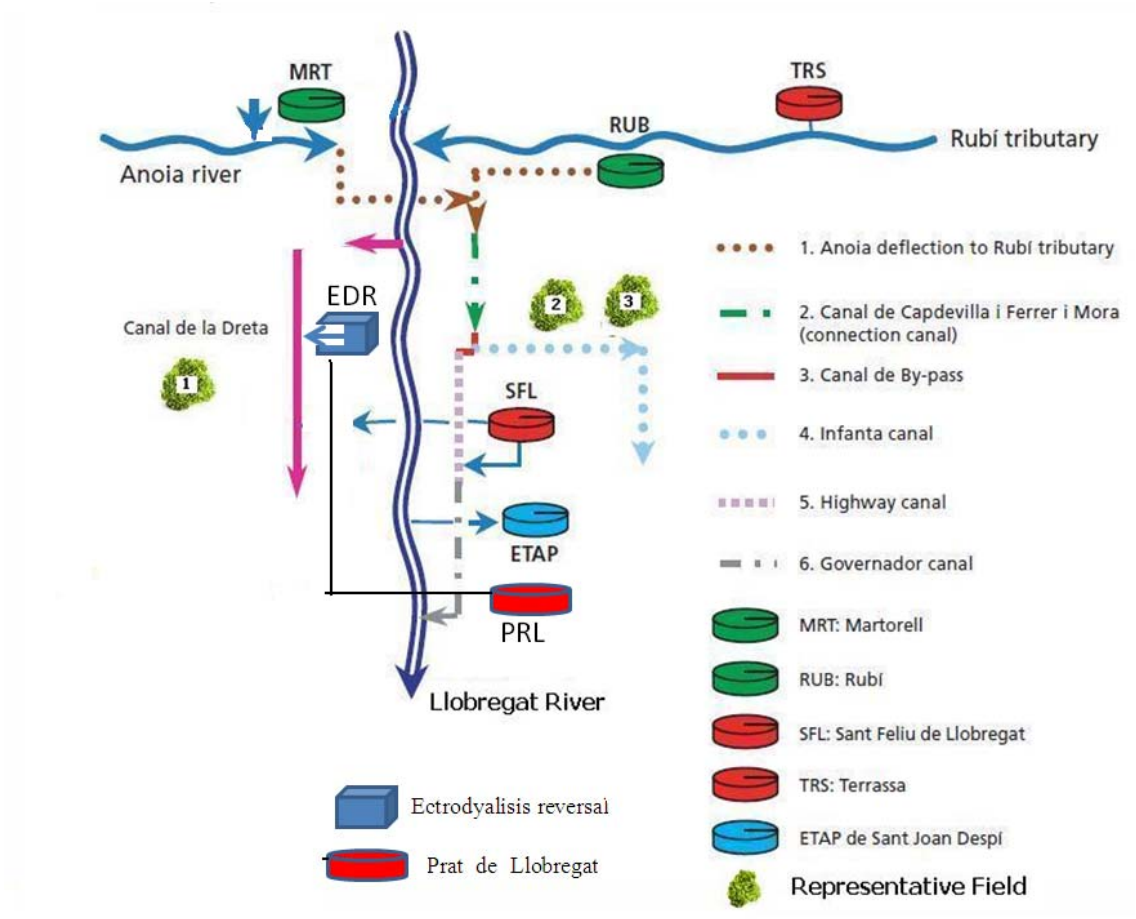

Fig. 1.2. Deflection channels in the lower Llobregat River course (adapted from FAO, 2010)

1.3 General Outlines

1.3.1 Background

For decades, numerous studies have been carried out in this area. In 1926, Antonia Burés Borrás the owner of a textile mill, which was located next to the Cardener, found that the metallic turbines of her factory were corroding. She realized that the concentration of salts was very high in the Cardener River upstream due to the mining industry´s wastes. Burés then initiated legal proceeding against the mining company in order to stop their pollution of the Cardener's waters. The Spanish Government began to study this issue seriously by doing two investigations on the effluent flowing out of Súria. Later, a lot of debates related to the affect of the salts flowing into the river from mines to the Llobregat aquifer carried out by the Commission for the Study of the Salinity of the Waters of the the Llobregat River (CESALL). In 1930, the CESALL released their conclusions and recommendation which was one of them is the salinity effluents should be limited to 250 mg L^{-1} in Palleja (CESALL, 1932). The study of Vilaró (1966) realized in the Llobregat River was the first research in Spain investigated in details the surface and underground water together. At the end of the 70's, when salinization problems became increasingly worrying, hydrochemistry works improved the knowledge of the aquifer systems and the mechanisms that caused seawater intrusion in the main aquifer of the Llobregat delta (Custodio et al., 1976; Custodio, 1981; Muñoz and Prat, 1991; Manzano et al., 1992; Bayó et al., 1977; Doménech et al., 1983; Iríbar et al., 1991). An interesting study was done by Llamas (1969) about recharge the groundwater in the Llobregat Delta. He found the infiltration due to irrigation and rainwater falling directly on the area or in the watersheds of the small streams running directly into the delta formed about 45% per year of the total natural recharge of water in the Llobregat delta groundwater. Guimerá and Candela (1991) discovered in their study, which was carried out in the coastal detrial Maresme aquifer located north of Barcelona, that there is an increase of up to 40% of seawater presence in the aquifer from 1989 to 1991. Soler et al. (2002) used the characteristics of the isotopes as geochemical tools to study the water pollution problems in the Llobregat River.

Many studies investigated in the practices of the Managed Artificial Recharge (MAR) to mitigate the negative effect of existing infrastructures in the influential area

of Llobregat River (roads, railroads, airport, etc) on the total amount of natural aquifer recharge that can be normally attributed to the area (Abarca et al., 2006; Gámez, 2007; Gasith and Resh, 1999; Luna et al., 2009; Prat and Rieradevall, 2006; Vázquez-Suñe et al., 2006).

The previous studies discussed the water resources and environmental problems in Llobregat River and Llobregat Delta from the hydrological, geological and geochemical point of view.

1.3.2 Structure

Our work will deal with the water resources and environmental situation in the Llobregat Delta from the agricultural point of view. In other words, within the complex situation that the Llobregat Delta area has, this research will evaluate the agricultural operations that the farmers are practicing and study its effect on the soil salinity, groundwater, and hence on the sustainability of irrigated area. Given limited time and resources for conducting the study, it will focus on the irrigation system adapted by the major farmers in the area and study its effect on the soil water content and soil salinity within the root zone.

Sustainable management of groundwater quality in agricultural areas requires efficiently irrigate the crops. This means keeping the soil water content at its field capacity, the soil salinity at adequate level for plant growth and minimizing percolation. In that case the fertilizers will settle in the root zone and away from groundwater. Furrow irrigation system is the most common method that adopted by farmer in the study area to irrigate their crops. We will evaluate the furrow irrigation system in the two representative fields of the area (one of them is irrigated by the water coming from the Canal de la Dreta and the other from the Canal de la Infanta). The research has been organized into five chapters:

Chapter one contains background and description of the study area, environmental problems face the area and the procedures that the public authority responsible has been adopted to mitigate it, studies have been done to deal with that problems and the objective of the study.

Chapter two will evaluate the furrow irrigation system that the farmers adopted it to irrigate their crops by using mathematical methods to calculate the performance indicators of the irrigation and using simulation to improve the irrigation efficiency.

Chapter three will include stochastic models to assess the irrigation management that the farmers apply it in their fields. We will conclude this chapter with tools that can help the farmers in scheduling irrigation (determining the next irrigation time).

Chapter four is related to the field soil salinity; advanced mathematical processes will be realized to develop the Hilhorst (2000) linear model to derive an accurate offset in order to convert the bulk electrical conductivity (σ_b) to pore water electrical conductivity (σ_p). After that, the relationship between the soil water content and soil temperature at the shallower depths with the soil salinity at deeper depths will be studied with the objective to predict the soil salinity at deeper depth by measuring soil moisture and soil temperature at shallow depth in order to help the farmers in keeping the root zone at adequate salinity level for plant growth.

Finally, the **conclusions**, that arising from this research, will be presented in the last chapter along with the implications of this research and the recommendations for future work.

1.3.3 Research problem and objective

In brief, the research objective could be divided into two parts: a) developing an integrated decision support for furrow irrigation used in the area study and; b) modeling the behavior of soil water content and soil salinity in the root zone to improve scheduling irrigation and maintain the sustainability of irrigated area.

Five **specific objectives** have been designed to solve the research problem:

1. Evaluating the furrow irrigation method used in the area study: determine the infiltration function and applied it in a simulation model to evaluate the performance and determine optimal design or management practices.
2. Improving the scheduling irrigation: determine the next irrigation time and its effect on the soil water at depth of interest, this objective will be achieved by 1)

studying the autocorrelation and partial correlation function for soil water content measured at a shallower depth as well as the cross-correlation function between soil water content at a shallower depth and various greater depths, including average soil water content (W_{AVG}) in the top 0.60 m of soil profile; 2) develop models for predicting the soil water content at various greater depths and water storage in the soil profile from a single shallower depth; and 3) examine the effectiveness of the irrigation event in the soil water profile.

3. Deriving an offset value for the linear relationship between soil dielectic constant (ε_b) and bulk electrical conductivity (σ_b) that would ensure the accurate prediction of electrical conductivity of pore water (σ_p) from measurements of soil bulk electrical conductivity (σ_b).
4. Developing models for predicting the soil salinity at various greater depths by measuring soil water content and soil temperature at shallow depth, this will be achieved by: a) studying the autocorrelation and partial correlation function for soil water content and temperature measured at a shallower depth; b) studying the cross-correlation function between soil water content and temperature at a shallower depth and various greater depths for soil salinity, including average soil salinity in the top 0.60 m profile.
5. Studying the evolution of soil salinity during the crop vegetative stage in the study area and examine the effect of irrigation frequency and depth on the soil salinity.

1.4. References:

Abarca, E., Vázquez-Suñé, E., Carrera, J., Capino, B., Gámez, D., Batlle, F., 2006. Optimal design of measures to correct seawater intrusion. Water Resources Resarch 42: W09415. doi: 10.1029/ 2005WR004524.

Bayó, A., Batista, E., Custodio, E., 1977. Sea water encroachment in Catalonia coastal aquifers, in General Assembly IAH. Birmingham 1977, vol. XIII, pp. F.1–14.

Catalan Water Agency (ACA). 2008. Water in Catalonia. Diagnosis and proposed actions. Significant water management issues raised within the compilation of the River Basin District Management Plan for Catalonia. Pursuant to Article 14(b) of the Hydrological Planning Regulation (Decret 380/2006).

CESALL., 1932. Comisión para el Estudio de la Salinidad de las Aguas del Llobregat. National Archives of Catalonia. Fons 547. Agencia Catalana de l'Aigua. Unitat 479, Barcelona.

Custodio, E., 1981. Sea water encroachment in the Llobregat delta and Besós areas, near Barcelona (Catalonia, Spain). In Sea Water Intrusion Meeting: Intruded and Fosil Groundwater of Marine Origin., vol. 27, edited by U. S. G. undersökning: 120–152.

Custodio, E., Cacho, F., Peláez, M., 1976. Problemática de la intrusión marina en los acuíferos del Delta del Llobregat. In Segunda Asamblea Nacional de Geodesia y Geofísica, Barcelona., Instituto Geofísico y Catastral Madrid, 2069–2101

Doménech, J., Batista, E., Bayó, A., Custodio, E., 1983. Some aspects of sea water intrusion in Catalonia (Spain). In 8th SWIM. Bari., edited by I. di Geología Appicata e Geotecnia, Bari. p. 15.

FAO, 2010. The wealth of waste: The economics of wastewater use in agriculture. FAO Water Report 35. Food and Agriculture Organization of the United Nations, Rome, Italy.

Gámez, D, 2007. Sequence stratigraphy as a tool for water resource management in alluvial coastal aquifers: application to the Llobregat delta (Barcelona, Spain). PhD Thesis, UPC Barcelona Tech.

Gasith, A., Resh, V. H., 1999. Streams in Mediterranean climate regions: abiotic influences and biotic responses to predictable seasonal events. Annual Review of Ecology and Systematics 30, 51-81.

Ghassemi, F., Jakeman, A. J., Nix, H. A., 1995. Salinization of land and water resources. University of New South Wales Press, Sydney, Aust., 526 pp.

Guimerá, J., Candela, L., 1991. Quality variability of groundwater resources in the Maresme coastal aquifer, Barcelona, Spain. In Proceedings of IAH XXIII International Congress, Aquifer Overexploitation. Canary Islands, Spain, 520–530.

Hilhorst, M. A., 2000. A pore water conductivity sensor. Soil Science Society of America Journal 64, 1922-1925.

Iríbar, V., Manzano, M., Custodio, E., 1991. Evaluation of overexploitation effects in the Baix Llobregat aquifers by means of environmental isotope techniques. In Proceedings of IAH XXIII International Congress, Aquifer Overexploitation. Canary Islands, Spain, 535–538.

Llamas, M. R., 1969. Combined use of surface and groundwater for the water supply to Barcelona (Spain), International Association of Scientific Hydrology. Bulletin, 14, 119-136.

Luna, M., Salas, J., Molinero, J., Queralt, E., Rull, M., Colomer, V., Trevisan, L., Ruiz, E., Guimerá, J., Niñerola, J. M., 2009. Evaluación de la capacidad de infiltración e impacto hidrogeológico de las balsas de recarga artificial del Baix Llobregat (Santa Coloma de Cervello). Jornadas sobre la Investigación de la zona no saturada del suelo –ZNS'09. Vol IX.

Manzano, M., Custodio, E., Carrera, J., 1992. Fresh and salt water in the Llobregat delta aquifer: application of ion chromatography to the field data, in SWIM Study and Modelling of Saltwater Intrusion into Aquifers, edited by E. Custodio and A. Galofre, , CIMNE–UPC, Barcelona, 207–228.

Muñoz, I., Prat, N., 1991. Cambios en la calidad del agua de los ríos Llobregat y Cardener en los últimos 10 años. Tecnología del Agua 91, 17–23.

Prat, N., Rieradevall, M., 2006. 25-years of biomonitoring in two mediterranean streams (Llobregat and Beso`s basins, NE Spain). The ecology of the Iberian inland waters: Homage to Ramon Margalef 25, 541–550.

Rhoades, J. D. Lesch, S. M., Lemert, R. D., Alves, W. J., 1997. Assesssing irrigation /draingage/salinity management using spatially referenced salinity measurements. Agricultural Water Management 35, 147-165.

Sabater, S., Ginebreda, A., Barcelo, D., 2012. The Llobregat River Basin: A Paradigm of Impaired Rivers Under Climate Change Threats. Springer Berlin Heidelberg.

Soler, A., Canals, A., Goldstein, S. L., Otero, N., Antich, N., Spangenberg, J., 2002. Sulphur and strontium isotope composition of the Llobregat river (NE Spain): Tracers of natural and anthropogenic chemicals in stream waters. Water, Air, and Soil Pollution 136, 207–224.

Vázquez-Suñé, E., Abarca, E., Carrera, J., Capino, B., Gámez, D., Pool, M., Simó, T., Batlle, F, Niñerola, J. M., Ibáñez, X., 2006. Groundwater modelling as a tool for the European Water Framework Directive (WFD) application: the Llobregat case. Physics and Chemistry of the Earth 31, 1015–1029.

Vilaró, F., 1966. Estudio de los recursos hidráulicos totales de las cuencas de los ríos Besós y bajo Llobregat, 2º Informe. Comisaría de Aguas del Pirineo Oriental y Servicio Geológico de Obras Públicas. Barcelona.

"Model-making, the imaginative and logical steps which precede the experiment, may be judged the most valuable part of scientific method because skill and insight in these matters are rare. Without them we do not know what experiment to do. But it is the experiment which provides the raw material for scientific theory. Scientific theory cannot be built directly from the conclusions of conceptual models."

HERBERT GEORGE ANDREWARTHA

Introduction to the Study of Animal Population (1961), 181.

2. Soil water: Evaluation of furrow irrigation performance

2. Soil water: Evaluation of furrow irrigation performance

Table of contents

Abstract

The efficiency of the application of furrow irrigation for lettuce and artichoke production was studied in the Llobregat Delta area. Average irrigation efficiencies in the study area were found to vary between 31 and 52 %. Differences in efficiency were found to be directly related to farm design and specific management practices. Application efficiency was found to increase with decreasing cut-off time. 30 % and 43 % of the applied water would have been saved in Field 1 and Field 2 respectively, if irrigation stopped as soon as soil water deficit was fully compensated taking into account the amount of water needed for salt leaching. More water was used for fields irrigated by poor water quality to ensure salt leaching. These results indicate that significant improvements in irrigation efficiency could be achieved through the adoption of design and management practices that are appropriate to meet the farms' environmental and management constraints.

Keywords: Furrow; Irrigation; Farm design; Efficiency.

1. Introduction

Furrow irrigation relies on gravity to distribute water to farm fields. Following the direction of gravitational fore, the water flows across the fields from one end to the other, and infiltrates into the soil as it flows. The purpose of furrow irrigation techniques is to supply water in the right quantity, at the right time and in an even layer, to achieve a uniform crop stand and minimize water losses. The success of the techniques depends on proper design and operation of furrow irrigation systems at field level, which help farmers to achieve good crop yields, use precious water resources more efficiently, and limit water- logging, salinization and pollution of resources.

Field dimensions, field slope, flow rate, cut-off time, soil-infiltration characteristics, and flow resistance are the variables used in the mathematical models describing the entire process of surface irrigation and developed by engineers to improve irrigation efficiencies. Interactions between the variables determine advance time, recession time, infiltrated depths and corresponding irrigation efficiencies and uniformities.

Four major categories of mathematical models have been developed to evaluate surface irrigation: fully hydrodynamic, zero-inertia, kinematic wave and volume balance models. A fully hydrodynamic model is the most complex and the most accurate. It is based on the complete Saint-Venant equations for conservation of mass and momentum. A zero-inertia model is a slightly simplified version of the complete Saint-Venant equations that leaves out the acceleration or inertia terms in the momentum equation. A kinematic wave model uses further simplifications and uniform flow assumptions. The simplest model, which involves the largest number of assumptions, is a volume balance model. It is based on the analytical or numerical solution of temporally and spatially-lumped mass conservation, commonly referred to as the "volume balance approach" (Jurriens et al., 2001). This approach has become more refined over time, both conceptually and numerically.

The volume balance model has been widely used for design and field evaluation procedures and has been validated with field and laboratory data (Elliott and Walker, 1982; Walker and Skogerboe, 1987; Guardo, 1988). It is applied primarily to the advance phase of any irrigation condition (i.e., border and furrow). Guardo et al. (2000) determined the advance-infiltration phase in level basin irrigation system by zero-inertia and volume balance models. They found that the volume balance model provides satisfactory predictions of the advance-infiltration phase, although it is less complex and less mathematically demanding than the zero-inertia model.

We used the volume balance model to evaluate the efficiency of the furrow irrigation system in the study area, futher details about its operations and methodology will be presented in the material and method section.

The main objective of this research is assessing field irrigation performance in terms of application efficiency, storage efficiency, deep percolation and distribution uniformity, as well as assessing the impact of improved management options for a furrow irrigation system, based on surface irrigation simulations, the Monserrat (1988) EVSUP model and the WinSRFR model (Bautista et al., 2009). While the specific goals include:

1. Assessing the current field irrigation performance for selected irrigation events on different fields.
2. Developing management options to improve (i.e. optimize) the irrigation efficiency for the selected fields.

2. Materials and Methods

With the help of technicians from the Parc Agrari del Baix Llobregat, two lettuce and artichoke fields established on silty loam soil were selected for irrigatin trails (Fig. 1.1), one located in the Canal de la Dreta (Field 1, lettuce and artichoke crops) and the other in the Canal de la Infanta (Field 2, lettuce crop). Sites were selected as representative of the soils, water quality (electrical conductivity, EC: 1 dS m^{-1} in field 1 and 2 dS^{-1} m in field 2), irrigation design, area and management practices of the region. Irrigations were scheduled according to the farmer's normal management practice.

Irrigation water was applied from the upper part of the furrow and passed through a long throated flume device; the lower part of each furrow was closed at the end. Five neighboring furrows for in Field 1 and eight neighboring furrows for in Field 2 were selected for monitoring at each site. Analysis were conducted using the Monserrat (1988) EVASUP model to calculate the parameters of infiltration function. Moreover, to identify the optimum of application efficiency, analysis to examine the effect of changes in cut-off time and inflow were conducted using the surface irrigation model WinSRFR (Bautista et al., 2009). In each case, input parameters required for model operation were obtained from the measured field irrigations. Field slope, length and geometry furrow were measured at each site. A long throated flume device was used to measure flow rate. The water lost as tailwater is zero since the lower end of each furrow was closed. Stakes were placed at 5 meter intervals along the furrow length to measure water advance time, recession time and depth of flow. Capacitance soil moisture sensors (5TE, Decagon Devices, Inc., Pullman, WA) were installed in each field, with readings taken immediately prior to irrigation and two days after the irrigation was completed to measure the plant available soil water replaced by irrigation (root zone soil water deficit). These measurements were used to determine an average soil water deficit for each site, which was used in the subsequent determination of application irrigation efficiency.

In our case, we assumed that the total infiltrated volume was equal to that of the water applied because there was no loss by tailwater. Below we will present the way to calculate the performance indicators.

2.1 Evaluating furrow irrigation system

Various parameters and variables are involved in the surface irrigation process, and they can be categorized according to whether they are field parameters, decision variables, or evaluation variables. Field parameters are situational data (i.e. data that describe the field situation), so the irrigation designer or farmer cannot assign them another value. Decision variables are those parameters or variables that an irrigation designer can adapt to find the best irrigation performance for given or selected field parameters. Evaluation variables are basically indexes for determining the irrigation performance.

2.1.1 Field parameters

Field parameters include the infiltration characteristics, the surface roughness or flow resistance, the field slope and the required irrigation depth.

a) Soil infiltration characteristics

Infiltration is the fundamental variable in irrigation, since it has the strongest influence on the movement of water over the soil. It is also the most difficult one to measure.

The infiltration function is empirically determined to yield the relationship between the infiltrated water and the opportunity time (the time during which the water contact the soil). The power type- Kostiakov function is the most widely accepted to describte the infiltration characteristics:

$$Z = KT^{a}$$

where:

K, a : are empirical parameters.

Z : is the infiltrated water m^3/m.

T : is the intake opportunity time, min.

There is another derived function suggested by Wallender et al. (1985):

$$Z = KT^a + CT + D$$

When $D = 0$ a Kostiakov – Lewis dominated equation is obtained, and when $C = 0$ a function suggested by the S.C.S is obtained.

The volume balance method was used to determine the infiltration, based on the volume of water entering the field ($Q.t$) being equal to the volume of surface water (V_{sur}) plus the volume of infiltrated water (V_{inf}).

$$Q.t = V_{sur} + V_{inv}$$

Q: is the flow, m^3/min/furrow or unit width.

t: is the moments when the water reaches the points where water height is measured(min).

V_{sur}, V_{inf} are the volume of surface and infiltration water (m^3).

There are different methods to calculate infiltration using this equation (Elliot and Eisenhawer, 1983; Smerdon et al., 1988; Burt et al., 1982). In our study we follwed the method adapted by Monserrat (1988) EVASUP model[1] to measure infiltration. This method has some assumptions:

- The type of infiltration function is $Z = KT^a$;
- The infiltration function is the same across the field;
- The advance front is uniform;
- The surface volume is estimated by two or three measurements of the water height during the flow of water along the furrow.

[1] For more information about the EVASUP model see (Curso de Tecnología del Riego (4rt. : 1990 : E.T.S.E.A. Agrònoms, Lleida)

This type of infiltration has two unknown parameters *K* and *a*, that means, we need two equations: generally they are calculated when water reaches at the middle and the end of the furrow. At these two points, the applied volume of water and the surface volume of water can be known, thus, mathematically the infiltrated volume could be expressed as follows:

For $t = t_1$

$$Q.t_1 - V_{sur1} = \int_0^{x_1} K(t_1 - t_x)^a dx$$

For $t = t_2$

$$Q.t_2 - V_{sur2} = \int_0^{x_2} K(t_2 - t_x)^a dx$$

where:

Q: is the flow, m^3/min/furrow or unit width.

t_1, t_2: are the moments when the water reaches the points where water height is measured (min).

V_{sur1}, V_{sur2}: are the volumes of surface water at moment *t1*, *t2*, (m^3).

t_x: is the time of advance at distance x, (m).

K, a : are parameters of the Kostiakov function.

K and *a* were determined using the equations of Monserrat (1988) model.

In our study, two-point approximations for expressing the mass balance of water in the field during the advance phase were selected. For example, furrow length in Field 1 was 50 m, so when the advancing front of water reaches at 20 m during the irrigation event, the water heights at 5 m and 15 m were measured. Then, when the advancing front of water reached at 45 m, the water heights at 5, 15 and 40 m were measured. Fig. 2.1 explains the locations of these points.

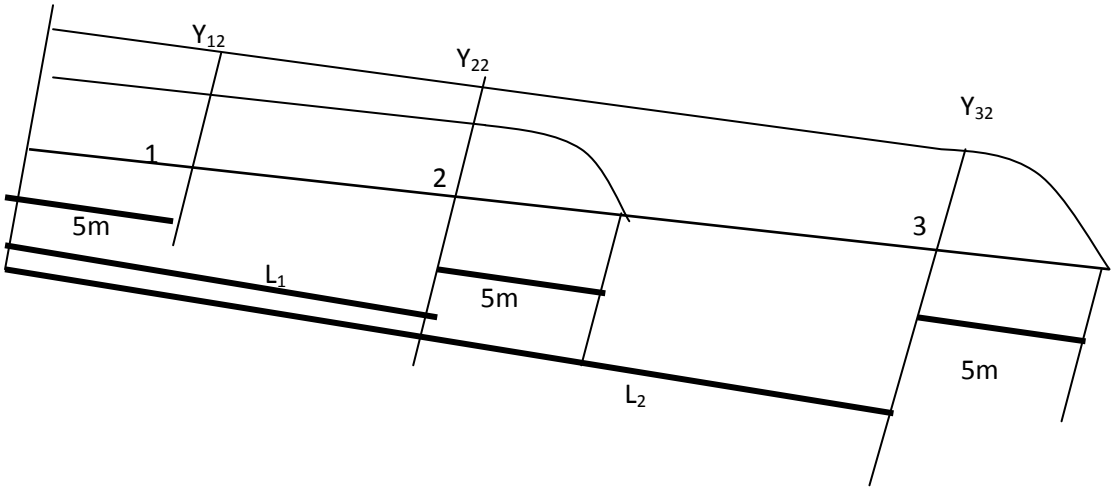

Fig. 2.1. Water advance at two moments

Supposing that the height of water from the beginning of the furrow to the 5 m before the advance front is stabled, we could get the volume water surface as following:

$$V_{sur} = \frac{(Y_{12} + Y_{22})}{2} L_1 + \frac{(Y_{22} + Y_{32})}{2} (L_2 - L_1) + \sigma_y . Y_{32} . 5$$

where σ_y is the surface shape factor generally equal to 0.8, which is the ratio between the average cross-sectional flow area and that at the head of the field. For the infiltrated volume that factor called subsurface shape factor, is the ratio between the average infiltrated cross-sectional area (infiltrated depth time width), and the infiltrated cross-sectional area (depth times width) at the head of the field.

b) Flow resistance

Flow resistance or roughness (n) is a basic input parameter in simulations of surface irrigation. It has a direct effect on flow velocity and, consequently, on advance time, infiltration pattern and total irrigation performance. The higher the flow resistance the longer the advance time; the longer the advance time, the higher heterogeneous infiltrated-depth distribution.

It is difficult to determine the roughness of the field, and generally a hydraulic form is used to measure it. The Manning equation is the most used one to calculate

roughness. This equation is valid when normal flow is reached, that is when water height is constant, which first occurs at the beginning of the field. Hydraulic roughness calculates as follows:

$$Q = A\, R^{0.67} S_0^{0.5} \,/n$$

where:

Q : is the water flow, in $m^3 sec^{-1}$

n : is the hydraulic roughness.

S_0: is the field slope.

R: is the hydraulic radius, in m.

A: is the cross-sectional area of the flow, in m^2.

c) Required depth

The required maximum depth can be determined from the total soil-moisture holding capacity, i.e., the total available moisture between field capacity and wilting point **(**TAM). Stress conditions in the root zone are defined by the Ready Available Moisture (RAM); it is a fraction of TAM. The Soil Moisture Deficit (SMD) is a measure of soil moisture between field capacity (θ_{fc}) and existing moisture content (θ_i), multiplied by the rooting depth (*RD)* :

$$SMD = \left(\theta_{fc} - \theta_i\right) RD$$

A similar term expressing the moisture that is allotted for depletion between irrigations is the Management Allowed Deficit (*MAD***)**. This is the value of (*SMD***)** when irrigation should be scheduled and represents the depth of water the irrigation system should supply. Later this will be referred to as Z_{req}, indicating the 'required depth' of infiltration. In this case, the leaching fraction should be added to the soil moisture deficit to calculate the required depth. The leaching fraction (*LF*) is the fraction of supplied water that passes through the entire rooting depth and percolates below, and calculated as follows:

The total water applied through the irrigation system during each irrigation event (D_i) is the crop water requirement (*SMD*) plus a drainage depth (D_d) due to the leaching requirement:

$$Z_{req} = SMD + D_d = SMD / (1\text{-}LF)$$
$$LF = D_d / Z_{req} = EC_i / (5EC_e - EC_i)$$

LF : leaching fraction (dimensionless)

D_d : depth of water drained (mm)

Z_{req} : depth of water applied through irrigation (mm)

EC_i : electrical conductivity of irrigation water (dSm^{-1})

EC_e : electrical conductivity of soil saturated extract salinity level affecting the crop at the root zone ($dS\ m^{-1}$).

d) Soil moisture depletion prior to irrigation:

There are numerous techniques to evaluate soil moisture such as gravimetric samples, the neutron probe and the touch-and-feel method. In our study, capacitance soil moisture sensors (5TE, Decagon Devices, Inc., Pullman, WA) were installed to hourly measure soil moisture at five depths within the root zone (0.10, 0.20, 0.35, 0.50 and 0.60 m). Depending on root depth, we took readings prior to irrigation and, knowing the field capacity, we calculated soil moisture depletion taking the leaching fraction (as described above) into account.

e) Field slope

Field slope and length were measured by survey before the first irrigation.

f) Furrow spacing

Furrow spacing (*W*), the distance from center to center of two adjacent furrows, is a field dimension used primarily to convert volumes to depths ($D = Q / [LW]$), where L is the field length and Q is the water flow rate, and it is also an input that assists in the modeling of the infiltration process.

g) Furrow geometry

Measuring the cross-sectional geometry is very important for furrow evaluation. In our study we used a profilometer which provides data to plot furrow depth as a function of the lateral distance, and these data can then be used to obtain the geometric relationship between depths and areas. Simple power functions can be used to relate the cross-section area and the wetted perimeter with depth:

$$A = \sigma_1 Y^{\sigma_2}$$

where:

A: is the cross-sectional area (m^2).

Y: is the depth of the furrow.

σ_1, σ_2: are empirical parameters determined by the adjusted data.

By using a computer program, we numerically integrated the data to develop geometric relationship between the area and the depth.

2.1.2 Decision variables

Decision variables are those parameters or variables that a design engineer can manipulate to find the best irrigation performance for given or selected field parameters. The decision variables in surface irrigation are normally the field dimensions (length and width), the flow rate and the cut-off time.

a) Field dimensions

For furrows, there is only one field dimension: the furrow length. Furrow spacing is important only in the context of field parameters.

b) Flow rate

This variable is fundamental for the evaluation and it should be measured at the point where water enters the field. In our study, the flow was measured by using a long throated flume device (Fig. 2.2).

$$Q = 0.0004581\ (h + 4.56)^{2.0023}$$

where Q is the volume flow rate, in Ls^{-1}, h is the water head, in mm, when it enters the long throated flume.

c) The advance and recession of water across the field surface

This requires determining points (stakes) along the furrow. In order to determine the intake opportunity time, it is necessary to record the advance and recession data at each point.

d) Cutoff time

Cut-off time (Tco) is the amount of time that elapses since irrigation starts until it is cut off.

e) Cutback ratio and tailwater reuse ratio

In our fields the furrows were closed, so there was no cutback ratio.

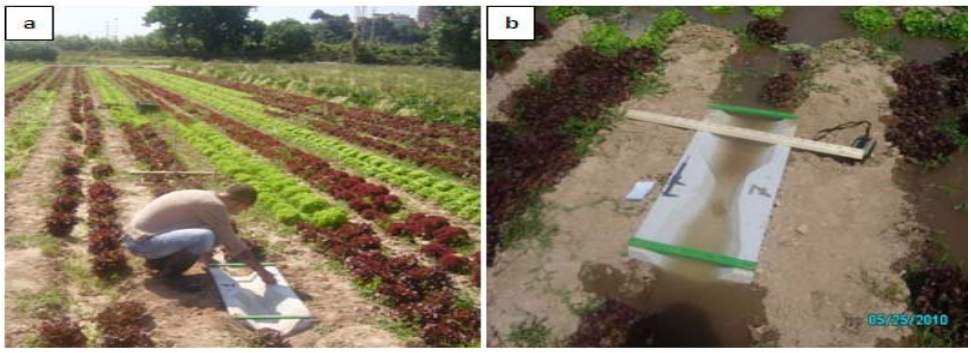

Fig. 2.2. Throated flume device, a) installation and b) measuring the inflow rate

2.1.3 Performances measurements

Many performances measurements have been suggested; we applied the traditional ones which are based on volume –balance principles. They are 1) Application Efficiency; 2) Storage Efficiency; 3) Application Uniformity; 4) Deep Percolation; and 5) Tailwater Ratio. We did not calculate Tailwater Ratio because in our study fields, the outlets were closed and we assumed that all the water entering the field did infiltrate.

a) Application Efficiency (*AE*)

It relates to the amount of water stored in the root zone to meet the crop water needs in relation to the water applied to the field:

$$AE = \frac{volume\ of\ water\ added\ to\ the\ root\ zone}{volume\ of\ water\ applied\ to\ the\ field}$$

Fig. 2.3 shows the distribution of applied water along the field length stemming. The differences in intake opportunity time produce applied depths that are non-uniformly distributed with a characteristic shape skewed toward the inlet end of the field.

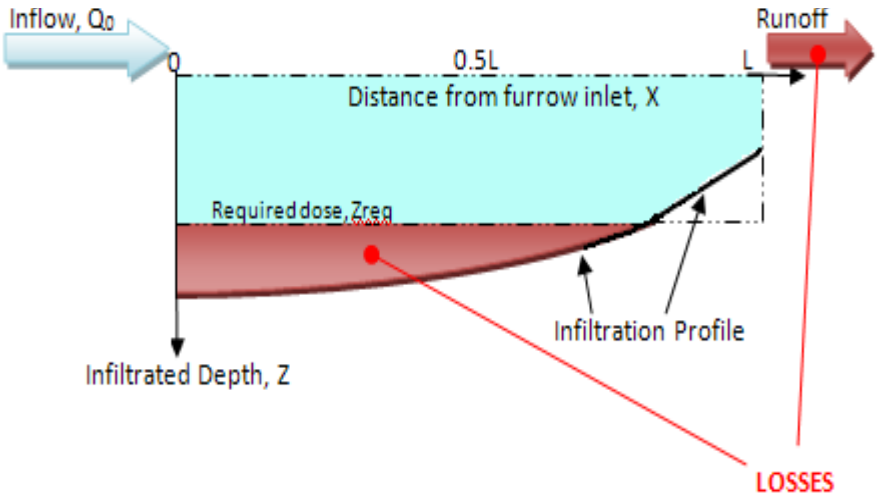

Fig. 2.3. Distribution of applied water along a surface irrigated field, also showing the depth required to refill the root zone.

b) Storage Efficiency (*SE*)

It relates to the volume of water stored in the root zone (defined by Z_{req}) to meet the crop water needs in relation to the total storage capacity of the root zone (Fig. 2.3).

$$SE = \frac{volume\ of\ water\ added\ to\ root\ zone\ storage}{potential\ soil\ moiture\ storage\ volume}$$

c) Application Uniformity (*DU*)

It is defined as the average infiltrated depth in the lowest quarter of the field, divided by the average infiltrated depth in the field (Merriam and Keller, 1978).

d) Deep Percolation (*DP*)

It relates to the water lost through drainage beyond the root zone:

$$DP = \frac{volume\ of\ deep\ percolation}{voluem\ of\ water\ applied\ to\ the\ \ field}$$

We used two models to evaluate furrow irrigation: Monserrat (1988) EVASUP model to get the parameters of Kostiakov (k and a) and to present the performance indicator, and WinSRFR model for simulation and to optimize the infiltration parameters. The WinSRFR model is an integrated hydraulic analysis application for surface irrigation systems that combines a simulation engine with tools for irrigation system evaluation, design, and operational analysis. WinSRFR is the successor of the irrigation modeling software developed over the past 20 years by the USDA Agricultural Research Service (Bautista et al., 2009).

3. Results and discussion

We evaluated the furrow irrigation system in two fields. Two tests for irrigation were done in Field 1 (one for a lettuce crop on April 2010-*IR1*- and another for an artichoke crop on May 2011-*IR11*), and one test was done in Field 2 (for a lettuce crop on April 2010-*IR2*). Tables 2.1, 2.2 and 2.3 show the inputs and outputs of the Monserrat (1988) EVASUP model to calculate the performance indicators. Z_{req} were estimated from field measurements of soil water contents before irrigation. The observed soil moisture deficits, *SMD* (mm), were assumed as the best estimates of Z_{req}. Moreover, the amount of water required to leach the salts was added to Z_{req}. For all irrigation events, the root zone depths for lettuce and artichoke crop were assumed to equal 0.20 and 0.35 m, respectively, based on phenological estimations of the development of lettuce and artichoke root mass. Tables 2.1 to 2.4 show the way to calculate Z_{req}. To measure the cross- sectional geometry we used a profilometer, which provides data to plot furrow depth as a function of the lateral distance; these data can then be used to get geometric relationships between depths and areas. With a computer program we numerically integrated the data to develop geometric relationships between the areas and the depths (Fig. 2.4).

Table 2.1. Threshold and zero yield salinity levels for four salinity rating

Salinity rating	Threshold salinity dS m^{-1}	Zero yield level dS m^{-1}
Sensitive	1.3	8.0
Moderately sensitive	3.0	16.0
Moderately tolerant	6.0	24.0
Tolerant	10.0	32.0

Adopted from Ayers and Westcot, 1985

Table 2.2. Crops in four salinity rating groups

Sensitive	Moderately sensitive	Moderately tolerant	Tolerant
Lettuce		Artichoke	

Adopted from Ayers and Westoct, 1985

Table 2. 3. Data to calculate Z_{req} (*IR1*: Field 1, lettuce. *IR11*: Field 1, artichoke. *IR2*: Field 2, artichoke)

Field	Crop	Field capacity θ_{fc} (m^3 m^{-3})	Soil water content before irrigation θ_i (m^3 m^{-3})	Rooting depth *RD* (mm)	Electrical conductivity of irrigation water (dS m^{-1})
IR1	Lettuce	0.35	0.25	200	1
IR11	Artichoke	0.35	0.24	350	1
IR2	Lettuce	0.30	0.24	200	2

Table 2. 4 Calculation of the depth of water required through irrigation Di

IR1: Field 1, lettuce	SMD = (0.35-0.25) 200 = 0.020 m $LF = D_d / Z_{req} = ECi$ / (5ECe - ECi) = 1 / (5 x 1.3-1) = 0.18 Z_{req}=SMD / (1-LF) = 0.020 / (1-0.18) = 0.024 m
IR11: Field 1, artichoke	SMD = (0.35-0.24) 350 = 0.0385 m $LF = D_d/Z_{req} = ECi$ / (5ECe - ECi) = 1 / (5 x 6-1) = 0.034 Z_{req}= SMD / (1-LF) = 0.0385 / (1-0.034) = 0.039 m
IR2: Field 2, lettuce	SMD = (0.30-0.24) 200 = 0.012 m $LF = D_d / Z_{req} = EC\ i$ / (5ECe - ECi) = 2 / (5 x 1.3-2) = 0.44 Z_{req}= SMD / (1-LF) = 0.012 / (1-0.44) = 0.021 m

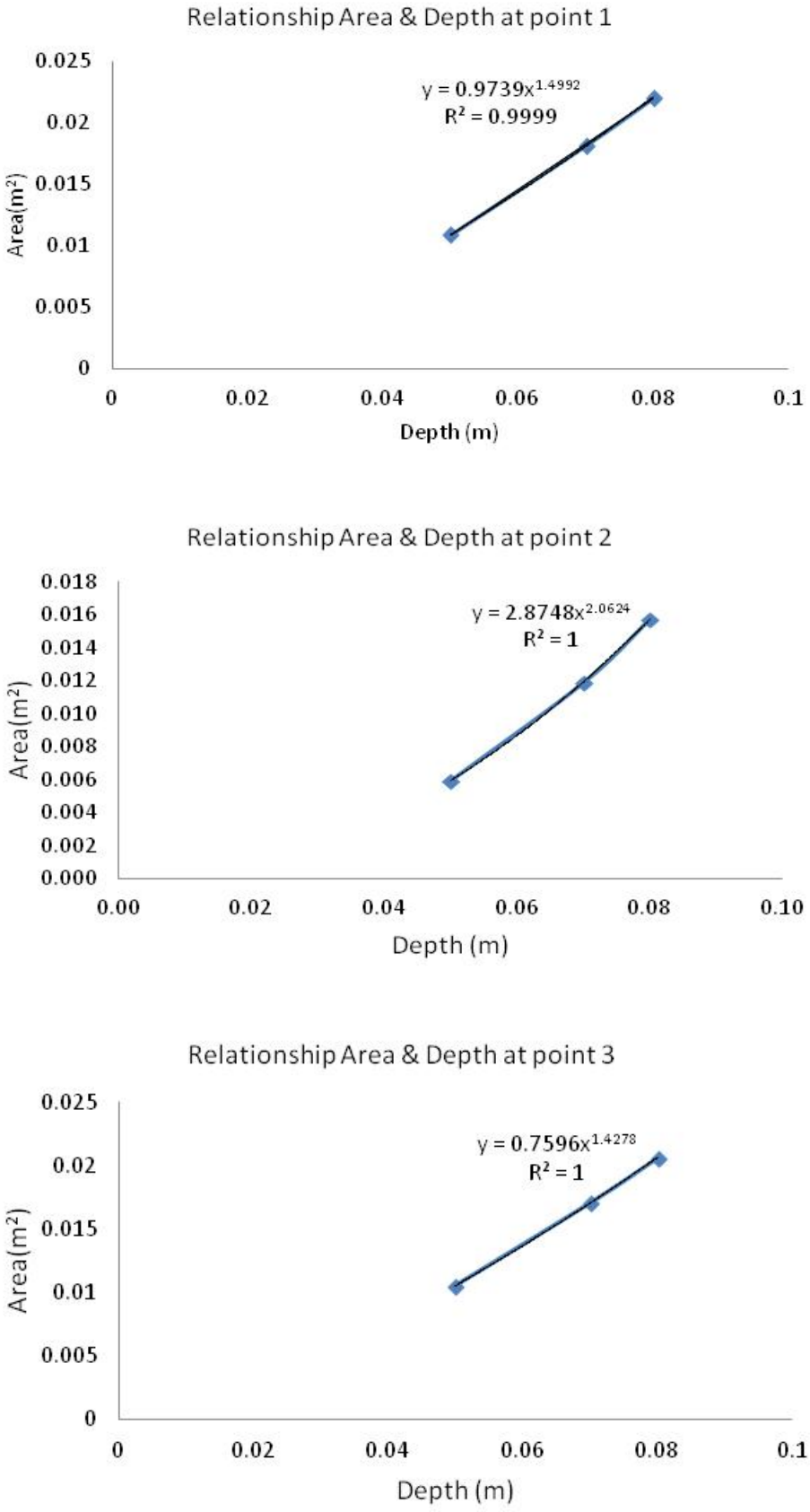

Fig. 2.4. Relationship between the area and the depths at three points in the furrow (for Field 1, IR1)

In the actual condition of irrigation in Field 1, the application efficiency was 52.45% for *IR1* and 32% for *IR11*. Tables 2.5, 2.6 and 2.7 present the low values of final mass balance error (MBE) which is the difference between measured and predicted infiltration volume relative functions and reflects the validation of the estimated infiltration function.

The application efficiency under *IR2* actual conditions was 38.12%. Tables 2.8 and 2.11 show scenarios simulated by the WinSRFR model for the lettuce crops in the two fields. In table 2.8, optimized discharge in *IR1* was evaluated in scenario 2, with a cut-off time of 12.3 min obtained without changing discharge compared to the actual conditions. In table 2.9 optimized discharge in *IR2* was evaluated in scenario 3, with a cut-off time of 10.3 min obtained without changing discharge compared to the actual conditions. For Field 1, Fig. 2.5 shows the actual status of *IR1*, and Fig. 2.6 shows its simulation. For Field 2, Fig. 2.7 shows the actual status of *IR2*, and Fig. 2.8 shows its simulation.

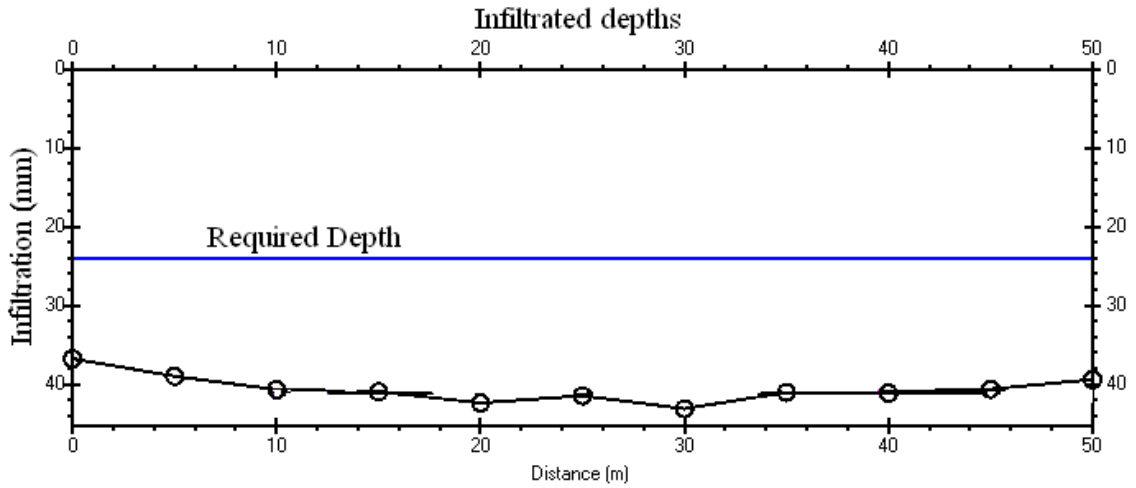

Fig. 2.5. Over irrigation status as applied under actual farm conditions (*IR1*)

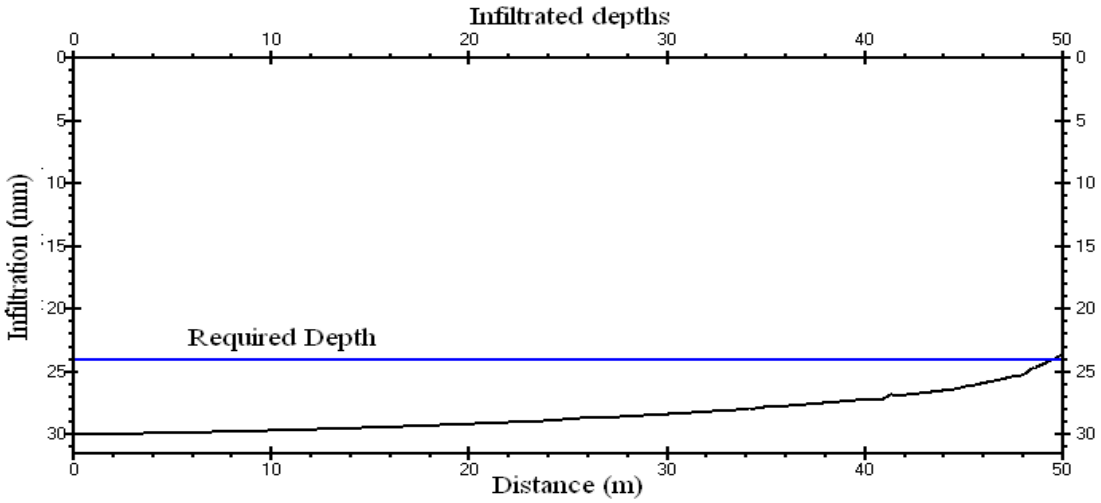

Fig. 2.6. Full irrigation status as applied with optimized cut-off time by the WinSRFR model (scenarios 2-IR1)

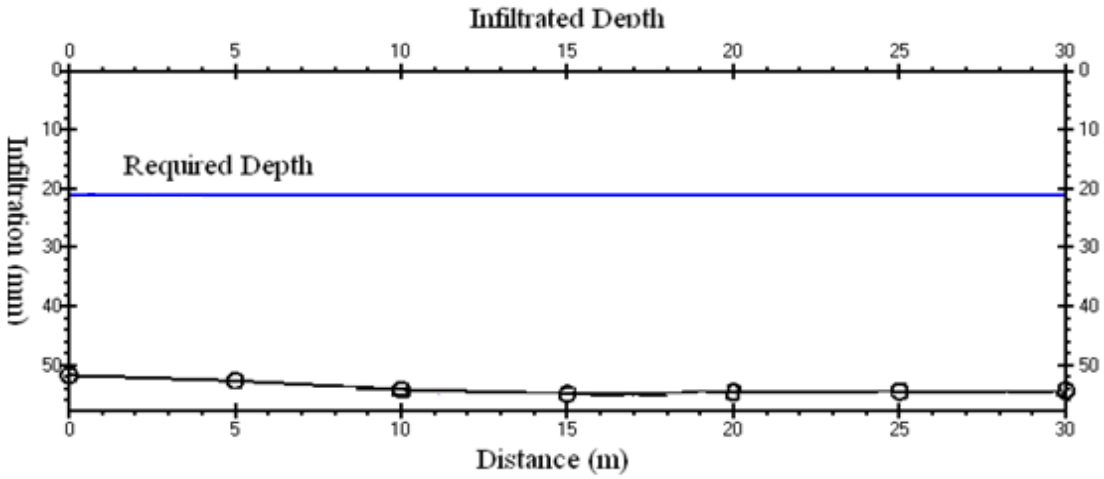

Fig. 2.7. Over irrigation status as applied under actual farml conditions (IR2)

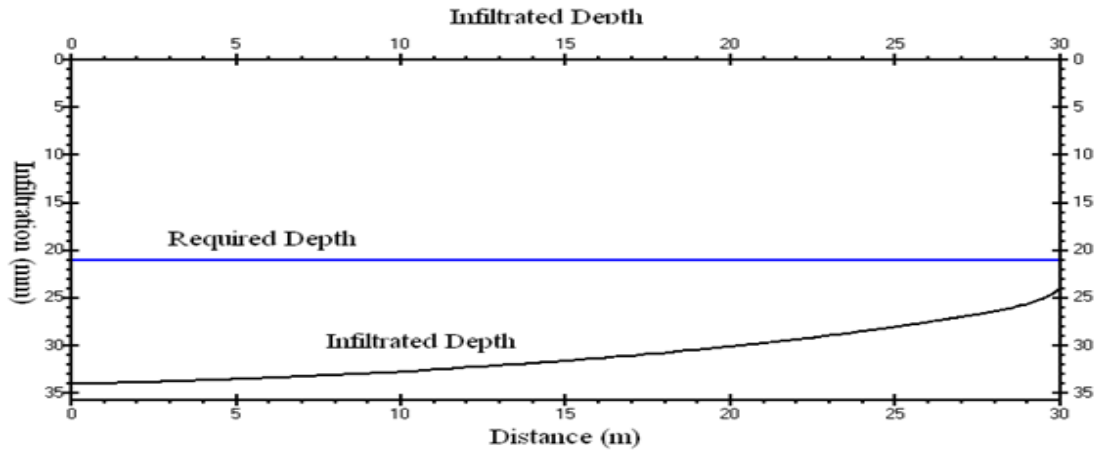

Fig. 2.8. Full irrigation status as applied with optimized cut-off time by the WinSRFR model (scenarios 3-*IR2*)

Table 2.5. Inputs and output of Monserrat (1988) EVASUP model for calculation of performance indicators (first field, lettuce crop- *IR1*)

Input data										
Distance between stakes = 5.000 m										
T1 time at instant 1						6.50 min				
T2 time at instant 2						15.00 min				
Q inflow rate						0.001290 m^3/seg/unit width				
Surface shape factor						0.770				
Subsurface shape factor						0.800				
Advance Time										
X (m)	5.00	10.00	15.00	20.00	25.00	30.00	35.00	40.00	45.00	50.00
T (min)	1.50	3.50	5.00	6.50	8.50	9.00	11.00	13.00	15.00	17.00
Parametors for Monsserat (1988) EVASUP model										
T = 6.50 min *advance time when water front reach 20 m stake*										
X = 0 m	H = 0.080 m									
X = 15.00 m	H = 0.060 m									
T = 15.00 min *advance time when water front reach 45 m stake*										
						Parameters of Relationship between the area and the depth at three points in the furrow ($A = \sigma_1 Y^{\sigma_2}$ *,Fig. 2.4)*				
X = 0 m	H = 0.110 m					σ_1 = 0.900			σ_2 = 1.470	
X = 15.00 m	H = 0.070 m					σ_1 = 2.8748			σ_2 = 2.0624	
X = 40.00 m	H = 0.020 m					σ_1 = 0.7596			σ_2 = 1.470	
Output										
Balance for the two instants										
T = 6.50 min										
VOL. Applied	0.503 m^3/unit width									
VOL. Superficial	0.286 m^3/unit width									
VOL. Infiltrated TEO.	0.217 m^3/unit width									
ERROR BAL. VOL. (%)	0.0758									
T = 15.00 min										
VOL. Applied	1.161 m^3/unit width									
VOL. Superficial	0.563 m^3/unit width									
VOL. Infiltrated TEO.	0.598 m^3/unit width									
ERROR BAL. VOL. (%)	.0000									
K	0.0037951 m^3/m.l./unit width /seg^A									
	90.04 cm^3 /cm/unit width /min^A									
	213.60 cm^3 /cm/unit width /H^A									
A	0.211									

Continued Table 2.5

Input data for calculating performance indicators					
Inflow rate			0.00129 m^3/seg/unit width		
Application time			20.00 min		
Required infiltrated volume			0.0161 m^3/m.l./unit width (the depth times the furrow spacing)		
Distance between furrows			0.75 m		
Infiltration parameters :					
K	0.00379/m.l./UA/S**A				
A	0.211				
C	0.00 m^3/m.l./UA/S				
D	0.00 m^3/m.l./UA				
X(m)	T. advance (min)	T. recession (min)			
.0	0.0	165			
5.0	1.50	220			
0.0	3.50	270			
5.0	5	280			
0.0	6.50	330			
5.0	8.50	300			
30.0	9	360			
5.0	11	290			
40.0	13	295			
45.0	15	280			
0.0	17	250			
Output					
Runoff flow =0 (No Cutback)					
Performance indicators (%)					
Application Uniformity = 97.64					
				m^3/ unit depth	m^3/unit width /m.l.
Application Efficiency		52.05 %	V. Applied	1.548	0.031
Deep Percolation		47.92 %	V. Percolated	0.742	0.016
Runoff		0.00 %			
Storage Efficiency		100.00 %	V. Runoff	0.000	0.000
Volum balnace error		5.20 %	V. Infiltrated	1.467	0.031

Table 2.6. Inputs and outputs of Monserrat (1988) EVASUP model for calculation of performance indicators (first field, artichoke crop-*IR11*)

Input data										
Distance between stakes					5.00 m					
T1 time at instant 1					12.00 min					
T2 time at instant 2					17.50 min					
Q inflow rate					0.002230 m^3/seg/unit width					
Surface shape factor					0.77					
Subsurface shape factor					0.80					
Time advance										
X (m)	5.00	10.00	15.00	20.00	25.00	30.00	35.00	40.00	45.00	50.00
T (min)	4.00	7.50	9.50	12.00	15.00	17.50	19.50	22.00	25.00	29.50
Parametors for Monsserat (1988) EVASUP model										
T = 12.00 min *advance time when water front reach 20 m stake*										
X = 0 m	H = 0.089 m									
X = 15.00 m	H = 0.036 m									
T = 17.50 min *advance time when water front reach 30 m stake*										
					Parameters of Relationship between the area and the depth at three points in the furrow ($A = \sigma_1 Y^{\sigma_2}$, *Fig2. 4.)*					
X = 0 m	H = 0.089 m				$\sigma_1 = 1.110$			$\sigma_2 = 1.800$		
X = 15.00 m	H = 0.030 m				$\sigma_1 = 0.690$			$\sigma_2 = 1.400$		
X = 25.00 m	H = 0.020 m				$\sigma_1 = 0.620$			$\sigma_2 = 1.800$		
Output										
Balance for the two instants										
T = 12.00 min										
VOL. Applied	1.60 m^3/unit width									
VOL. Superficial	0.18 m^3/unit width									
VOL. Infiltrated TEO.	1.40 m^3/unit width									
ERROR BAL. VOL. (%)	1.2138									
T = 17.50										
VOL. Applied	2.34 m^3/unit width									
VOL. Superficial	0.19 m^3/unit width									
VOL. Infiltrated TEO.	2.14 m^3/unit width									
ERROR BAL. VOL. (%)	.0000									
Empirical constants for Kostiakov function										
K	0.0736203 m^3/m.l./unit width /seg^A									
A	0.001									

Continued Table 2.6

Input data for calculating performance indicators				
Inflow rate			0.00223 m^3/seg/unit width	
Application time			30.00 min	
Required infiltrated volume			0.0320M3/m.l./unit width (the depth times the furrow spacing	
Distance between furrows			1.20 m	
Infiltration parameters :				
K	0.07362030 m^3/m.l./ unit width /s^A			
A	0.001			
C	0.00000000000 m^3/m.l./ unit width /s			
D	0.00000000 m^3/m.l./ unit width			
X(m)	T. advance (min)	T. recession (min)		
0.0	0.0	160.0		
5.0	4.0	219.0		
10.0	7.5	270.0		
15.0	9.5	278.0		
20.0	12.0	332.0		
25.0	15.0	285.0		
30.0	17.5	357.0		
35.0	19.5	262.0		
40.0	22.0	256.0		
45.0	25.0	281.0		
50.0	29.5	343.0		
Runoff flow =0 (No Cutback)				
output				
Performance indicators (%)				
Application Uniformity = 99.99				
			m^3/unit depth	m^3/unit width /m.l.
Application Efficiency	31.39 %	V. Applied	4.014	0.080
Deep Percolation	68.61 %	V. Percolated	2.754	0.055
Runoff	0.00 %			
Storage Efficiency		V. Runoff	0.000	0.000
volume balance error	3 %	V. Infiltrated	3.888	0.080

Table 2.7. Inputs and outputs of Monserrat (1988) EVASUP model for calculation of performance indicators (first field, artichoke crop-*IR11*)

Input data										
Distance between stakes	5.00 m									
T1 time at instant 1	12.00 min									
T2 time at instant 2	17.50 min									
Q inflow rate	0.00223 m^3/seg/unit width									
Surface shape factor	0.770									
Subsurface shape factor	0.800									
Time advance										
X (m.)	5.00	10.00	15.00	20.00	25.00	30.00	35.00	40.00	45.00	50.00
T (min)	4.00	7.50	9.50	12.00	15.00	17.50	19.50	22.00	25.00	29.50

Parameters for the Monsserat (1988) EVASUP model			
T = 12.00 min *advance time when water front reaches the 20 m stake*			
X = 0 m	H = 0.089 m		
X = 15.00 m	H = 0.036 m		
T = 17.50 min. *advance time when water front reaches the 30 m stake*			
		Parameters of Relationship between the area and the depth at three points in the furrow ($A = \sigma_1 Y^{\sigma_2}$, *Fig. 2.4.)*	
X = 0 m	H = 0.089 m	σ_1 = 1.110	σ_2 = 1.800
X = 15.00 m	H = 0.030 m	σ_1 = 0.690	σ_2 = 1.400
X = 25.00 m	H = 0.020 m	σ_1 = 0.620	σ_2 = 1.800

output	
Balance for the two instants	
T = 12.00 min	
VOL. Applied	1.60 m^3/unit width
VOL. Superficial	0.18 m^3/unit width
VOL. Infiltrated TEO.	1.40 m^3/unit width
ERROR BAL. VOL. (%)	1.2138
T = 17.50 min	
VOL. Applied	2.34 m^3/unit width
VOL. Superficial	0.19 m^3/unit width
VOL. Infiltrated TEO.	2.14 m^3/unit width
ERROR BAL. VOL. (%)	.0000
Empirical constants for the Kostiakov function	
K	0.0736203 m^3/m.l./unit width /seg^A
	739.22 cm^3/cm/unit width /min^A
	742.26 cm^3/cm/unit width /h^A
A	0.251

Continued Table.2.7

Input data for calculating performance indicators					
Inflow rate		0.00120 m^3/seg/unit width			
Application time		18.00 min			
Required infiltrated volume		0.0165 m3/m.l./unit width (the depth times the furrow spacing			
Distance between furrows		0.90 m			
Infiltration parameters :					
K	0.0048 m^3/m.l./ unit width /s^A				
A	0.251				
C	0.00 m^3/m.l./ unit width /s				
D	0.00 m^3/m.l./ unit width				
X(m)	T. advance (min)	T. recession (min)			
0.0	0.0	120.0			
5.0	4.0	133.0			
10.0	6.0	150.0			
15.0	8.0	160.0			
20.0	12.0	161.0			
25.0	14.5	162.0			
30.0	17.0	163.0			
Runoff flow =0 (No Cutback)					
Output					
Performance indicators (%)					
Application Uniformity = 98.56					
				m^3/unit depth	m^3/unit width /m.l.
Application Efficiency		38.12 %	V. Applied	1.296	0.043
Deep Percolation		61.87 %	V. Percolated	0.756	0.025
Runoff		0.00 %			
			V. Runoff	0.000	0.000
Storage Efficiency		100.00 %			
Volume balance error		1.4 %	V. Infiltrated	1.277	0.043

Table 2.8. Results from Field 1 (lettuce crop- IR1) using the WinSRFR model (performances measures)

	Qin (L/s)	tco (min)	Applied water (L)	DU (%)	AE (%)	DP (%)
actual conditions	1.29	20	1548	97.64	52.05	61.87
Scenario 1	1.29	15	1161	0.90	65	35
Scenario 2 (optimal cut- off time)	1,29	14	1083.6	85	84	16
Scenario 3	1.29	11	851.4	*Water front no reach to lower end*		
Scenario 4	0.95	20	1140	0.96	66	34
Scenario 5	0.90	20	1140	0.94	69	31
Scenario 6	0.80	20	960	*Water front no reach to lower end*		

Table 2.9. Results from Field 2 (lettuce crop- IR2) using the WinSRFR model (performance measures)

	Qin (L/s)	tco (min)	Applied water (L)	DU (%)	AE (%)	DP (%)
Actual conditions	1.2	18	1296	98.56	38.12	58.33
Scenario 1	1.2	15	1080	97	44	57
Scenario 2	1.2	12	864	93	56	45
Scenario 3 (optimal cut-off time)	1.2	10.3	741,6	80	68	32
Scenario 4	0.98	18	1058,4	96	45	56
Scenario 5	0.9	18	972	88	46.67	51
Scenario 6	0.75	18	810	81	59	41
Scenario 7	0.70	18	756	*Water front no reach to lower end*		

Farmers in the Llobregat Delta area generally maintain irrigation after water has reached the end of the furrows to ensure that soil water at the root zone is fully recharged. However, farmers generally do not know the period of time required to compensate soil water deficit. Irrigation controllers or timers are not widely used, and the irrigation is often maintained until it is convenient to manually switch it off. Thus, under commercial conditions, a significant component of the applied irrigation water may be lost as an excessive deep percolation (Tables 2.8 and 2.9). For the specific irrigation example presented in Table 2.8 and Fig. 6 (Field 1, *IR1*), 30% of the applied water would have been saved if irrigation had been stopped as soon as the soil water deficit was fully compensated. For Field 2 (*IR2*), 43% of the applied water would have

been saved if irrigation had been stopped as soon as soil water deficit was fully compensated, as presented in table 2.9 and Fig 2.8. Moreover, the area of the individual furrow in Field 1 (*IR1*) was 50 m^2 and the water supplied under actual conditions was 1548 L (table 2.8), while the individual area in Field 2 (*IR2*) was 27 m^2 and the supplied water was 1295 L (table 2.9). Hence, Field 2**,** *IR2*, used almost the same amount of water as Field 1*, IR1*, with half of its area. This may have been expected since water for irrigation had an electrical conductivity of 2 $dS \cdot m^{-1}$ in Field 2 and 1 dSm^{-1} in Field 1, and the farmer in Field 2 applied more water to leach the salts from the root zone. Moreover, by applying the winSRFR and EVASUP models we have obtained the same performance measures.

4. Conclusion

The application efficiency of furrow irrigation for lettuce and artichoke production was studied in the Llobregat Delta. Average irrigation efficiencies in this area were found to vary between 31 and 52%.

30% and 43% of the applied water would have been saved in Field 1 and Field 2 respectively, if irrigation was stopped as soon as the soil water deficit was fully compensated, taking into account the amount of water needed for salt leaching

More water was applied in Field 2 than in Field 1 due to poor water quality. Differences in efficiency were found to be directly related to farm design and specific management practices. Application efficiency was found to increase with decreasing cut-off time. These results indicate that significant improvements in irrigation efficiency could be achieved through the adoption of design and management practices that are appropriate to the farm's environmental and management constraints.

5. References

Ayers, R. S., Westcot, D. W., 1985. Water quality for agriculture. FAO Irrigation and Drianage. Paper 29, Rev. I. FAO, Rome, Italy.

Bautista, E., Clemmens, A.J., Strelkoff, T.S., Schlegel, J., 2009. Modern analysis of surface irrigation systems with WinSRFR. Agricultural Water Management 96: 1146–1154.

Burt, CM, Robb, G. A., Hanon, A. 1982. Rapid evaluation of furrow irrigation efficiencies, ASE Paper No, 82-2537. Presented at the 1982 Winter Meeting of ASAE, Chicago, III

Burt, C.M., Robb, G.A., Hanon, A., 1982. Rapid evaluation of furrow irrigation efficiency. American Society of Agricultural Engineers Paper No, 82-2537.

Elliott, R. L., Walker, W. R., 1982. Field evaluation of furrow infiltration and advance function. Transactions of the American Society of Agricultural Engineers 396–400.

Elliott, R. L., Eisenhauer, D. E., 1983. Volume-balance techniques for measuring infiltration in surface irrigation, American Society of Agricultural Engineers Paper Non 83-2520, Presented at the 1983 Winter Meeting of the ASAE Chicago III.

Guardo, M., 1988. Kinematic model for designing level basins. Doctoral dissertation, Colorado State University, Fort Collins, Colorado.

Guardo, M., Oad, R., Podmore, T. H., 2000. Comparisoin of zero-inertia and volume balance advance-infiltration models. Journal of Hydraulic Engineering 126: 457-465.

Jurriens, M., Zerihun, D., Boonstra J., Feyen, J., 2001. SURDEV: Surface Irrigation Software, Design, Operation, and Evaluation of Basin, Border, and Furrow Irrigation. International Institute for Land Reclamation and Improvement, ILRI, Wageningen.

Merriam, J. L., Keller,J.,1978. Farm Irrigation System Evaluation: A Guide for Management. Department of Agricultural and Irrigation Engineering, Utah State University, Logan, Utah.

Monserrat, J. 1988. Estudio y evaluación de un modelo para la simulación del riego por surcos. Final Project. E. T. S.I .A. University of Lleida.

Smerdon, E.T., Blair, A.W., Reddell, D.L., 1988. Infiltration from irrigation advance: I theory. II Experimental . Journal of Irrigation and Drainage Engineering 114, nº1.

Walker, W. R., Skogerboe, G. V., 1987. Surface irrigation, theory and practice. Prentice-Hall, Englewood Cliffs, N.J.

Wallender, W. W., Rayej, M., 1985. Zero inertia surge model with wet-dry advance. Transactions of the American Society of Agricultural Engineers, 28: 1530-1534.

When modeling nature within the context of the scientific method, one should always employ a mathematical model that is realistically designed for capturing the key characteristics of the physical process being examined. One should always strive to design a mathematical model to fit the physical problem and never try to distort the physical process to fit a given mathematical model."

KEITH W. HIPEL and A. IAN MCLEOD

Developments in Water Science: Time Series Modeling of Water Resource and Environmental Systems (1994), 1053

".

3. Soil water: Time series outlier and intervention analysis: irrigation management influences on soil water content in silty loam soil

---

This study was published in (Agricultural Water Management by Elsevier and cited as:

Aljoumani, B., Sànchez-Espigares, J.A., Cañameras, N., Josa, R., Monserrat, J., 2012. Time series outlier and intervention analysis: irrigation management influences on soil water content in silty loam soil. Agricultural Water Management 111, 105-114.

3. Soil water flow. Time series outlier and intervention analysis: irrigation management influences on soil water content in silty loam soil

Table of contents

Abstract

Understanding the field soil water regime is fundamental in scheduling irrigation as well as for monitoring water flow and solute transport. This study was carried out on variable interval irrigation and used time series analysis techniques to predict the soil water content at the interested depth by measuring one single depth in order to precisely determine the next irrigation time and its effect on soil water content at the interested depth. Volumetric water content of silty loam soil in Barcelona was measured in situ with capacitance soil moisture sensors at five depths within the root zone for a horticultural crop during its life cycle in 2010. The time series consisted of hourly measurements of soil water content and was transformed to a stationary situation. Subsequently, the transformed data were used to conduct analyses in the time domain in order to obtain the parameters of a seasonal autoregressive integrated moving average (ARIMA) model. In the case of variable interval irrigation, predicting the soil water content time series cannot be properly explained by the ARIMA model and its underlying normality assumption. By completing the ARIMA model with intervention analysis and outlier detection, the prediction of soil water content in variable interval irrigation can be made. The transfer function models were then used to predict water contents at depths of interest (0.20, 0.35, 0.50 and 0.60 m depths) as well as the average water content W_{AVG} in the top 0.60 m soil profile by measuring water content at 0.10 m depth. As a result, the predictions were logical. Also, the next irrigation time and its effect on soil water content at the depth of interest were correctly estimated. To confirm results of the models, the experiment was repeated in 2011, and the predicted and observed values agree reasonably well.

Keywords: Soil volumetric water content; Autoregressive integrated moving average (ARIMA); Outlier detection; Transfer function model.

1. Introduction

Surface soil water is the water that is in the upper 0.10 m of soil, whereas root zone soil water is the water that is available to plants, which is generally considered to be in the upper 2 m of soil (Wang et al. 2009). Soil water has been studied in many soil science fields due to its great influences in the most of soil components as well as in the atmospheric conditions. Soil water in the top 2 m soil profile is considered the key variable in numerous environmental studies (Walker, 1999), including microbial, geological, meteorology, hydrology, agriculture and climate change (Topp et al., 1980; Jackson et al., 1999; Fast and McCorcle, 1991; Engman, 1992; Entekhabi et al., 1993; Betts et al., 1994; Saha, 1995).

Due to the development of new techniques for examining the structure and metabolic activities of microbial communities, many microbial studies showed that the changes in temperature and soil water content conditions along topographic gradient have been linked to changes in microbial community composition (Morris and Boerner, 1999; Carletti et al., 2009) or microbial metabolic diversity (Rogers and Tate, 2001). Soil microbial basal respiration was highly correlated with mean annual precipitation when comparing 24 sites along a precipitation transect in semi-arid and arid southern Africa (Wichern and Joergensen, 2009). In native Austrian forests, Hackl et al. (2005) found that microbial community structure was most closely correlated with soil water availability in azonal forests (which exhibit extreme site conditions). Chen et al. (2007) showed in a greenhouse pot experiment that total plant biomass of white clover and ryegrass increased with increasing soil moisture contents.

In irrigation studies understanding the field soil water regime is fundamental in scheduling irrigation. King et al. (2001) developed a device to aid in irrigation scheduling by visually indicating current soil water status relative to an upper and lower set point, two study fields, one with and one without soil water status indicators, Collectively, farm managers applied 7% (2.9 cm) less water to fields with the soil water status indicators than comparison fields. Average water application was significantly less (P=0.04) for fields with soil water status indicators.

In geological studies, soil water content plays a key role on the aggregate stability and determines the relationship between the variation in soil stability and soil physical properties (bulk density, texture, organic carbon, pore sizes distribution and saturated hydraulic conductivity), stable aggregates reduce detachment by raindrop and transport by overland flow and, also, reduce the formation of surface crusts and seals. In arid and semi-arid area where the soil water content at the onset of rain may be temporally and spatially variable so the antecedent soil water content in the field plays a key role in the rainfall-runoff relationship and soil loss (Puigdefabregas et al., 1992; Lopez-Bermudez et al., 1991). Martinez-Mena (1998) studied the effect of three soil water contents (close to saturation, field capacity and air-dry) on the aggregate stability for soils from arid and semi-arid area of southeast Spain, he found that the aggregate stability for wetter conditions was higher than for the air-dry conditions for 85% of the samples tested.

In hydrological and climate change studies, large-scale soil moisture dynamics and its verification are essential to improve the predictive capability of coupled hydrologic-meteorological models (Jackson et al. 1999).

Therefore, from what is mentioned above, it is important to accurately monitor and estimate spatial and temporal variations of soil moisture.

1.1. Measuring soil water content

Soil water content can be determined by direct or indirect methods. Direct method is referred to as the gravimetric methods, it is usually requires oven drying of a known volume of soil at 105 ºC and determining the weight loss (Walker et al. 2004). Indirect methods measure some physical or chemical properties of a soil which is correlated to the soil water content (Arguedas-Rodriquez, 2009), these properties include dielectric constant (relative permittivity), electrical conductivity, heat capacity, hydrogen content and magnetic susceptibility. These techniques include time domain reflectometry (TDR), frequency domain reflectometry (FDR), time domain transmission (TDT), amplitude domain refelectomerty (ADR), phase transmission and ground penetrating radar (GPR). They also include capacitance sensors, radar scatterometry or active microwave, passive microwave, electromagnetic induction (EMI), neutron

thermalization, nuclear magnetic resonance, and gamma ray attention (Dane and Topp, 2002).

Direct method is not appropriate for understanding of the spatial and temporal behavior of soil moisture. Due to the heterogeneity of soil type, land use and topography, soil moisture may change considerably in space and time. Among indirect methods, we choose for our study capacitance sensors, which are relatively cheap, rugged and portable.

Moreover, it is not sufficient to know simply the amount of water in the soil, because depending on conditions, given amount of water might be held so tightly by the force fields of a soil that it is essentially immobile. The energy states characterises the effects of forces exerted on a soil water by its surroundings and hence express the water`s availability.

1.2. Soil water flow

The traditional approach to modelling soil water flow is based on deterministic models using Richards' equation (Bresler and Dagan, 1981, 1983a, 1983b; Butters and Jury, 1989; Dagan and Bresler, 1983; Destouni and Cvetkovic, 1991; Schulin et al., 1987; Shani et al., 2007; Wagenet and Hutson, 1989; Wildenschild and Jensen, 1999). Many studies have indicated that the average moisture profile in a heterogeneous field could not be correctly predicted by the classical differential equations using effective soil properties (Alessi et al., 1992; Wu et al., 1996).

Due to soil profile heterogeneity, some experimenters have found it more desirable to use stochastic models rather than constant values in describing the future evolution of soil water, assuming that water transport has random variables (Comegna et al,. 2010; El-Kadi, 1987; Freeze, 1975; Greenholtz et al., 1988; Indelman et al., 1998; Makkawi, 2004; Sarangi et al., 2006).

A stochastic process amounts to a sequence of random variables known as a time series. The time series method has been applied in several agricultural and hydrologic studies. Gupta and Chauhan (1986) and Marino et al. (1993) used time series modeling

approaches, respectively, to study the stochastic nature of weekly irrigation that paddy crops required in India, and to forecast the monthly grass reference crop evapotranspiration (ET_0) values. A series of papers by Raghuwanshi and Wallender (1996, 1997, 1998, 1999) began by developing a seasonal irrigation model, then applied autocorrelation and partial autocorrelation to the standardized ET_0, and finally built up the autoregressive moving average ARMA (1,1) model. The same model was used to predict both irrigation schedules and optimum furrow irrigation designs (inflow rate and cut-off time).

Many researchers found that soil water content is highly correlated to different depths and they developed models to evaluate irrigation water management and to demonstrate the use of irrigation scheduling tools (Jones et al., 2003; Panda et al., 2004). Wu et al. (1997) used squared coherency, cross-amplitude and cross-correlation analysis to study the relationship between water content that was measured hourly at various depths of the soil profile (0.25, 0.50, 0.75 and 1 m) over 55 days. They later developed models that could predict water content at deeper depths from water content at a superficial depth. Zou et al. (2010) worked on silt loam soil profile data, collected monthly from 2001 to 2006, to compare two mathematical models: the back propagation neural network (BPNN) model and the autoregressive integrated moving average (ARIMA) model. The objective was to predict both the average water content in the top 1 meter profile from water content measured at 0.60 m depth, and the average salt content measured at various depths of the soil profile (0.10, 0.20 and 0.45 m).

Previous models assumed that the spacing between irrigation events is fixed; therefore, ARIMA models can be applied for predicting soil water content because ARIMA models save the behaviour of past observations in order to make the prediction. For example, if the farmer irrigates the field every ten days, the identified ARIMA model on the field data set for soil water content would expect an increase in the soil water content on the tenth day after the previous irrigation event. In the case of variable interval irrigation, ARIMA models do not have the ability to make an effective prediction if the farmer in the above example should decide to reduce the spacing between irrigation events to 9 days. In that case, the previous identified ARIMA model could not thoroughly predict the future behaviour of the soil; it would give an increase in soil water content after ten days and not after nine days. To allow ARIMA models to

work on variable interval irrigation systems and be able to detect new outliers, it is necessary to complement the ARIMA model with intervention analysis models and outlier detection (Wei, 1989).

Our study was carried out on variable interval irrigation and used time series analysis techniques with two objectives: to predict the soil water content of an interested depth by measuring one single depth, and to evaluate the effect of an irrigation event on the soil water content. An important distinction is made between outliers and intervention variables in the time series of soil water content. In case there is a priori information about a special event that may have caused abnormal observations (the irrigation event, in our case), the effect of the irrigation event should be captured through intervention analysis. An outlier, on the other hand, represents anomalies in the observations for which there is no a priori information on the date of its occurrence or on the dynamic pattern of its effect (i.e. precipitation event). We enabled the ARIMA model to be applied on variable interval irrigation and to examine the effectiveness of the irrigation event. This could be achieved by:

1) Detecting the outliers and removing them; thus, soil water forecasts will undergo a downward trend because no effect from irrigation events (outlier) will appear,

2) Evaluating the effect of the intervention (irrigation event) and including it in the model; thus, the soil water forecasts increase at the moment of irrigation, and this increase depends on the weight of the irrigation coefficient. The benefit of this complementary analysis comes from the probability of a well-realized irrigation schedule that is of a short duration (one day or within hours); i.e., the next irrigation event will be determined when the prediction for soil water content is below the field capacity.

There are two advantages to including the time series outlier and intervention analysis in the ARIMA model for describing soil water fluctuations:

First, by using intervention analysis, the input series will be in the form of a simple pulse or step indicator function to indicate the presence or absence of the irrigation event. So the effectiveness of the irrigation event can be included in the ARIMA model in order to improve the efficiency of irrigation scheduling. The main purpose of outlier

correction is to modify the data in such a way that the normality hypothesis of the ARIMA model can be accepted.

The second advantage is that, by including outlier analysis in the ARIMA model, we reduce the residual variance of the model, which then becomes more precise.

The objective of this study was to evaluate soil water content in the field regime by using time series analysis techniques. The specific objectives were:

1) To study the autocorrelation and partial correlation function for soil water content measured at a shallower depth as well as the cross-correlation function between soil water content at a shallower depth and various greater depths, including average soil water content W_{AVG} in the top 0.60 m profile;

2) To develop models for predicting the soil water content at various greater depths and water storage in the soil profile from a single shallower depth; and

3) To use outlier and intervention analysis to examine the effectiveness of the irrigation event in the soil water profile.

2. Materials and methods

2.1. Experiment

The experiment was carried out for 55 days, starting on 23 April 2010 in the Agricultural Park of Baix Llobregat, 5 km south of Barcelona, Spain. A field was planted with lettuce (*Lactuca sativa*) and irrigated by a furrow system; the experimental area was 275 m^2 (55 m x 5 m); four irrigation events were applied; each irrigation dose was almost 26 L m^{-2}; and the application time ranged between 20-26 minutes. The site had fairly uniform, silty loam with a bulk density ranging between 1.4 and 1.5 g cm^{-3} to a depth of 0.75 m and the water table was 4 m below the soil surface. In the test furrow, the water content distribution of the soil profile was measured with capacitance soil moisture sensors (5TE, Decagon Devices, Inc., Pullman, WA). The installation depths were at 0.10, 0.20, 0.35, 0.50 and 0.60 m from the soil surface (Fig 3.1). The study focused on the root zone. A total of 1318 observations were used to estimate the models, of which 659 observations were used to validate its forecast. To confirm the results of the models, the experiment was repeated in 2011 with 1199 observations. The

same transfer function models obtained from the 2010 set of data were applied in the 2011 one to predict the soil water content at deeper depths from a single shallower depth.

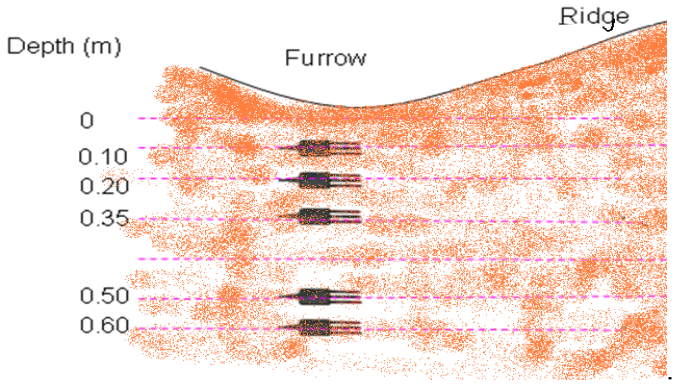

Fig.3.1. Chart shows sensors distribution in the top 0.60 m soil profile

2.2. Capacitance sensor

Capacitance senor used electromagnetic (EM) techniques for soil water content estimation (Blonquist et al., 2005). The capacitance technique determines the dielectric permittivity of a medium by measuring the charge time of a capacitor which uses that medium as a dielectric. Capacitance techniques introduced into agriculture by smith Rose (1933; cited by Dane and Topp, 2002). One of the first workers to use a high frequency capacitance technique for soil water content determination was Thomas (1966). 5TE probe model (Decagon Devices, Inc., Pullman, WA) was used in this study, it is an electromagnetic sensor which measures the dielectric permittivity of soil and related it with the soil water content by an empirical relationship, since EM signal properties strongly depend on volumetric water content that stems from the high permittivity of water ($\varepsilon_w = 80$) compared to mineral soil solids ($\varepsilon_s = 2\text{-}9$), and air ($\varepsilon_a = 1$). The equivalent circuit diagram of the 5TE probe is illustrated in Fig. 3.2. The 5TE sensor circuitry measures the dielectric permittivity of the material surrounding a thin, fiberglass enclosed probe. The circuit board includes an electronic oscillator that generates a repetitive square waveform with a characteristic frequency (70 MHz). The total sensor capacitance is then made up of the capacitance of medium C and the capacitance Cs due to stray electric fields (Kelleners et al., 2004). Soil permittivity is

determined by measuring the relationship between the time, t, it takes to charge a capacitor from a starting voltage (Vi), to a voltage (V) with an applied voltage (Vf) of capacitor which uses the soil as a dielectric. If the resistance R, Vf and Vi are held constant, then the charge time of the capacitor, t, is related to the capacitance according to:

$$t = -RC \ln\left(\frac{v - v_f + v_i}{v_i - v_f}\right) \quad (1)$$

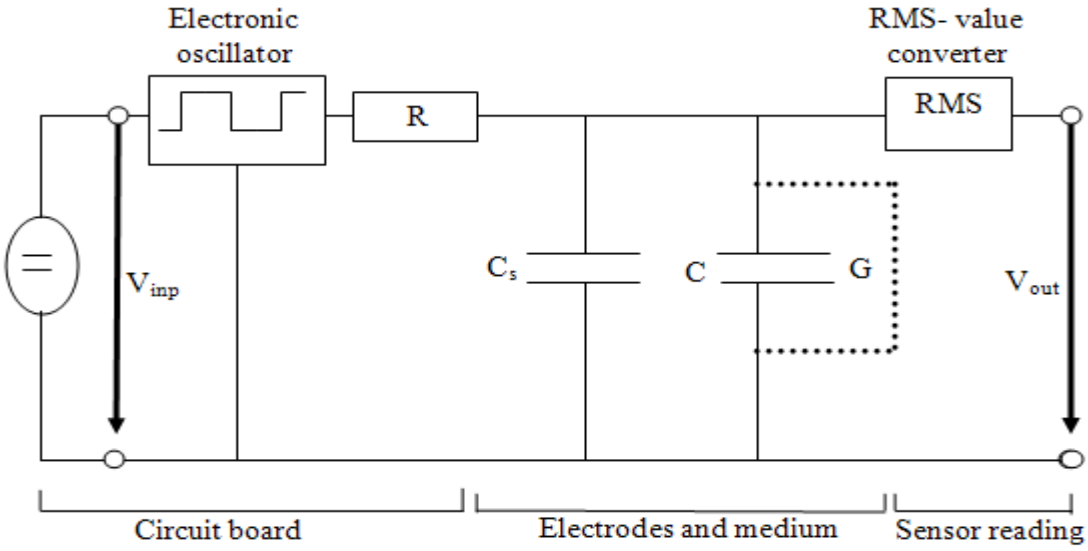

Fig. 3.2. Equivalent circuit diagram of a capacitance senor where R is a resistor, C is the capacitance of the medium, Cs is the stray capacitance, G is the energy loss due to relaxation and ionic conductivity and Vinp and Vout are the supply and senor reading voltage, respectively (From Bogena et al., 2007).

The capacitance is a function of the dielectric permittivity (ε) of the medium and a geometrical factor g, it can be calculated by:

$$C = g\varepsilon \quad (2)$$

The factor $g = \frac{A}{S}$

where A is the area of the plates and S is the separation between the plates. By assuming that the charge time of the capacitor is a linear function of the dielectric permittivity of the surrounding medium, ε can be calculated as follows:

$$\frac{1}{\varepsilon} = \frac{1}{t}\left[Rg \ln\left(\frac{v - v_f + v_i}{v_i - v_f} \right) \right] \quad (3)$$

A graphic representation from a capacitance senor reading is shown in Fig. 3.3 (Bogena et al., 2007), where it can be seen how the water content alters the time of the pulse length ΔT with fixed supply voltage V_t. Thus, high water content will result in a longer pulse length time, because the sensor output is directly related to the average voltage over the period of change in pulse length time (Bogena et al., 2007).

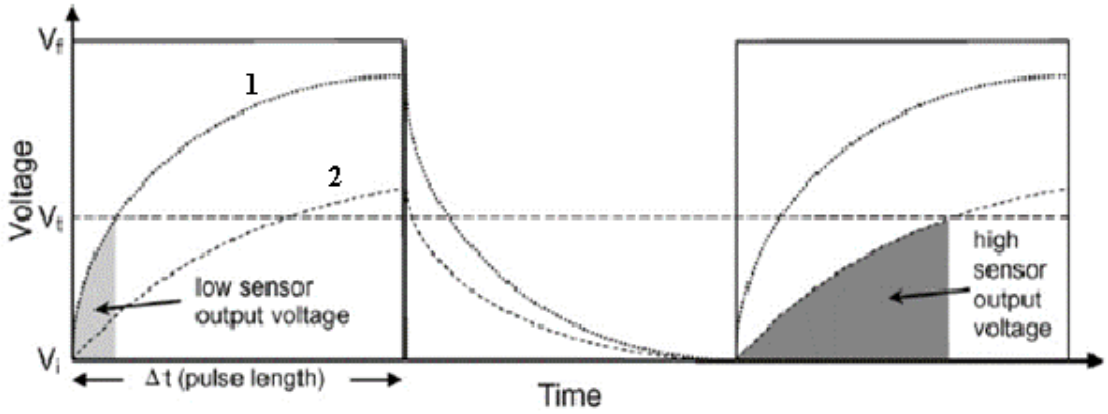

Fig. 3.3. The charge and discharge curves of two capacitance with either high or low permittivity, using a repetitive square pulse with a pulse length Δt (after Bogena et al., 2007).

2.3. **Calibrating**

In the laboratory, the sensors were immersed in soil columns to calibrate the soil water content. The volumetric soil water content determined from the soil columns

samples was regressed against the sensors probe readings. Regression equations transforming the sensors probe reading to volumetric water content were developed. These equations were used for calibration all the the measurements of soil water content used in this study.

2.4. Model identification and forecast

Stochastic models are mathematical models for describing systems which evolve over time according to probabilistic laws; it can be categorized according to the two criteria of time and state space. Table 3.1 shows a method for classification stochastic models. Our study deals with stochastic models that model continuous observations (soil water content values) measured at discrete points in time (hourly), they are usually referred to as time series models. The application of time series models to actual data is popularly referred to as time series analysis (Hipel et al., 1994).

Table 3.1. Classification of stochastic models

		STATE SPACE	
		Discrete	Continuous
TIME	Discrete	Markov Chains	Time Series Models
	Continuous	Point Processes	Stochastic Differential Equations

The time series analysis of soil water content was made in four steps. The first one involved applying the Box-Jenkins method (Box et al., 1994) in order to identify an appropriate univariate model for time series of soil water at 0.10 m depth. This study used the seasonal autoregressive integrated moving average (ARIMA) $(p, d, q) \times (P, D, Q)_S$ model, where p, q are the order of the regular autoregressive and moving average

factors, and *P, Q* are the seasonal autoregressive and moving average factors, respectively; *d* and *D* are the order of differencing for the regular and seasonal part, respectively; sub-index *S* denotes the seasonal period (24 hours in this study).

The second step was evaluating the effects of irrigation time by including it in the model as intervention analysis and searching for the presence of outliers in the univariate series. The third was identifying the appropriate transfer function approach by modelling the linear system, using the soil water content time series at 0.10 m depth as input, while the output was the soil water content time series at various depths (0.20, 0.35, 0.50, 0.60 m and W_{AVG}).The final step was applying the transfer function models obtained from the 2010 data set for predicting the soil water content to the 2011 data set at various greater depths in the soil profile.

2.4.1 Univariate Time Series Analysis

Univariate seasonal (ARIMA) $(p, d, q) \times (P, D, Q)_S$ modelling techniques were used to show the patterns of soil water content data at 0.10 m depth. The four steps of Box-Jenkins modelling approach for identifying and fitting ARIMA models were used: model identification, model parameter estimation, diagnostic checking, and forecasting. Fig 3.4 displays the overall procedures for Box-Jenkins modelling approach.

a) Identification

Applying the exploratory analysis -time series plots- sample autocorrelation function (ACF) and partial autocorrelation function (PACF) - on the time series data under consideration helps to reveal the essential mathematical features of the data. Plotting the data enables to capture the identification information by perusal of a graph includes:

1. Autocorrelation: shows the linear dependence existing among the observations.
2. Seasonality: series quite commonly display seasonal behaviour where a certain basic pattern tends to be repeated at regular seasonal intervals.
3. Nonstationarity: Most series time of nature resources are nonstationarity. Stationarily is analogous to the concept of isothermal within the field of physics. For example, in order to be able to derive soil physical laws that are

deterministic, it is often assumed that the soil water is isothermal, so that energy changes associated with temperature changes do not have to be taken into account. Likewise, in stochastic modelling, the statistical properties of a process are invariant with the time (variance and mean are constant) if the process is stationary.

4. Need for transformation: Box-Cox transformation (Box and Cox 1964) keep the series time stationary and it is achieved by several steps:
    a. Get the variance constant
    b. Get the mean constant
5. The nonstationarity is removed from the series using a technique called differencing. After differencing the data, the fitted model called ARIMA model. Subsequently, appropriate AR and MA parameters contained in the ARIMA models are estimated for resulting stationary series formed by differencing the original nonstationary series.
6. Known or unknown intervention: The effects of a known intervention can often be detected by an examination of the plot of the time series and observe when the general trend of the observations has changed.

When the time series become stationary, sample autocorrelation function (ACF) and partial autocorrelation function (PACF) were used to identify time series models (Pankratz, 1983; Hoff, 1983). ACF measures the relation between X_t and X_{t+k}, where k is the time lag, and PACF was used to take into account the dependence on the intermediate elements (those within the lag) (Wei, 1989). If the sample ACF of the differenced series still does not damp out quickly, the series should be differenced again. The data should be differenced just enough times to remove the homogeneous nonstationarity which in turn will cause the sample ACF to die off rather quickly. When differencing is required, usually it is not greater than 2 for nonstationary series which arise in practice. According to the sample ACF and PACF, how many AR and MA terms will be determined.

In brief, Identification has two steps prior to deciding upon the form of the ARMA model:

1. Transformation using the Box-Cox transformation in order to alleviate problems with nonnormality and/or changing variance. Additionally, the differencing may be required for removing nonstationarity.
2. Select one or more appropriate ARIMA models depend on ACF and PACF.

b) Estimation

For an identified ARIMA model, the following parameters must be estimated using the available data: a) mean of the series; b) AR parameters; c) MA parameters; d) innovation series; and e) variance of the innovations.

In our study we used method of maximum likelihood for estimating the parameters of ARIMA models. Significance of parameters was determined by constructing the Wald test statistic. Automatic selection criterion such as the Akaike information criterion can be employed for choosing the best overall model when more than one model is calibrated.

c) Validation

The residuals sequences for AR, MA, ARMA and ARIMA models are assumed to be independently distributed in the theoretical definition of these models. This implies that the estimated innovations or residuals are uncorrelated or white.

For checking that the residuals are white the recommended procedure is to plot the RACF (residual autocorrelation function) along the 95% confidence limits. And for ascertaining whether or not the residuals are uncorrelated. The suggested procedure is to use the Ljung-Box statistic test. Moreover, if the residuals are correlated this implies that the model is inadequate and a more appropriate model can be found by repeating the earlier stages of model construction.

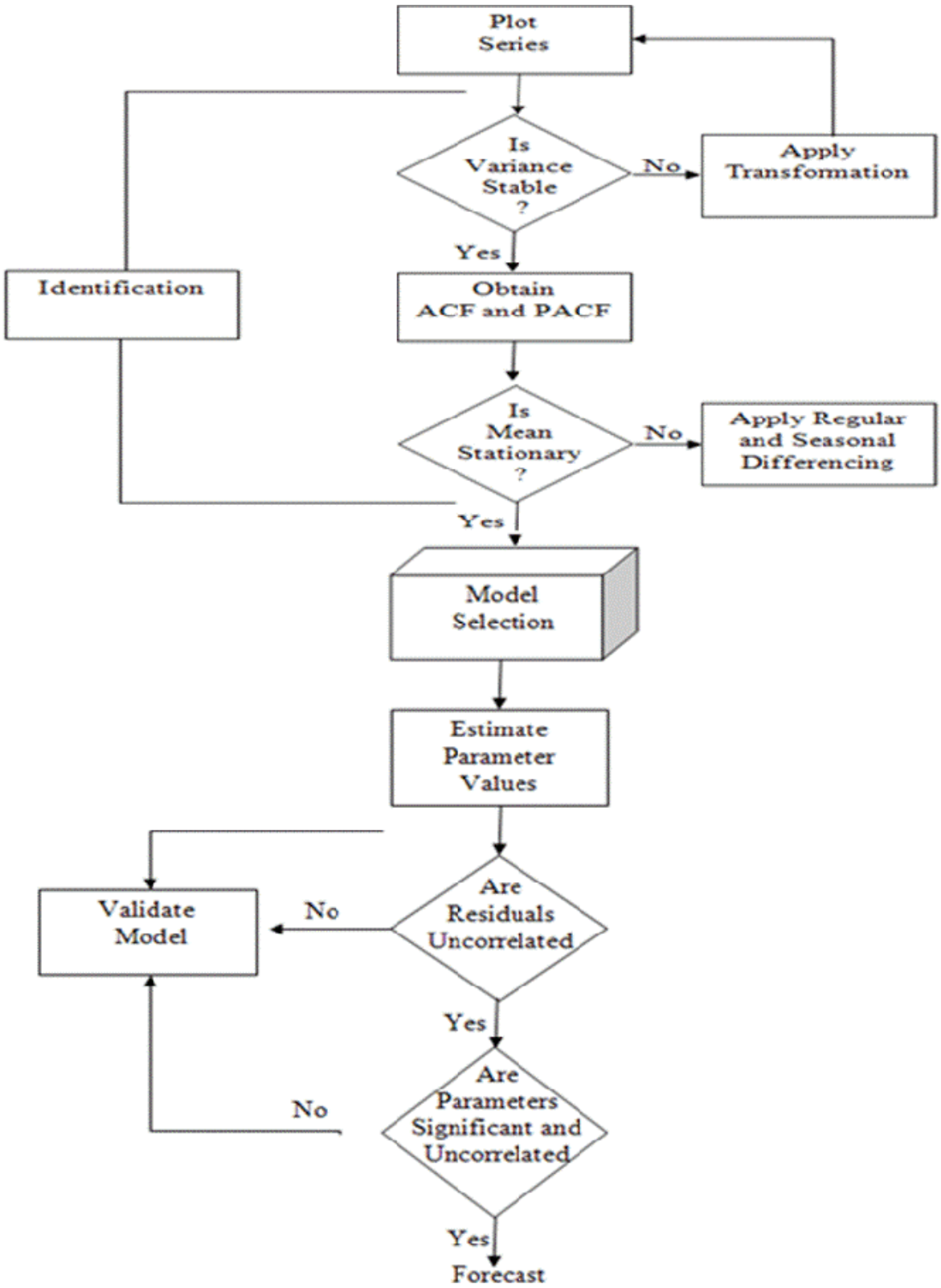

Fig. 3. 4. Overall procedures for Box -Jenkins modelling approach

d) Forecasting

Once the appropriate model has been found, it can be integrated (trend introduced into the model) and future forecasts can be found. Confidence intervals can also be computed for each of the observation forecasts.

One useful criterion to obtain the most accurate forecasts is to use what is called minimum mean square error.

Forecasting can be used as an approach for model discrimination. A variety of time series models can be fitted to the first portion of one or more time series and then used to forecast the remaining observations. By comparing the accuracy of the forecasts from the models, one can determine which set of models forecasts the best.

In the autoregressive (AR) process, the present values of time series depend on the preceding value plus a random shock. The AR model for a centred time series with order p is defined as:

$$X_t = \phi_1 X_{t-1} + \phi_2 X_{t-2} + ... + \phi_p X_{t-p} + a_t$$

$$\text{or } (1 - \phi_1 B - \phi_2 B^2 - ... - \phi_p B^p) X_t = a_t \qquad (4)$$

where ϕ_j is the j[th] AR parameter, a_t is the Gaussian white-noise error, and B is the backshift operator where $B^p X_t = X_{t-p}$. For the moving average (MA) model, errors are the average of this period's random error and the previous random error. MA time series of order q is defined as

$$X_t = a_t + \theta_1 a_{t-1} + \theta_2 a_{t-2} + .. + \theta_q a_{t-q} \text{ , or}$$

$$X_t = (1 + \theta_1 B + \theta_2 B^2 + .. + \theta_q B^q) a_t \qquad (5)$$

where θ_q is the q[th] MA parameter.

A stationary time series is required for identifying AR and MA models, which implies that the variance and mean values are constant while some transformation is necessary before identifying the model.

No trends in mean were identified by taking successive differences of the data on the regular and seasonal components. The number of differences needed to attain the stationary time series was denoted by *d* and *D*. No trend in variance is normally achieved by applying a logarithmic transformation (Soebiyanto et al., 2010; Quinn, 1985; Vandaele 1983).

For any time series, X_t, the ARIMA *(p, d, q)×(P, D,Q)S* of X_t is

$$\phi_{\mathrm{p}}(B)\,\Phi_P(B^s)(1-B)^d(1-B^s)^D X_t = \theta_q(B)\,\Theta_Q(B^s)a_t \qquad (6)$$

where $\phi_p(B)$ and $\theta_q(B)$ are the regular autoregressive and moving average factors, and $\Phi_P(B^s)$ and $\Theta_Q(B^s)$ are the seasonal autoregressive and moving average factors, respectively.

Autocorrelation function (ACF) and partial autocorrelation function (PACF) were used to identify time series models (McCleary and Hay, 1980; Pankratz, 1983; Hoff, 1983). ACF measures the relation between X_t and X_{t+K}, where *K* is the time lag, and PACF was used to take into account dependence on the intermediate elements (those within the lag) (Box et al., 1994; McDowall et al., 1980; Wei, 1989).

In this study, the maximum likelihood method was used to estimate the model parameters. The significance of parameters was determined by constructing the Wald test statistic.

Diagnostic checking tests were used to check if the residuals showed any autocorrelation at any lags. The assumptions would be satisfied if the ACF and PACF of residuals at all lags were non-significant.

2.4.2. Intervention analysis and outlier detection

Outliers in the soil water content data at a depth of 0.10 m were removed using the Grubbs' test for detecting outliers (Grubbs, 1969).

$$Z = \frac{/M - V/}{SD} \tag{7}$$

where Z is the test statistic, M is the mean of the values, V is the value being tested, and SD is the standard deviation of the values. In total 1318 observations of soil water content were available. Based upon an outlier probability level of 5%, the outlier test statistic was set at 4 (Grubbs, 1969). Soil water content values which yielded test statistics larger than or equal to 4 were removed from the data set. To assess the impact of precipitation and other observed irregularities in the times series of water content, two types of outliers were considered: additive outlier (*AO*) and temporary change (*TC*). At the same time, level shift (*LS*) was used as an intervention analysis to assess the impact of the irrigation event on the time series of soil water content. AO is a pulse that affects the time series at one period only. *TC* is an event that decays exponentially according to a pre-specified dampening factor. *LS* is an event that permanently affects the subsequent level of a series (Chen and Liu, 1993) (Fig. 3.5).

Let Z_t denote the underlying time series process which is free of the impact of outliers and is prior to the irrigation event, and let X_t denote the observed time series. We assume that Z_t follows the seasonal ARIMA *(p, d, q) (P, D, Q)*$_S$ model $\phi_p(B)\Phi_P(B^s)(1-B)^d(1-B^s)^D X_t = \theta_q(B)\Theta_Q(B^s)a_t$, based on these assumptions, the appropriate model for assessing the impact of the control is:

$$X_t = \sum_{r=1}^{n_r} \omega_r S_{T_r}^{(LS)} + \sum_{i=1}^{n_i} \omega_i P_{T_i}^{(TC)} + \sum_{j=1}^{n_j} \omega_j P_{T_j}^{(AO)} + Z_t$$

$$= \sum_{r=1}^{n_r} \omega_r S_{T_r}^{(LS)} + \sum_{i=1}^{n_i} \omega_i P_{T_i}^{(TC)} + \sum_{j=1}^{n_j} \omega_j P_{T_j}^{(AO)} + \frac{\theta_q(B)\ \Theta_Q(B^S)}{\phi_p(B)\Phi_p(B^S)(1-B)^d(1-B)^D} a_t \tag{8}$$

where ω_r represents the permanent change in the mean level after the intervention (irrigation event), $S_{T_r}^{(LS)}$ is referred to as a step indicator at irrigation time T_r , where

$$S_{T_r}^{(LS)}\begin{cases}0 & t < T_r\\ 1 & t \geq T_r\end{cases} \tag{9}$$

ω_i represents the transitory change in the mean level after the unusual observations (such as precipitation), $P_{T_i}^{(TC)}$ and $P_{T_j}^{(AO)}$ are referred to as a pulse indicator at unusual observation time T_i and T_j respectively , where

$$P_{T_i}^{(TC)}\begin{cases}0 & t < T_i\\ \dfrac{1}{(1-\delta B)} & t = T_i\end{cases} \tag{10}$$

and

$$P_{T_j}^{(AO)}\begin{cases}0 & t \neq T_j\\ 1 & t = T_j\end{cases} \tag{11}$$

δ is the dampening factor that takes a default value of 0.7 (Chen and Liu, 1993).

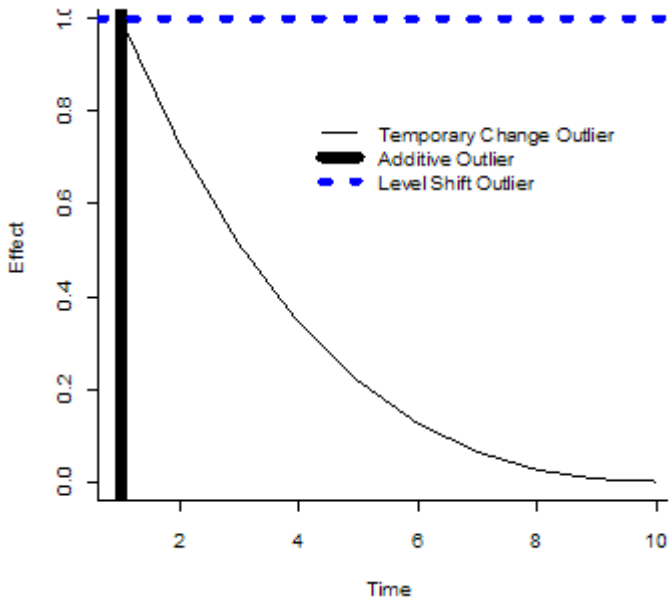

Fig. 3.5. Plot illustration of the effect of additive outlier, temporary change outlier with $\delta = 0.7$, and level shift outlier on later periods.

2.4.3 Transfer function approach

Observations and predictions of one time series (input X_t) may be used to estimate the outcome of another time series (outputG_t) by modelling the linear system with a relatively small number of parameters. The model takes the form

$$G_t = \frac{A(B)}{C(B)} X_{t-b} + a_t \qquad (12)$$

where $A(B)$ and $C(B)$ are a polynomial of the s and r orders, respectively

$A(B) = (A_0 - A_1 B - A_2 B^2 - \ldots - A_s B^s)$

$C(B) = (1 - C_1 B - C_2 B^2 - \ldots - C_r B^r)$

where $A_0, A_1, A_2, \ldots, A_s$ and $C_1, C_2, \ldots, C_r$ are the parameters of the model, b is the latent parameter, B is the backshift operator, and a_t is a disturbance (noise).

$A(B)/C(B)$ is called the transfer function of the system. The procedure for building a transfer function model involves three steps: a) identification, b) estimation and c) model checking. By using a univariate model for input X_t with white noise residuals, the same filter can be applied to the output series G_t (pre-whitening). Cross-correlation of the two residuals allows us to identify the transfer function form.

In this study, the transfer function approach was applied by choosing the soil water observations at 0.10 m as a primary series (X_t), while the output series (G_t) was chosen from the soil water content time series at various depths (0.20, 0.35, 0.50, 0.60 m and W_{AVG}). W_{AVG} represents the average soil volumetric water content in the top 0.60 m profile, calculated from the formula that Wu et al. (1997)[2] used to estimate total water storage.

[2] $W_{AVG} = \left[\frac{1}{2}(D_1 - D_0)\theta_1 + \sum_{i=1}^{n-1} \frac{1}{2}(D_{i+1} - D_{i-1})\theta_i + \frac{1}{2}(Z_n - Z_{n-1})\theta_n \right] / (D_n - D_0)$

where D is depth downward (m), and θ_i is volumetric water content at depth D_i

R software version 2.13.0 (R Development Core Team, 2010) was used to execute all model identifications and subsequent predictions of soil water content at various depths (Cryer and Chan, 2008; Shumway and Stoffer, 2006).

3. Results and discussion

Fig.3.6 shows soil water content by sensor probe regressed against soil water content by gravimetric method.

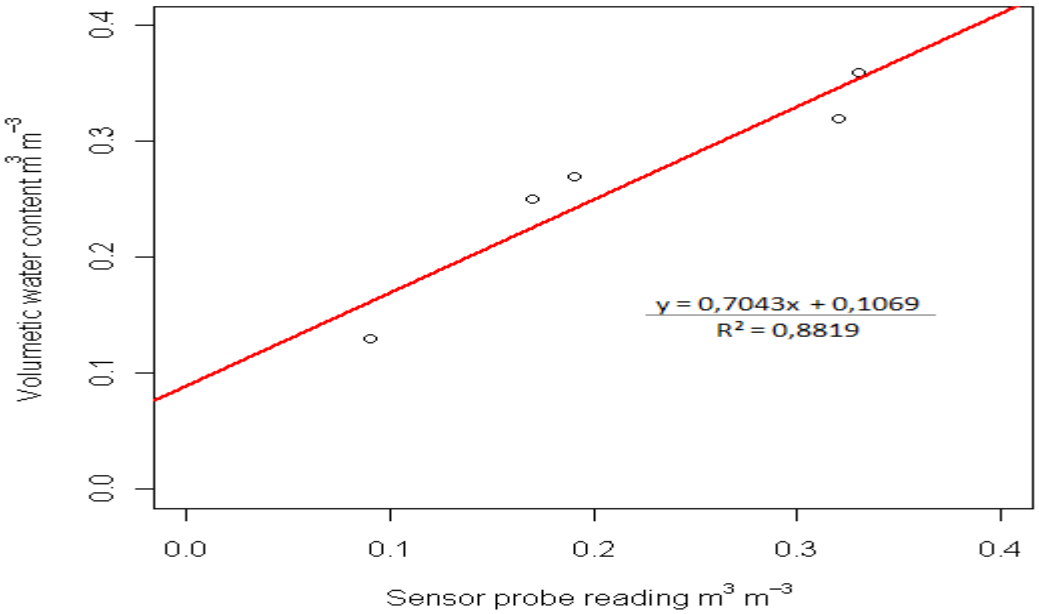

Fig.3.6. Soil water content by sensor probe regressed against soil water content by gravimetric method.

Fig. 3.7 shows the soil water content at five depths versus time. Fluctuation of soil water content at deeper layers corresponds to the changing of water content at upper layers; this fluctuation dampens as the layer becomes deeper. This could be used to identify a model to explain the water content behaviour of one depth, which in turn is used to predict the behaviour of water content at another depth (Wu et al., 1997). Irrigation events that were applied at 4.29, 27.20, 32.04 and 46.33 days, and precipitation occurring at 9.33, 20.50 and 52.54 days had significant effects on soil water content fluctuations. Fig. 3.8 shows the soil water content at 0.10 m depth and its response to each irrigation event and rainfall; capturing these two events well and

including them in models for soil moisture fluctuations will provide reasonable predictions for soil water content. Later, we developed ARIMA models and completed them by including the irrigation event as an intervention analysis and the precipitation as outlier detections.

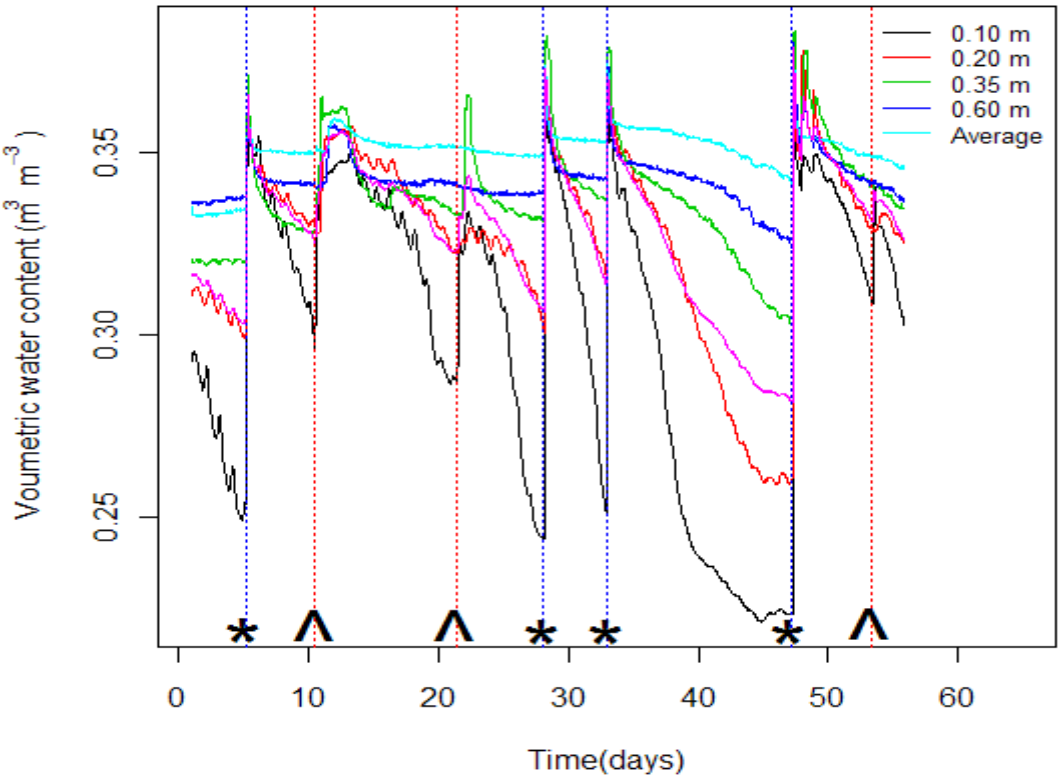

Fig. 3.7. Soil water content at five depths versus time ,and the average water content of the top 0.60 m soil profile WAVG; * indicates the irrigation time,^ indicates the precipitation time.

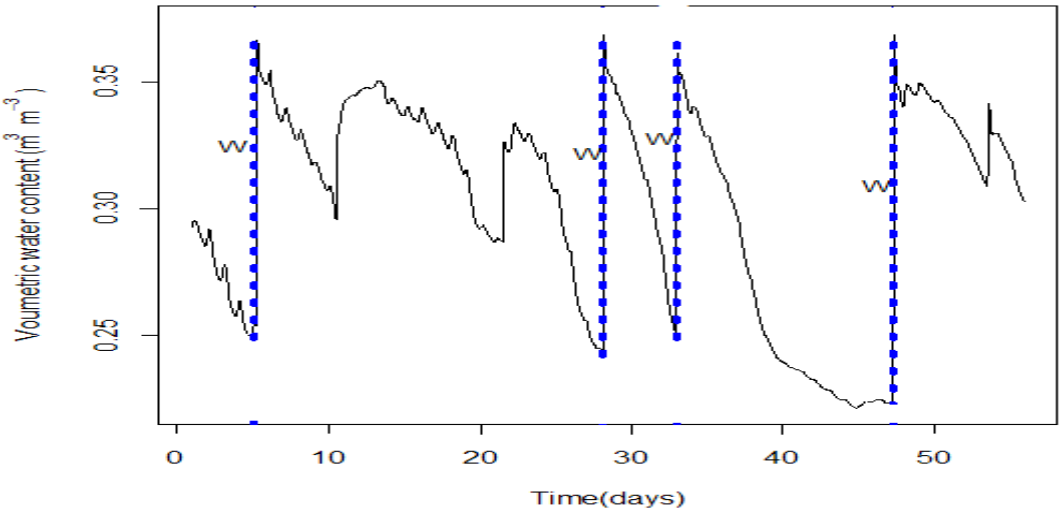

Fig.3.8. Soil water content at 0.10 m depth, W is a step indicator caused by the irrigation event.

3.1. Univariate modeling of the soil water content time series at 0.10 m depth.

The ACF of the original time series of water content at 0.10 m depth converges very slowly, indicating that the time series is non-stationary (Fig. 3.10 A). To obtain a stationary time series, the original series were differentiated (first order-difference and seasonal first order difference). No trend in variance is observed in this series, so there is no need to apply a logarithmic transformation.

The ACF and PACF of differentiated time series indicated that the series was approximately AR (2) for the regular component and MA (1) for the seasonal component, because the ACF (Fig. 3.10B) and PACF (Fig. 3.10C) showed that only the correlation at the first two lags of ACF and the 24^{th} lag of PACF were significant.

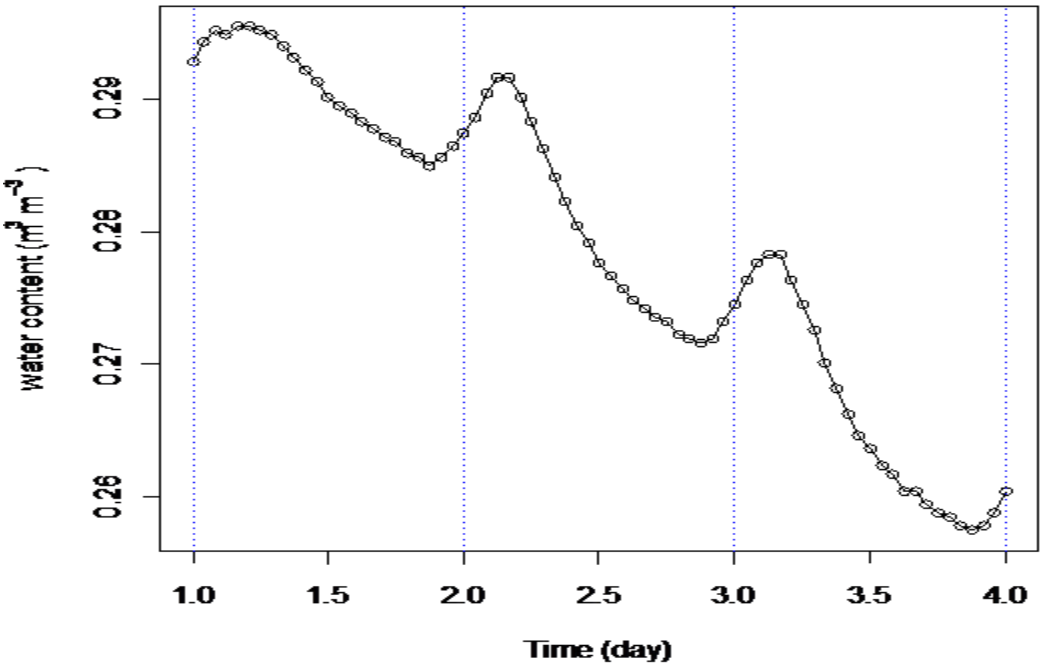

Fig. 3.9. Time series of soil water content at 0.10 m depth (m^3 m^{-3}) for the first 4 days at 0.10 m depth.

The ARIMA *(p, d, q) (P, D, Q)$_S$* model of time series of water content at 0.10 m depth was ARIMA (2, 1, 0) $(0, 1, 1)_{24}$. The model in usual notation is given by:

$$(1-\phi_1 B-\phi_2 B^2)(1-B)(1-B^{24})X_t = (1+\Theta_{24}B^{24})a_t \qquad (13)$$

where a_t is an independent, identically distributed white noise term with zero mean and variance = $2.8.10^{-7}$, ϕ_1 = 0.3841, and ϕ_2 = -0.17 are AR parameters. The Θ_{24} = 0.99 parameter of the seasonal MA part indicates that the model is almost non-invertible. Therefore, it is inadequate and needs to be improved in structure. An exploratory method, which is well-established in other fields, is a seasonal-trend decomposition based on locally-weighted regression (loess), widely known as "STL" (Cleveland et al., 1990; Hafen et al., 2009).

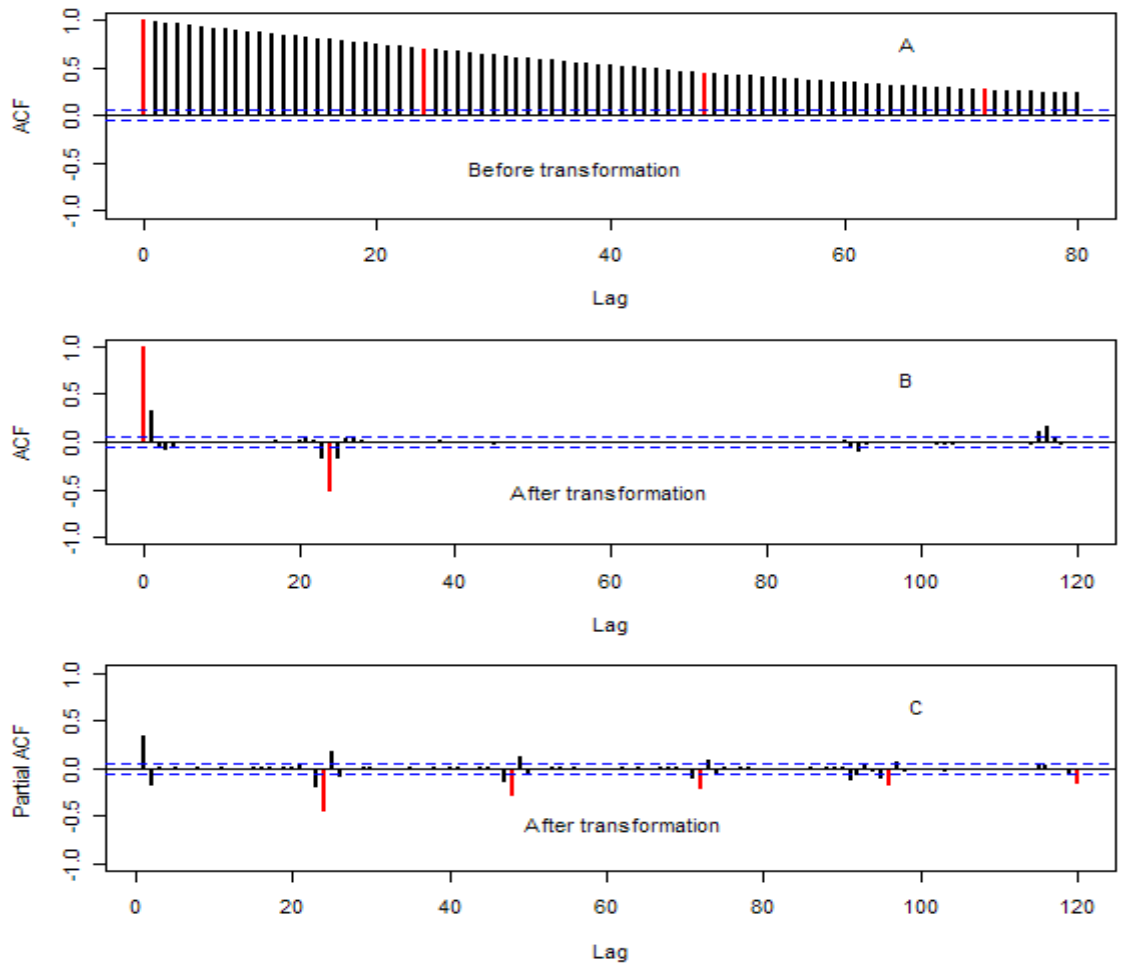

Fig. 3.10. (A) Autocorrelation function (ACF) of the original data, (B) autocorrelation function, and (C) partial autocorrelation function (PACF) of the transformed time series of water content at 0.10 m. The ACF of the original data indicates that the series is not stationary. The dotted line is 2 x standard errors.

The STL method is straightforward to use; it allows for flexibility in specifying the amount of variation in the trend and seasonal components of time-series; and it produces robust estimates that are not distorted by transient outliers (Cleveland et al., 1990). Fig. 3.11 shows that the large outliers of the remainder (random) are backed to the irrigation event. Since the timing of the irrigation event is previously known, the model could be completed with intervention analysis (irrigation event) and outlier detection (model 10), making it invertible and in order to reduce its residual variance (Wei, 1989).

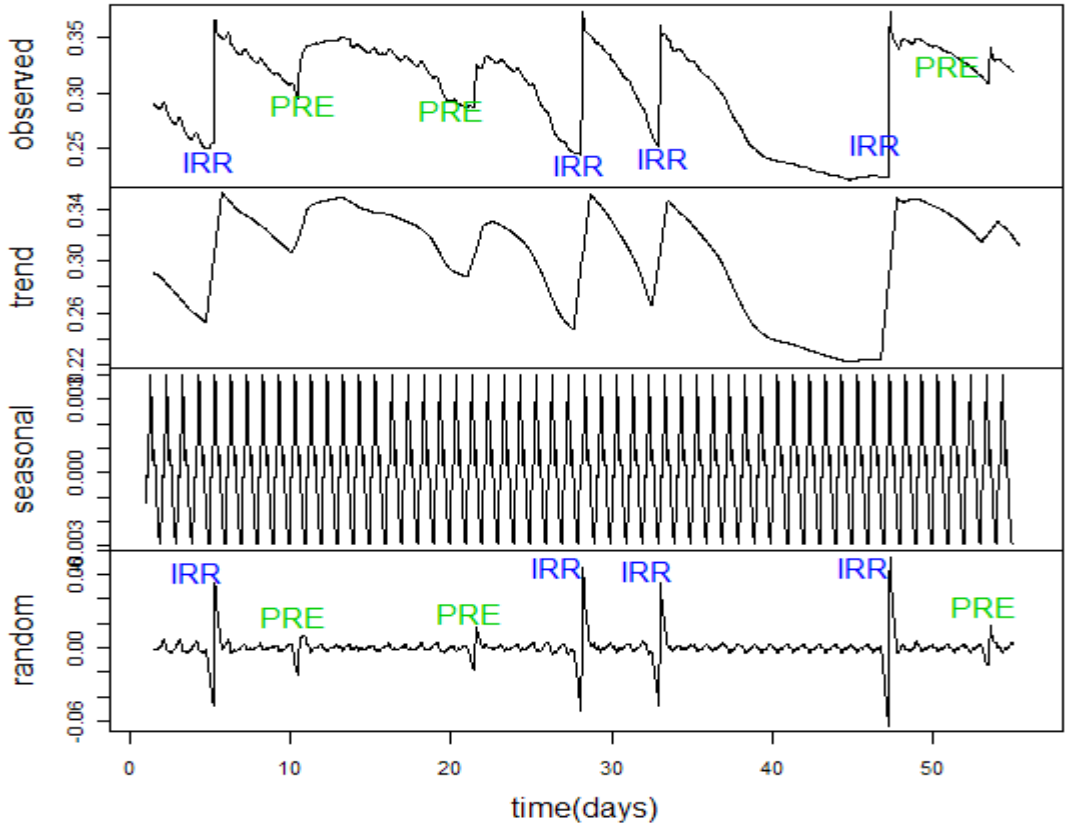

Fig. 3.11. Decomposition plot of the soil water content at 0.10 m depth affected with intervention variable (irrigation event in our case) and irregular variables (such as precipitation) over 55 days, STL method. This plot assists evaluation of the trend, seasonality and remainder (random) against the raw data. The graph (observed) represents the hourly time series of water content affected with irrigation and irregular events like precipitation. The graph (trend) is the fitted trend. The graph (seasonal) is the seasonal pattern per 24 hours. The graph (random) represents the remainder after the trend and the seasonal pattern have been fitted to the time-series values. The sum of the trend, the seasonal pattern and the random equals exactly the time-series. IRR is the time of irrigation event, and PRE is the precipitation time. The large peaks of the remainder correspond to the irrigation time which has to take into account when building up ARIMA model on the series.

3.2. Outlier and intervention analysis on the ARIMA model for time series of water content at 0.10 m depth: the effectiveness of the irrigation event on soil water content.

Intervention analysis and automatic outlier detection were applied on the previous ARIMA (2, 1, 0) $(0, 1, 1)_{24}$ model to improve it and to assess the effect of irrigation events on the soil water at 0.10 m depth. Applying the Grubb's test (Eq. 7) detected 28 outliers (Table 3.2) for time series of soil water content at 0.10 m depth.

Table 3.2 Outlier detection and parameter estimation for time series of water content at 0.10 m

observation time (hour)	type	ω	observation time (hour)	type	ω
103	TC	-0.0137	494	TC	0.0249
104	TC	0.0323	495	TC	0.0047
105	TC	0.0053	653	TC	-0.0267
128	TC	-0.0076	654	TC	0.0578
151	AO	0.0044	769	TC	-0.0136
175	AO	0.0038	770	TC	0.0310
224	TC	-0.0056	1110	TC	-0.0043
225	TC	-0.0046	1111	AO	-0.0037
226	TC	-0.0045	1112	TC	0.0291
227	TC	-0.0048	1113	TC	0.0313
228	TC	-0.0059	1114	TC	0.0123
229	AO	-0.0074	1261	TC	0.0087
231	TC	0.0139	1262	TC	0.0199
492	AO	-0.0051	1263	TC	0.0053

Including the outlier detection and intervention analysis, the observed value of time series of soil water content at 0.10 m can be described according to Eq. (8) as

$$X_t = \omega_r (S_{4.29}^{(t)} + S_{27.20}^{(t)} + S_{32.04}^{(t)} + S_{46.33}^{(t)}) + \sum_{i=1}^{23} \omega_i P_{T_i}^{(TC)} + \sum_{j=1}^{5} \omega_j P_{T_j}^{(AO)} + Z_t \qquad (14)$$

where X_t is the observed time series, Z_t *i*s the time series free of outliers, and ω_r = 0.087 represents the permanent change in the mean level after the irrigation event, which characterizes the effectiveness of the irrigation event on the soil water content. In this study, the flow rate and cut-off time for the four applied irrigations were almost equal. Therefore, we used one average coefficient for $\omega_r$to estimate the weight of the peak caused by four irrigation events. The part $(S_{4.29}^{(t)} + S_{27.20}^{(t)} + S_{32.04}^{(t)} + S_{46.33}^{(t)})$ represents the step indicator at four irrigation times T_r (4.29, 27.20, 32.04, and 46.33 days). The part $\sum_{i=1}^{23} \omega_i P_{T_i}^{(TC)} + \sum_{j=1}^{5} \omega_j P_{T_j}^{(AO)}$ represents the effects of 28 outliers which were detected.

By applying the Box-Jenkins approach to the time series of water content Z_{t_t} obtained from Eq. (14), the ARIMA (1, 1, 2) $(0, 1, 2)_{24}$ model was determined. The model, in usual notation, is given by:

$$(1-\phi_1 B)(1-B)(1-B^{24})Z_t = (1+\theta_1 B+\theta_2 B^2)(1+\Theta_{24}B^{24}+\Theta_{48}B^{48})a_t \qquad (15)$$

The model (15) is free of outliers, it is invertible, and the ACF and PACF of residuals at all lags are non-significant. Table 3.3 shows the comparison between the two models (13 and 15) in terms of statistical parameters.

Table 3.3. Comparison of the two models for the soil water observations at 0.10 m depth in terms of statistical parameters (one based on observed data X_t and the second based on outlier-free data Z_t)

Model	ϕ_1	ϕ_2	θ_1	θ_2	Θ_{24}	Θ_{48}	σ^2
Model based on observed data X_t (13)	0.38	-0.17			0.99		$2.7.10^{-5}$
Model based on Outlier free data Z_t (15)	0.87		-0.51	0.09	0.76	-0.13	$5.48.10^{-7}$

3.3. Transfer function approach

The cross-correlation between the pre-whitened primary time series (0.10 m depth), and the target soil water content time series at various depths (0.20, 0.35, 0.50, 0.60 m and W_{AVG}), showed that the primary series affects the target series, but the target series cannot in turn have a bearing upon the primary series. Fig. 3.12 proofs that the present value of soil water content at 0.10 m has a significant effect on the present values of soil water content at various depths (0.20, 0.35, 0.50, 0.60 m and W_{AVG}). Models for predicting the soil water content at individual depths and W_{AVG} from the soil water content at 0.10 m depth were identified (Table 3.4). The coefficients of X_t in the equations of Table 3.3 show that the present value of soil water content at 0.10 m has an effect of 61, 40, 25 and 19%, respectively, on the present values of soil water content at 0.20, 0.35, 0.50 and 0.60 m and its effect on the present value of W_{AVG} is 55%.

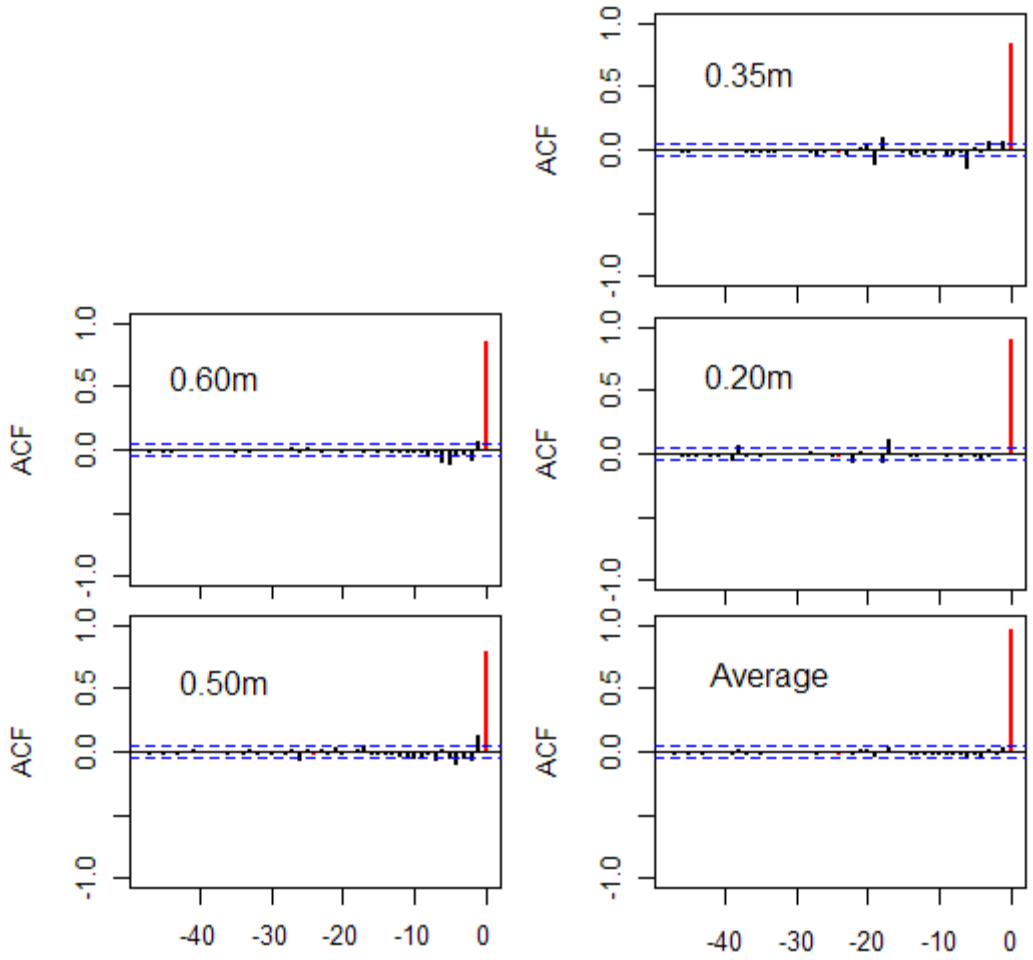

Fig. 3.12. Cross-correlation function for soil water content hourly time series at 0.10 and 0.20, 0.10 and 0.35, 0.10 and 0.50, 0.10 and 0.60 m, 0.10 m and average soil water profile, respectively. Dashed lines indicate 95% confident limits.

Table 3. 4. Time series transfer function model for the various depths and average soil water content of the top 0.60 m profile.

X_t at 0.10 and Y_t at 0.60 m:

$$Y_t = \frac{(0.19 + 0.15B)X_t + a_t}{(1 - 0.14B - 0.21B^2 - 0.7B^3)}$$

$$a_t \sim N(0,\ 2.8\ 10^{-7})$$

X_t at 0.10 and Y_t at 0.50 m:

$$Y_t = \frac{(0.25 + 0.04B)X_t + a_t}{(1 - 0.16B - 0.26B^2 - 0.03B^3 + 0.16B^4)}$$

$$a_t \sim N(0,\ 8.8\ 10^{-7})$$

X_t at 0.10 and Y_t at 0.35 m:

$$Y_t = \frac{(0.4 + 0.04B + 0.0085B^2 + 0.039B^3)X_t + (1 - B^{24})a_t}{(1 - B)(1 - B^{24})(1 - 0.227B - 0.0225B^2 - 0.053B^3 + 0.67B^4 - 0.045B^5 + 0.11B^6)}$$

$$a_t \sim N(0,\ 1.8\ 10^{-6})$$

X_t at 0.10 and Y_t at 0.20 m:

$$Y_t = \frac{0.61X_t + (1 - B^{24})a_t}{(1 - B)(1 - B^{24})(1 - 0.28B + 0.17B^2 - 0.08B^3 + 0.068B^4)}$$

$$a_t \sim N(0,\ 2.062\ \ 10^{-6})$$

X_t at 0.10 and Y_t as the average of the top 0.60 m soil profile:

$$Y_t = \frac{0.55X_t + (1 - 0.28B)(1 - B^{24})a_t}{(1 - B)(1 - B^{24})(1 - 0.59B + 0.23B^2 - 0.16B^3)}$$

$$a_t \sim N(0,\ 4.684\ \ 10^{-7})$$

3.4. Forecasting

Fig. 3.13 shows the model calibration and prediction for 0.20, 0.35 and 0.60 m soil depths. The first 659 observations of each time series were used for model identification. The calibrated model represented the values before these 659 observations very well for each depth. The predicted and observed values after the 659 observation agreed reasonably. The relative difference between predicted and observed values was sometimes large; it increased as the distance of separation between the primary and target increased. The absolute difference between the prediction and measurement never exceeded 0.03 $m^3\ m^{-3}$.

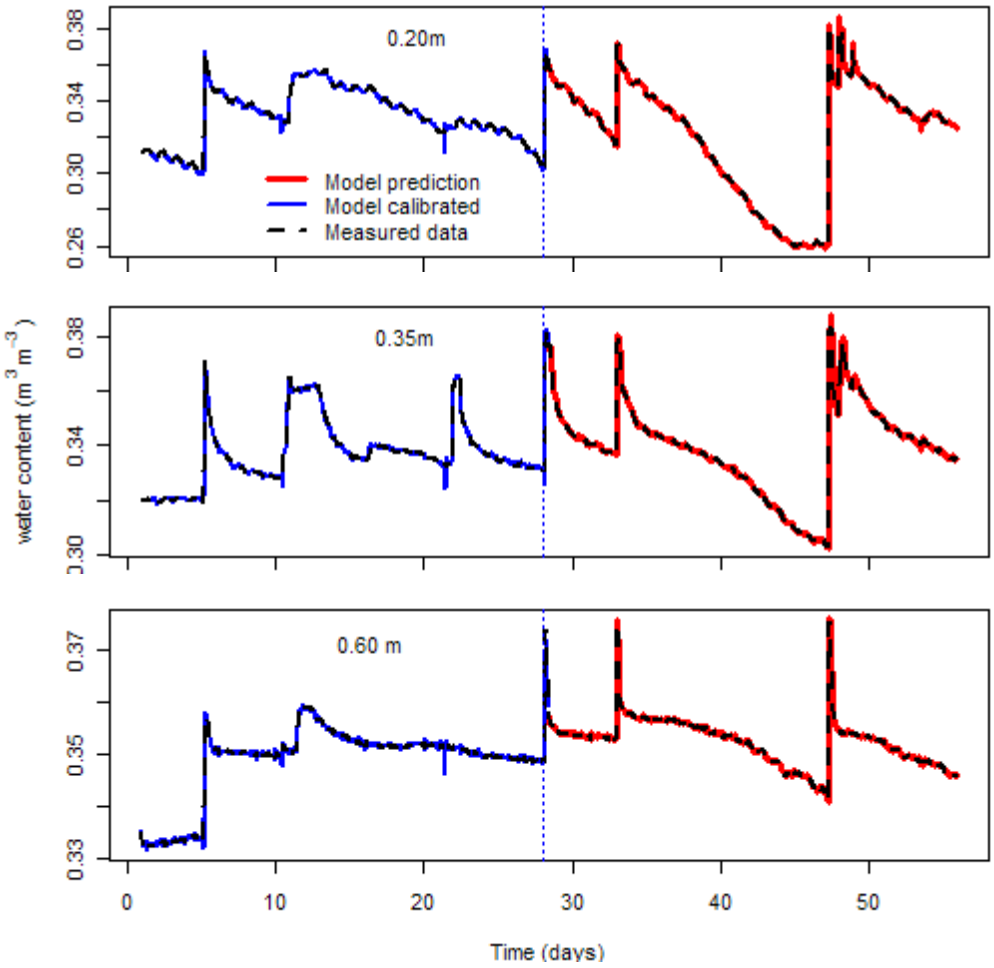

Fig. 3.13. Measured and predicted water content versus time at 0.20, 0.35, and 0. 60 m depths. Prediction was based on the identified transfer function models for each depth. The curve before the vertical dashed line refers to model calibration and after the vertical dashed line to model prediction.

The model of forecasting the average water content W_{AVG} (Fig. 3.14) behaved similar as the individual models for soil depths. The absolute difference between prediction and measurement never exceeded 0.025 m^3 m^{-3}. Measured versus predicted average water content are shown in the Fig. 3.15. Many data points were very close to the 1:1 line. Overall, the models represented the dynamics of field soil water fluctuation very well.

In the case of variable interval irrigation, we were able to determine the time of the next irrigation and its effect on soil water content by predicting the time series of soil water Z_t without outliers (model 11), and then by adding the irrigation effect ω_r to the prediction when the soil water content dropped below the field capacity. In Fig. 3.16

there is an example of two prediction days. The observed values of soil water content covered 55 days, and the prediction is for the 56th and 57th day. It includes the effect of the next irrigation if the farmer chooses to irrigate on the 56.5th day.

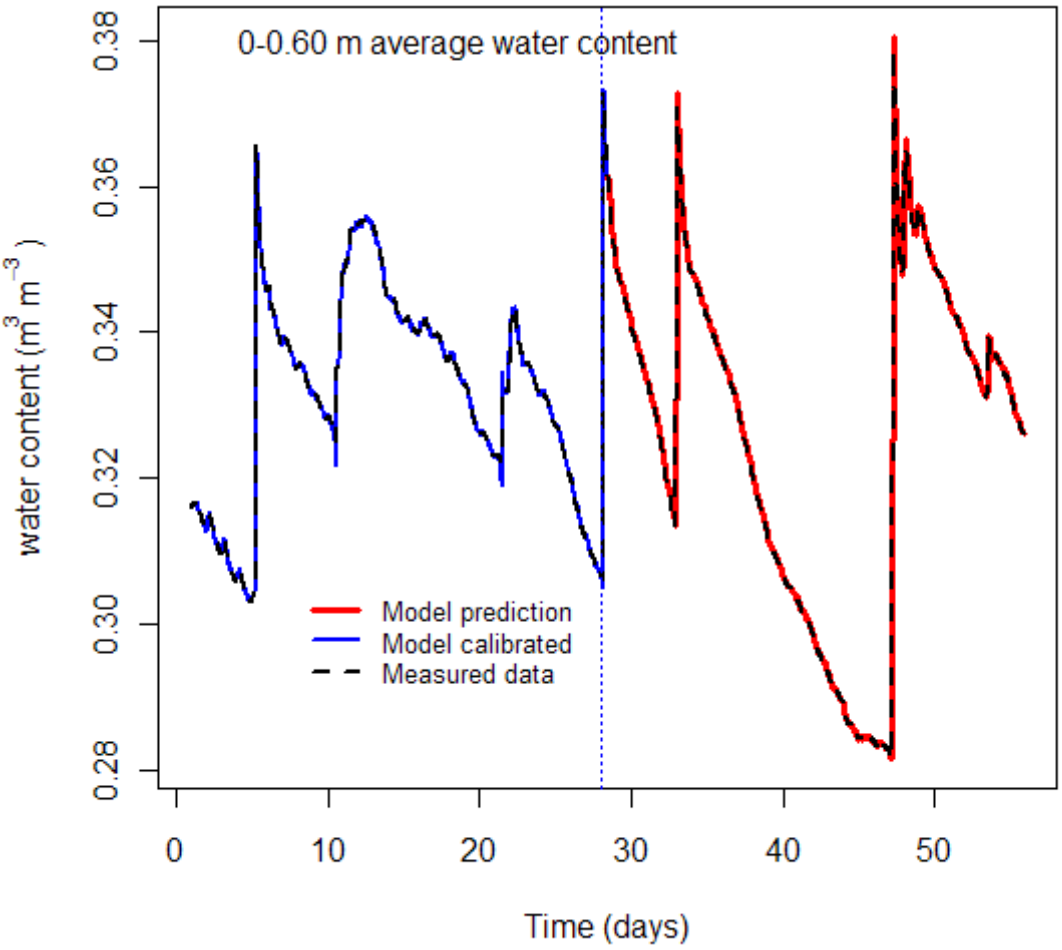

Fig. 3.14. Measured and predicted average water content WAVG versus time in the top 0.60 m profile. Prediction was based on the indentified transfer function models for WAVG. The curve before the vertical dashed line is model calibration and that after the vertical dashed line is model prediction.

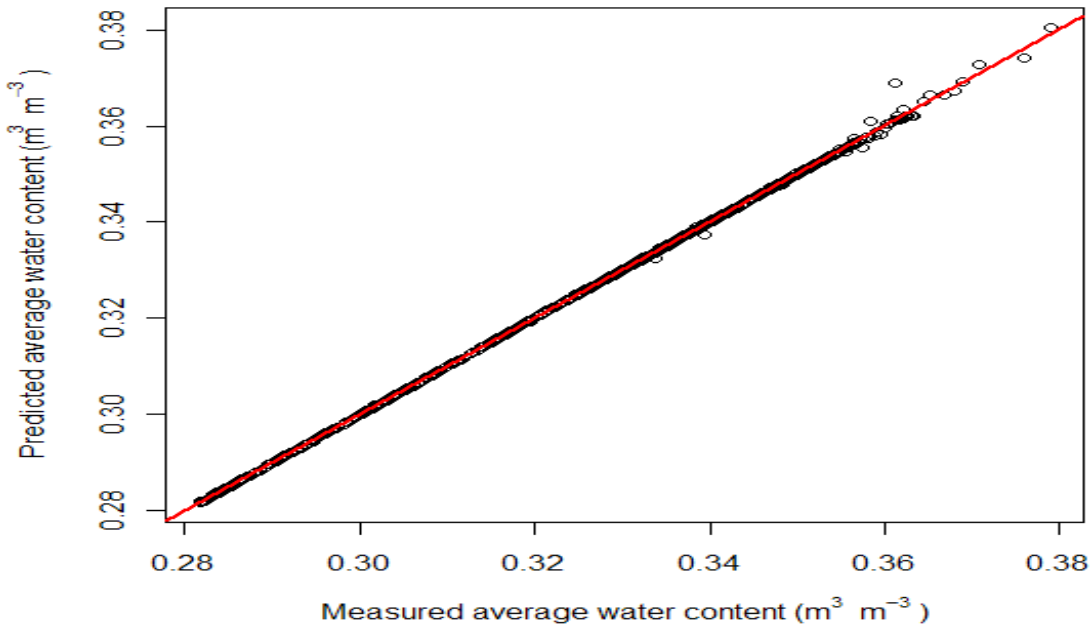

Fig. 3.15. Measured versus predicted average water content in the top 0.60 m soil profile.

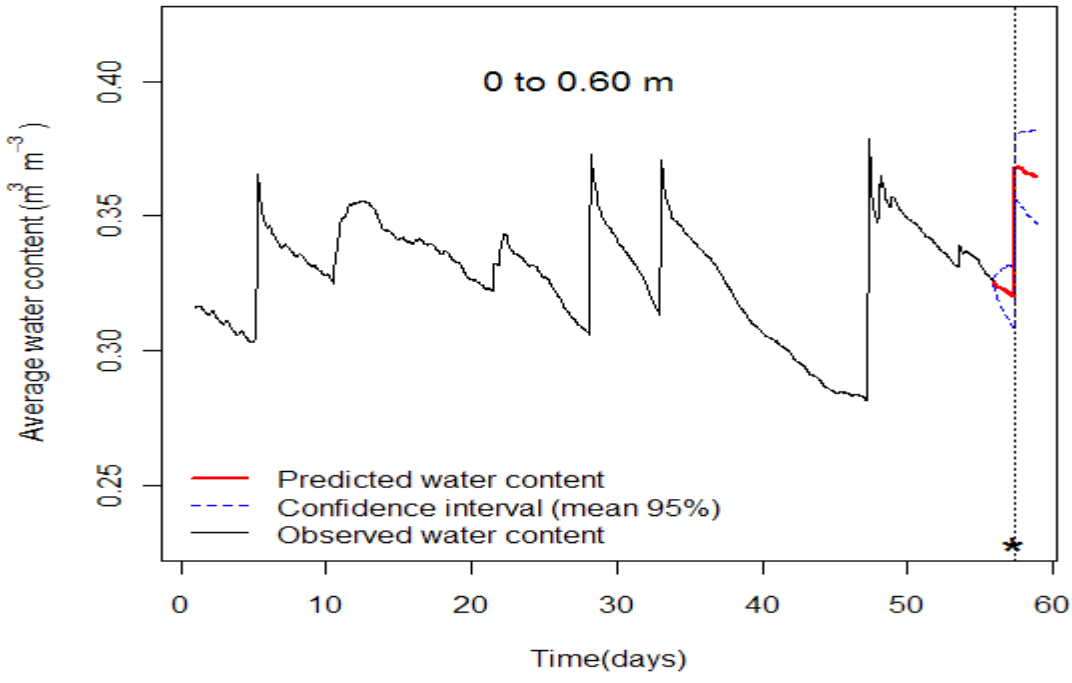

Fig. 3.16. Prediction models for average soil water content WAVG. Prediction was based on the indentified transfer function models for WAVG. We have observed data for 55 days, the model predicts the 56th and 57th day taking into account the effect of next irrigation if the farmer choose to irrigate on 56.5th day (*is the irrigation time at 56.5th day).

To confirm the results of the models, the experiment was repeated in 2011. The field was planted with artichokes and 1199 observations were made starting on 23 April 2011 (Fig. 3.17). The same transfer function models obtained from the 2010 data set were applied to the 2011 data set to predict the soil water content at deeper depths from one single shallower depth. Fig. 3.18 shows the time series of soil water content at 0.20 m depth and the average water content in the top 0.60 m soil profile W_{AVG} for the 2010 data set (1318 observations) and the 2011 data set (1199 observations). The transfer function model obtained from the 2010 data set was applied to the 2517 total observations (1318+1199) for each time series. The calibrated model represented the values very well up to 1318 observations (2010 data set) for each series. The predicted and observed values after the 1318 observations agreed reasonably (which is represented by the 2011 data set). The absolute difference between the prediction and measurement for the time series of soil water content at 0.2 m depth and W_{AVG} never exceeded 0.01 and 0.005 m^3 m^{-3}, respectively.

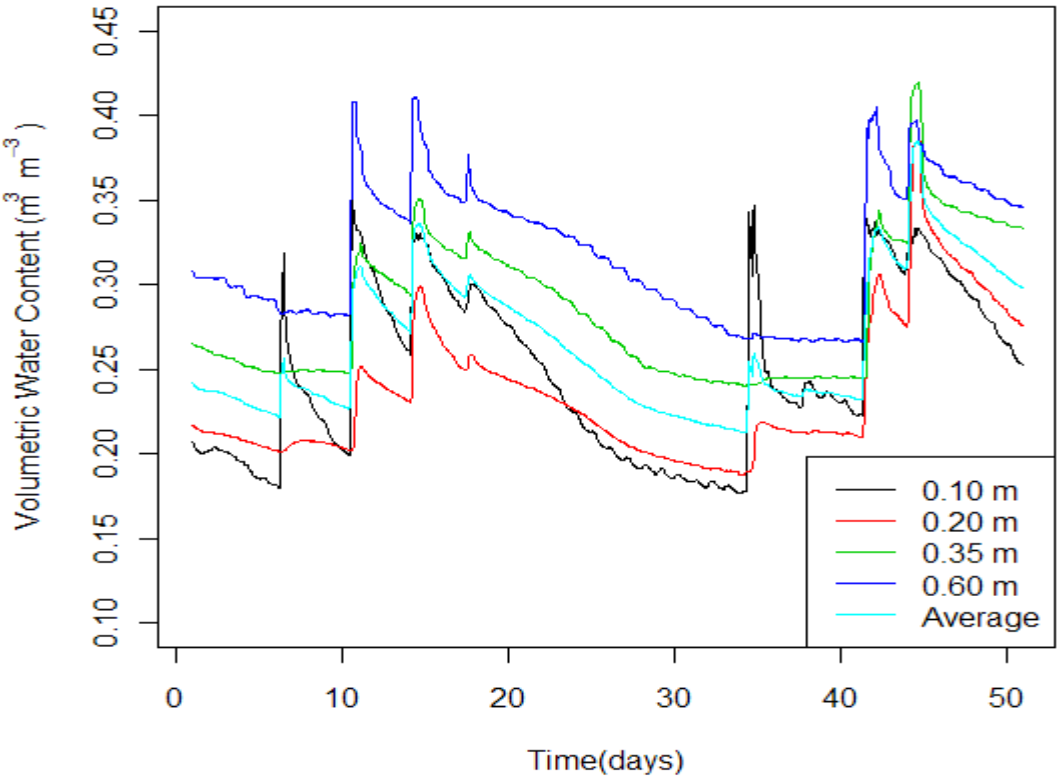

Fig. 3.17. Soil water content at five depths versus time, and the average water content of the top 0.60 m soil profile WAVG (1199 observations starting on 23 April 2011).

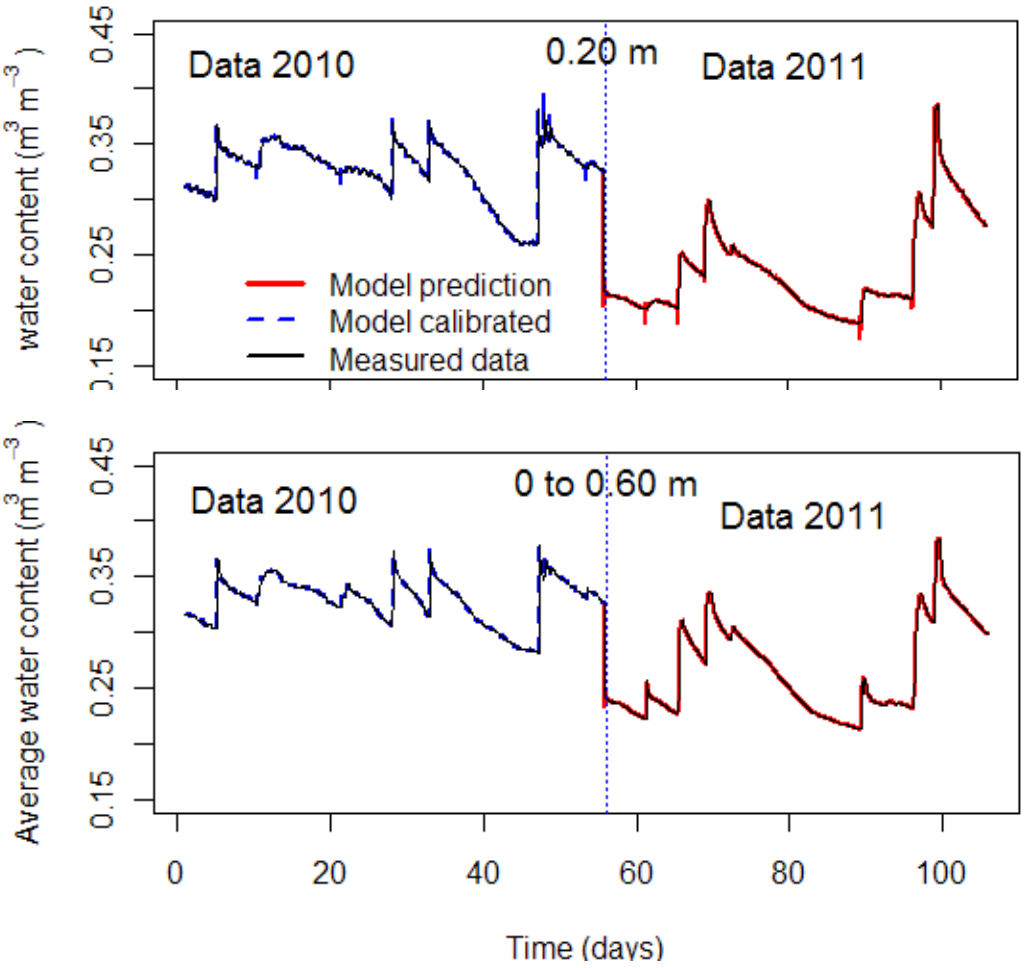

Fig. 3.18. Measured and predicted water content versus time at 0.20 m depth and average water content WAVG. Prediction was based on the identified transfer function 2010 data set of models for each one. The curve before the vertical dashed line refers to model calibration and after the vertical dashed line to model prediction (2011 data set).

4. Conclusions

The time series of soil water content at the root zone for a lettuce field (silty loam soil) was studied at five depths 0.10, 0.20, 0.35, 0.50 and 0.60 m; each one was transformed to a stationary situation; then, ARIMA models were constructed to study each time series and make predictions. In the case of variable interval irrigation, predictions of irrigation effects on the soil water content could not be properly explained by the ARIMA model and its underlying normality assumption. To avoid this obstacle and let the ARIMA model work in variable interval irrigation, we used intervention analysis (irrigation events) and outlier detection for unusual observations in

order to complete the model. The transfer function models were then used to predict water contents at depths of interest (0.20, 0.35, 0.50 and 0.60 m) and the average water content in the top 0.60 m soil profile W_{AVG} from the measured water content at 0.10 m depth. The predictions were rational. The next irrigation and how much the soil water content would rise after the irrigation event were correctly estimated.

Since the irrigation dose for four irrigation events in this study were almost the same, we used one average mean level ω_t = 0.087 to depict the effectiveness of an irrigation moment on the time series of soil water content. In the case of variable irrigation doses, we suggest studying the effect of each irrigation event and include their effects separately in the model.

5. References

Alessi, S., Prunty, L., Schuh, W.M., 1992. Infiltration simulations among five hydraulic property models. Soil Science Society of America Journal 56, 675–682.

Arguedas-Rodriguez, F. R., 2009. Calibrating capacitance sensors to estimate water content, matric potential, and electrical conductivity in soilless substrates. University of Maryland, MS Thesis. 118p.

Betts, A. K., Ball, J. H., Baljaars, A. C. M., Miller, M. J., Viterbo, P., 1994. Coupling between land –surface, boundary – layer parameterizations and rainfall on local and regional scales: Lessons from the wet summer of 1993. Fith Conf. Global changes studies: American Meteorological Society. Nashville, 174-181.

Bogena, H. R., Huisman, J. A., Oberdorster, C., Vereecken, H., 2007. Evaluation of a low cost water content sensor for wireless network applications. Journal of Hydrology 344, 32-42.

Bonquist Jr., J. M., Jones, S. B., Robinson, D. A., 2005. Standardizing characterizatin of electromagnetic water content sensors. Par 2. Evaluation of seven sensing systems. Vadose Zone Jouranl 4, 1059-1069.

Box, G.E.P., Jenkins, G.M., Reinsel, G.C., 1994. Time Series Analysis: Forecasting and Control. Englewood Cliffs, New Jersey.

Bresler, E., Dagan, G., 1981. Convective and pore scale dispersive solute transport in unsaturated heterogeneous fields. Water Resources Research 17 (6), 1683–1693.

Bresler, E., Dagan, G., 1983a. Unsaturated flow in spatially variable fields. 2. Application of water flow models to various fields. Water Resources Research 19 (2), 421–428.

Bresler, E., Dagan, G., 1983b. Unsaturated flow in spatially variable fields. 3. Solute transport models and their application to two fields. Water Resources Research 19 (2), 429–435.

Butters, G.L., Jury, W.A., 1989. Field scale transport of bromide in an unsaturated soil. 2. Dispersion modeling. Water Resources Research 25 (7), 1583–1589.

Carletti, P., Vendramin, E., Pizzeghello, D., Concheri, G., Zanella, A., Nardi, S., Squartini, A., 2009. Soil humic compounds and microbial communities in six spruce forests as function of parent material, slope aspect and stand age. Plant and Soil 315, 47-65.

Chen, C., Liu, L., 1993. Joint estimation of model parameters and outlier effects in time series. Journal of the American Statistical Association 88 (421), 284–297. Cleveland, R.B., Cleveland, W.S., McRae, J.E., Terpenning, I., 1990. STL: a seasonaltrend decomposition procedure based on loess. Journal of Official Statistics 6, 3–73.

Chen, M. M., Zhu, Y. G., Su, Y. H., Chen, B. D., Fu, B. J., Marschner, P., 2007. Effects of soil moisture and plant interactions on the soil microbial community structure. European Journal of Soil Biology 43,31-38.

Comegna, A., Coppola, A., Comegna, V., Severino, G., Sommella, A., 2010. State-space approach to evaluate spatial variability of field measured soil water status along a line transect in a volcanic-vesuvian soil. Hydrology and Earth System Sciences 14, 2455–2463.

Cryer, J.D., Chan, K.S., 2008. Time Series Analysis with Applications in R, second ed. Springer, New York.

Dagan, G., Bresler, E., 1983. Unsaturated flow in spatially variable fields. 1. Derivation of models of infiltration and redistribution. Water Resources Research 19 (2), 413–420.

Dane, J. H., Toop, C., 2002. Methods of soil analysis. Part 4. Physical Methods SSSA, Segoe Road, Madison, WI 53711, USA.

Destouni, G., Cvetkovic, V., 1991. Field scale mass arrival of sorptive solute into the groundwater. Water Resources Research 27 (16), 1315–1325.

El-Kadi, A., 1987. Variability of infiltration under uncertainty in unsaturated zone parameters. Journal of Hydrology 90, 61–80.

Engman, E. T., 1991. Soil moisture needs in earth sciences. In. Proceedings of international geoscience and remote sensing symposium (IGARSS), 477-479.

Entekhabi, D., Nakamura, H., Njoku, E. G., 1993. Retrieval of soil moisture by combined remote sensing an modelling, In: Choudhury, B. J., Kerr, Y. H., Njoku, E. G., Pampaloni, P., eds. ESA/NASA International workshop on passive microwave remote sensing research related to Land-Atmosphere Interactions, St. Lary, France, 485-498.

Fast, J. D., McCorecle, M. D., 1991. The effect of heterogenous soil moisture on a summer barcolinic circulation in the central united states. Monthly Weather Review 119, 2140-2167.

Freeze, R.A., 1975. A stochastic conceptual analysis of one-dimensional groundwater flow in nonuniform heterogeneous media. Water Resources Research 11 (5), 725–741.

Greenholtz, D.E., Yeh, T.C.J., Nash, M.S.B., Wierenga, P.J., 1988. Geostatistical analysis of soil hydrologic properties in a field plot. Journal of Contaminant Hydrology 3 (2–4), 227–250.

Grubbs, F., 1969. Procedures for detecting outlying observations in samples. Technometrics 11 (1), 1–21.

Gupta, R.K., Chauhan, H.S., 1986. Stochastic modeling of irrigation requirements. Journal of Irrigation and Drainage Engineering: ASCE 112, 265–276.

Hackl, E., Pfeffer, M., Dona, C., Bachmann, G., Zechmeister-Boltenstern, S., 2005. Composition of the microbial communities in the mineral soil under different types of natural forest. Soil Biology & Biochemistry 37, 661-671.

Hafen, R., Anderson, D., Cleveland, W., Maciejewski, R., Ebert, D., Abusalah, A., Yakout, M., Ouzzani, M., Grannis, S., 2009. Syndromic surveillance: STL for modeling, visualizing, and monitoring disease counts. BMC Medical Informatics and Decision Making 9, 21.

Hipel, K. W., Mcleod, A. I., 1994. Time series modelling of water resources and environment systems, Elsevier.

Hoff, J.C., 1983. A Practical Guide to Box–Jenkins Forecasting. Lifetime Learning Publications, London.

Indelman, P., Touber-Yasur, I., Yaron, B., Dagan, G., 1998. Stochastic analysis of water flow and pesticides transport in a field experiment. Journal of Contaminant Hydrology 32 , 77–97.

Jackson, T. J., Hwley, M. E., O'Neill, P. E., 1987. Preplanting soil moisture using passive microwave sensors. Water Resources Bulletin 23, 11- 19.

Jackson, T. J., Le Vine, D. M., Hsu, A. Y., Oldak, A., Starks, P. J., Swift, C. T., Isham, J. D., Haken, M., 1999. Soil moisture mapping at regional scales using microwave radiometry: The Southern Great Plains hydrology experiment. IEE Transactions on Geoscience and Remote Sensing 37.

Jones, J.W., Hoogenboom, G., Porter, C.H., Boote, K.J., Batchelor, W.D., Hunt, L.A., Wilkens, P.W., Singh, U., Gijsman, A.J., Ritchie, J.T., 2003. DSSAT cropping system model. European Journal of Agronomy 18, 235–265.

Kelleners, T. J., Soppe, R. W. O., Robinson, D. A., Shape, M.G., Ayars, J.E. Skaggs, T. H., 2004. Calibration of capacitance probes sensors using electric circuit theory. Soil Science Society of America Journal 68, 430-439.

King, B. A., Wall, R. W., Taberna Jr, J. P., 2001. Visual soil water status indicator for improved irrigation management. Computers and Electronics in Agriculture 32, 31-43.

Lopez-Bermudez, F., Alias, L.J., Martinez Fernandez, P., Romero Diaz, M.A., Marin, P., 1991. Escorrentias y perdidas de suelo en calcisol petrico bajo ambiente mediterraneo semiarido. Cuaternario y Geomorfologia 5, 77-89.

Makkawi, M.H., 2004. Effect of porous medium heterogeneity on water flow: a stochastic hydrofacies approach. Hydrogeology Journal 12, 481–487.

Marino, M.A., Tracy, J.C., Taghavi, S.A., 1993. Forecasting of reference crop evapotranspiration. Agricultural Water Management 24, 163–187.

Martinez-Mena, M., Williams, A. G., Ternan, J. L., Fitzjohon, C., 1988. Role of antecedent soil water content on aggregates stability in a semi-arid environment. Soil and Tillage Research 48, 71-80.

McCleary, R., Hay, R.A., 1980. Applied Time Series Analysis for the Social Sciences. Sage Publications Inc., Thousand Oaks.

McDowall, D., McCleary, R., Meidinger, E.E., Hay, R.A., 1980. Interrupted Time Series Analysis. Sage Publications, Beverly Hills, CA.

Morris, S.J., Boerner, R.E.J., 1999. Spatial distribution of fungal and bacterial biomass in southern Ohio hardwood forest soils: scale dependency and landscape patterns. Soil Biology & Biochemistry 31, 887-902.

Panda, R.K., Behera, S.K., Kashyap, P.S., 2004. Effective management of irrigation water for maize under stressed conditions. Agricultural Water Management 1, 181–203.

Pankratz, A., 1983. Forecasting with Univariate Box–Jenkins Models: Concepts and Cases. John Wiley and Sons, New York.

Puigdefábregas,J.,Solé-Benet,A.,Lázaro,R.,Nicolau, J. M. 1992. Factores que controlan la escorrentía en una zona semiárida sobre micaesquistos. F. López, Conesa and A. Romero, eds. En Estudios de Geomorfología en España, 1: 117 - 127. Sociedad Española de Geomorfología, Murcia.

R Development Core Team, 2010. R: A Language and Environment for Statistical Computing. R Foundation for Statistical Computing, Vienna, Austria, ISBN 3-900051-07-0, URL: http://www.R-project.org/.

Raghuwanshi, N.S., Wallender, W.W., 1996. Modeling seasonal furrow irrigation. Journal of Irrigation and Drainage Engineering: ASCE 122, 235–242.

Raghuwanshi, N.S., Wallender, W.W., 1997. Economic optimization of furrow irrigation. Journal of Irrigation and Drainage Engineering: ASCE 123, 377–385.

Raghuwanshi, N.S., Wallender, W.W., 1998. Optimization of furrow irrigation schedules, designs and net return to water. Agricultural Water Management 35, 209–226.

Raghuwanshi, N.S., Wallender, W.W., 1999. Forecasting and optimizing furrow irrigation management decision variables. Irrigation Science 19, 1–6.

Rogers, B.F., Tate III, R.L., 2001. Temporal analysis of the soil microbial community along a toposequence in Pineland soils. Soil Biology & Biochemistry 33, 1389-1401.

Saha, S. K., 1995. Assessment of regional soil moisture conditions by coupling satellite sensor data with a soil-plant system heat and moisture balance model. International Journal of Remote Sensing 16: 972-980.

Sarangi, A., Singh, A., Bhattacharya, A.K., Singh, A.K., 2006. Subsurface drainage performance study using SALTMOD and ANN models. Agricultural Water Management 84, 240–248.

Schulin, R., van Genuchten, M.T., Fliihler, H., Ferlin, P., 1987. An experimental study of solute transport in a stony field soil. Water Resources Research 23 (9), 1785–1794.

Shani, U., Ben-Gal, A., Tripler, E., Dudley, L.M., 2007. Plant response to the soil environment: an analytical model integrating yield, water, soil type, and salinity. Water Resources Research 43, W08418, http://dx.doi.org/10.1029/ 2006WR005313.

Shumway, R.H., Stoffer, D.S., 2006. Time Series Analysis and its Applications with R. Examples. Springer, New York.

Soebiyanto, R.P., Adimi, F., Kiang, R.K., 2010. Modeling and predicting seasonal influenza transmission in warm regions using climatological parameters. PLoSOne 5 (3), 10.

Thomas, A.M., 1966. In situ measurement of moisture in soil and similar substances by 'fringe' capacitance. Journal of Scientific Instruments 43, 21–27.

Topp, G. C., Davis, J. L., Annan, A. P., 1980. Electromagnetic determination of soil water content: Measurements in coaxial transmission lines. Water Resources Researcch 16, 574-582.

Vandaele, W., 1983. Applied Time Series and Box–Jenkins Models. Academic Press, New York.

Wagenet, R.J., Hutson, J.L., 1989. LEACHM: Leaching Estimation and Chemistry Model. A Process based Model for Water and Solute Movement Transformations, Plant Uptake and Chemical Reactions in the Unsaturated Zone. Water Resources Institute, Cornell University, Ithaca.

Walker, J. P., Willgoose, G. R., Kalma, J. D., 2004. In situ measurement of soil moisture: a comparsion of techniques. Journal of Hydrology 293, 85-99.

Walker, J., 1999. Estimating soil moisture profile dynamics from near surface soil moisture measurements and standard meteorological data. Ph.D. dissertation, the University of Newcastle, Australia.

Wang, L., Qu, J. J., 2009. Satellite remote sensing applications for surface soil moisture monitoring: A review. Earth Sci. China. 2, 237-247

Wei, W.W.S., 1989. Time Series Analysis: Univariate and Multivariate Methods. Person Addison-Wesley, New York.

Wichern, F., Joergensen, R.G., 2009. Soil microbial properties along a precipitation transect in southern Africa. Arid Land Research and Management 23, 115-126.

Wildenschild, D., Jensen, K.H., 1999. Numerical modeling of observed effective flow behavior in unsaturated heterogeneous sands. Water Resources Research 35, 29–42.

Wu, L., Allmaras, R.R., Lamb, J.A., Johnson, K.E., 1996. Model sensitivity to measured and estimated hydraulic properties. Soil Science Society of America Journal 60, 1283–1290.

Wu, L., Jury, W.A., Chang, A.C., Allmaras, R.R., 1997. Time series analysis of field measured water content of a sandy soil. Soil Science Society of America Journal 61, 736–742.

“The only reason for time is so that everything doesn't happen at once.”

ALBERT EINSTEIN

4. Soil salinity

4. Soil salinity

Table of contents

Abstract

Using the linear relationship between soil dielectric constant (ε_b) and the bulk electrical conductivity (σ_b) under laboratory conditions, Hilhorst (2000) model was able to convert σ_b to pore water electrical conductivity (σ_p). In the present study, the application of the linear relationship ε_b - σ_b to data obtained from field capacitance sensors, resulted in strong positive autocorrelations between the residuals of that regression. By including a stochastic component to the linear model , rearranging it to a Time-varying Dynamic Linear Model (DLM), and using Kalman filtering and smoothing, we were able to derive an accurate offset of the relationship ε_b - σ_b and to estimate the evolution of σ_p over time. It was shown that the offset varies for each depth in the same soil profile. A reason for this might be the changes in soil temperature along the soil profile. Once σ_p was estimated for each depth in the study fields, using a (multiple input-one output) transfer function model, we could predict soil salinity at the 0.10 m depth and in the top 0.60 m of the soil profile by measuring soil water content and soil temperature at the 0.10 m depth. Moreover, the effects of the usual irrigation frequency on soil salinity behaviour were evaluated. As a result, the offset and σ_p were precisely estimated for each depth, and predictions of soil salinity by measuring soil water and soil temperature were logical. Also, the next irrigation time and its effect on soil salinity at the depth of interest were correctly estimated. Finally, it was found that for each depth, farmers left the field with less soil salinity than at the beginning of the crop's vegetative stage. The study showed that the quality of irrigation water had a significant effect on soil salinity at the root zone in the study fields.

Key words: Capacitance sensor; Soil dielectric; Time-varying Linear Dynamic Model (LDM); Kalman filtering; Offset; Soil salinity; Transfer function model.

1. Introduction

A saline soil is defined as the accumulation of water-soluble salts in the soil profile to a level that impacts on agricultural production, water quality, environmental health, and economic welfare (Regasamy, 2006). Chloride, sulphate and bicarbonate salts of sodium, calcium and magnesium contribute in varying degrees to soil and water salinity. Salinity affects 7% of the world's land area, which amounts to 930 million ha (Szabolcs, 1994; based on FAO 1989 data). The area is increasing; a global study of land use over 45 years found that 6% had become saline (Ghassemi et al. 1995). This amounts to 77 million ha.

Salinization is an important process in land degradation and nutrient deficiency. Munns (2002) showed that if excessive amounts of salt enter the plant, salt will eventually rise to toxic levels in the older transpiring leaves, causing premature senescence, and reduce the photosynthetic leaf area of the plant to a level that cannot sustain growth. Maas and Hoffman (1977) demonstrated that salinity induces nutritional imbalances or deficiencies causing decreased growth and plant injury for which osmotic effects alone cannot account. Thiruchelvam and Pathmarajah (1999), who studied the salinity problems in Sri Lanka's Mahaweli River System "H" Irrigation Project, showed that salinity can lead to the following agricultural problems if left uncorrected: a) reduced crop intensity; b) decreased profitability and; c) land scarcity. Among a lot of studies are investigated in the links between dryland salinity and climate change, John (2005) has conducted a detailed analysis of the interaction between climate change and dryland salinity in the eastern wheat belt of Western Australia. She concluded that climate change may reduce farm profitability in that region by 50 per cent or more compared to historical climate, and that the reduced profitability of farms would probably would affect the capacity of farmers to adopt some practices that have been recommended to farmers to prevent land degradation through dryland salinization. Ghassemi et al. (1995) concluded in their study that extensive areas of irrigated land have been and are increasingly becoming degraded by salinization and water-logging resulting from over –irrigation and other forms of poor agricultural management. Thus, a practical methodology is needed for timely and spatially assessment of soil salinity in irrigated fields, for evaluating the appropriateness of related management practices.

1.1. Measuring salinity

Salinity is most commonly measured with an electrical conductivity (EC) meter that estimates the concentration of soluble salts in a soil slurry or water solution by how well an electrical current passes through the medium. The ability of a solution to conduct electricity increases with increasing salt content; therefore, a high EC value corresponds to high amounts of soluble salts, and vice versa. A soil is considered saline if the electrical conductivity of its saturation extract (EC_e) is above 4 dS m^{-1} 25ºC (US Salinity Laboratory Staff, 1954). However, the threshold value above which deleterious effects occur can vary depending on several factors including plant type, soil water regime and climatic condition (Maas, 1986).

Determining the electrical conductivity of the pore water of soil (σ_p) requires extraction of the pore water from the soil by suction, or to use saturated paste conductivity measurement, and both conventional methods are labour- intensive. And it is not certain that all ions are collected in the extract sample (Hilhorst, 2000). Additionally, in their study, Rhoades et al (1997) criticized two concepts that have been used by US Salinity Laboratory Staff (U.S. Salinity Laboratory Staff, 1954) to evaluate the appropriateness of irrigation and drainage systems and practices with respect to salinity control. These concepts are leaching requirement (L_r), which refers to the quantity of irrigation water required for transporting salts through the soil profile to maintain a favourable salt balance in the root zone for plant development, and salt-balance-index (SBI), defined as the relation between the quantity of dissolved salts carried to an area in the irrigation water and the quantity of dissolved salts removed by the drainage water. These two conventional procedures are criticized because they do not provide sufficiently detailed spatial information to adequately characterize salinity conditions and to determine its natural or management-related causes. SBI fails because it provides no information about the soil salinity level existing within any specific field of the project. Many other studies on soil salinity assessment concluded that it is important to assess soil salinity temporally and spatially for correctly evaluating its evolution and for reasonably predicting its values (Hajrasuliha et al., 1980; Mahmut et al., 2003; Rhoades et al., 1997; Shouse et al., 2010; Xiaoming et al., 2012).

A new way to evaluate the conductivity of σ_p temporally and spatially is to translate the electrical conductivity of the bulk soil (σ_b) to σ_p using methods, models and estimates. To measure σ_b, new devices have been developed, such as time-domain reflectometry (TDR) and frequency-domain refectomerty.

Temperature and water content have a significant effect on accurate σ_b determination, requiring that sensors have a temperature compensation capability for precise measurement (Scoggins and van Iersel, 2006). Electrical conductivity sensors therefore need to simultaneously measure three variables: water content, temperature and σ_b to provide a precise real-time measurement of σ_b.

However, we need to go one step further and calculate a soil specific offset value.to provide an accurate estimate of σ_p This offset eliminates the contribution of surface electrical conductivity σ_s and permittivity of dry soil ($\varepsilon'_{\sigma b=0}$) in the final estimation of σ_p, as described by the Rhoades (1976, 1989) and Hilhorst (2000) models. Such models estimate the σ_p by utilizing different physical parameters read directly by the sensor or estimated separately during laboratory experimentation. In the next section, a brief description of Rhoades et al. (1989) model and further details of the Hilhorst (2000) model are presented. The senores were used in this study applied the Hilhorst (2000) model to get σ_p by measuring σ_b**.**

1.2. Models to convert σ_b to σ_p

1.2.1. Rhoades et al. (1989) model

By dividing the mixed soil water system into three separate current-flow pathways, Rhoades et al. (1989) were able to build up a model explaining the expected electrical conductivity of the system. These pathways are demonstrated in Fig. 4.1 and they are as follows:

1. A solid–liquid interphase, the conductance pathway passing through alternating layers of soil particles and soil solution.
2. A liquid phase, the conductance pathway passing through continuous soil solution.

3. A solid phase, the conductance pathway passing through or along the surface of soil particles in direct and continuous contact.

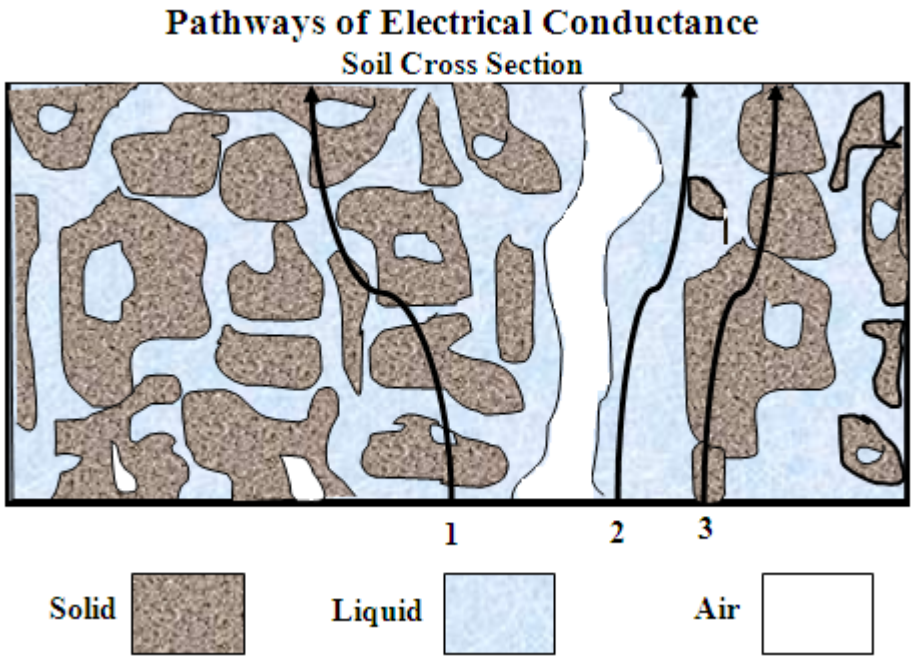

Fig. 4.1. Three conductance pathways for the σ_b measurements. Modified from Rhoades et al. (1989).

The model was proposed by Rhoades et al. (1989) intended to assess soil salinity as bulk electrical conductivity:

$$\sigma_b = \left[\frac{(\theta_s + \theta_{ws})^2 \sigma_{ws} \sigma_s}{(\theta_s)\sigma_{ws} + (\theta_{ws})\sigma_s} \right] + (\theta_w - \theta_{ws})\sigma_{wc} \quad (1)$$

Where:

Θ_s is the volumetric soil water content in the continuous liquid pathway,
Θ_{ws} is the volumetric soil water content in the series-coupled pathway,
σ_{ws} is the specific electrical conductivity of the series-coupled water phase,
σ_s is the electrical conductivity of the surface conductance soil phase, and

$\Theta_w = \Theta_{ws} + \Theta_{wc}$ where Θ_{wc} is the volumetric soil content in the continuous liquid pathway.

σ_{wc} is the specific electrical conductivity of the continuous water phase.

Equation 1 can be solved for σ_p with the assumption that $\sigma_{ws} \approx \sigma_{wc}$ and it can be re-arranged as a quadratic equation, and solved for its positive root as:

$$\sigma_p = \frac{-B + \sqrt{B^2 - 4AC}}{2A} \qquad (2)$$

where : $A = [(\theta_s)(\theta_w \theta_{ws})]$

$$B = [(\theta_s + \theta_{ws})^2 (\sigma_s) + (\theta_w - \theta_{ws}) * (\theta_{ws} \sigma_s) - (\theta_s \sigma_b)]$$

$$C = -[\theta_{ws} \sigma_s \sigma_b]$$

Rhoades et al. (1989) state the necessity for an offset value or estimation of the surface electrical conductivity σ_s in order to estimate pore water electrical conductivity σ_p. This offset value σ_s is calculated by plotting the σ_b versus the solution electrical conductivity σ_w.

1.2.2. Hilhorst (2000) model

The σ_b of the soil depends on both the σ_p and water content (θ) (Persson, 2002). Thus, the $\sigma_p$can only be predicted if θ is constant, or if the relationship between σ_p, σ_b, and θ is determined. Several different models of $\sigma_p - \sigma_b - \theta$ relationship have been developed (Rhoades et al., 1976; Mualem and Friedman, 1991; Malicki and Walczak, 1999). Malicki et al. (1994) discovered a high degree linear correlation between dielectric constant (ε_b) and σ_b values by using time domain reflectometry for most of soil types. Hilhorst (2000) took advantage of this relationship and enabled to convert σ_b to σ_p by using a theoretical model describing a liner relationship between σ_b and ε_b.

1.2.3. The Linear $\sigma_p - \sigma_b$ - θ Model

The σ_p can be determined according to Hilhorst (2000) from the equation (see the details about this equation in the Materials and methods section):

$$\sigma_p = \frac{\varepsilon_p * \sigma_b}{\varepsilon_b - \varepsilon_{\sigma_b=0}} \quad (3)$$

where σ_p is the pore water electrical conductivity (dS m^{-1}); ε_p is the real portion of the dielectric permittivity of the soil pore water (unitless); σ_b is the bulk electrical conductivity, (dS m^{-1}); ε_b is the real portion of the dielectric permittivity of the bulk soil (unitless); $\varepsilon_{\sigma b=0}$ is the real portion of the dielectric permittivity of the soil when bulk electrical conductivity is 0 (unitless). However, $\varepsilon_{\sigma b=0}$ appears as an offset of the linear relationship between ε_b and σ_b. Hilhorst (2000) found that the $\varepsilon_{\sigma b=0}$ depends on the soil type and varied between of 1.9 and 7.6 in the soils used in his study, he recommended 4.1 as a generic offset.

Many studies applied Hilhorst (2000) model in their experiments to convert σ_b into σ_p. Persson (2002) applied it in time domain-reflectometry (TDR) measurements, laboratory experiments using soil columns with different θ and σ_p. By rearranging Eq. 3, the slope can be calculated theoretically; $\varepsilon_b = \varepsilon_p / \sigma_p * \sigma_b + \varepsilon_{\sigma b=0}$ i.e. slope = ε_p / σ_p. The value of the offset $\varepsilon_{\sigma b=0}$ was obtained as a fitting parameter when the slope was fixed, assuming that ε_p equals the dielectric constant of free water at the specific temperature. He concluded his work by using different offset (within the range of 3.67 to 6.38) according to the soil type. Moreover, the manufacture of capacitance soil moisture senores 5TE (Decagon Devices, Inc., Pullman, WA) also uses Hilhorst (2000) model to convert σ_b into σ_p and they recommended to use offset = 6 for all agricultural soils, Arquedas-Rodriguez (2009) used 5TE sensors in his study and found that offset = 6 did not represent very good the linear relationship between ε_b and σ_b. The WET sensor (Delta- T Device Ltd, Cambridge, UK), is a frequency domain dielectric sensor and is designed to use the standard offset = 4.1 of Hilhorst (2000) model, Bouksila et a.l (2008) worked with a saline gypsiferous soil and found that the accuracy of the WET sensor to predict the σ_p was very poor using the standard value of $\varepsilon_{\sigma b=0}$ = 4.1. Compute

σ_p from σ_b is very important, but still not very well worked out (G. Campbell, Decagon Devices, personal communication, 2010).

1.3. Soil salinity movement models

Fickian-based convection-dispersion equation for predicting solute transport between the land surface and groundwater table will continue to provide convenient tools for analyzing specific experiments on solute movement, these deterministic models still have success for extrapolating information for a limited number of field studies to different soils, crop and climate conditions, as well as to different tillage and water management schemes (Van Genuchten, 1991). For one-dimensional vertical transfer the convection-dispersion equation could describe the solute movement in the unsaturated zone as:

$$\frac{\partial(\rho s)}{\partial t} + \frac{\partial(\theta c)}{\partial t} = \frac{\partial}{\partial z}(\theta D \frac{\partial c}{\partial z} - qc) + \phi \qquad (4)$$

Where θ is the volumetric water content, t is time, z is distance from the soil surface downward, s is the solute concentration associated with the solid phase of the soil, c is the solute concentration of the fluid phase, ρ is the soil bulk density, D is the solute dispersion coefficient, and ϕ is the sink for solutes.

Legal questions have arisen in the literature about the worth of equation 4 for describing solute transport in structured soils characterized by large continuous voids, such as natural interaggregate pores, interpedal voids, earthworm and gopher holes. The progress of solutes in such soils can be largely different from that in fairly homogeneous materials (Beven and Germann, 1982; White, 1985). The fact that most soils are heterogeneous raises significant questions about how to simulate the heterogeneous field-scale transport process (Van Genuchten, 1991).

Due to soil profile heterogeneity, some experimenters have found it more desirable to use stochastic models rather than constant values in describing the future evolution of soil solutes, where the parameters of stochastic transport models are treated as random variables with discrete values assigned according to a given probability distribution.

During the last decade, there has been a significant increase in stochastic models for agronomic applications, such as artificial neural networks (ANNs) (Huang et al., 2010),

including crop development modeling (Zhang et al., 2009; Fortin et al., 2010) and crop yield prediction (Park et al., 2005; Green et al., 2007; Khazaei et al., 2008). Zou et al. (2010) worked on silt loam soil profile data, collected monthly from 2001 to 2006, to compare two mathematical models: the back propagation neural network (BPNN) model and the autoregressive integrated moving average (ARIMA) model. The objective was to predict both the average water content in the top 1 meter profile from water content measured at 0.60 m depth, and the average salt content measured at various depths of the soil profile (0.10, 0.20 and 0.45 m). Sarangi et al. (2006) used artificial neural networks (ANNs) in modeling the root zone soil salinity and the salinity of drainage effluent from subsurface drained rice fields in the coastal clay soils of Andhra Pradesh, India. They observed that, the use of time lag procedure in feeding the input values to the ANNs resulted in better ANNs than the conceptual SALTMOD model for prediction of salinity of the drainage effluent.

Previous studies predicted soil salinity by assuming that historical values of soil water content and temperature do not change, maybe because data on soil water and temperature were not available simultaneously when data of soil salinity was collected (i. e., Zou et al. (2010) predicted soil water content and soil salinity in two separated models because they had data of soil water content and soil salinity from different moments). Soil water content has a significant effect on soil salinity at the root zone (Ben-Gal et al., 2008). In the case of variable irrigation system, predicting the soil salinity time series cannot be properly explained by the ARIMA model and its underlying normality assumption, for the same reasons that were explained in the chapter 2. Therefore, modelling soil salinity in oreder to predict its values for near future, shoud take into accoutnt the changes in irrigation patters. On the other hand, many studies found that calibration measurements of electromagnetic EM induction for prediction of σ_b is affected by soil texture, water content, and soil temperature (McKenzie et al., 1989; Slavich and Petterson, 1990). Sarangi et al. (2006) found that predicting of soil salinity is correlated to the state of soil water content and temperature.

Our study was carried out on variable interval irrigation and used capacitance soil sensors that measure σ_b, soil temperature and θ simultaneously, which enabled us to properly build up models capable to predict soil salinity taking the situation of θ and soil temperature into account.

The objectives of this chapter are:

1. To derive an offset value that would ensure the accurate prediction of σ_p from measurements of σ_b that we are obtained from our field experiments;
2. To study the autocorrelation and partial correlation function for θ and soil temperature measured at shallow depth as well as the cross-correlation function between θ and soil temperature at shallow depth and various greater depths of soil salinity, including average soil salinity in the top 0.60 m profile;
3. To develop models for predicting the soil salinity at various greater depths by measuring θ and soil temperature from a single shallow depth;
4. To use outlier and intervention analysis to examine the effectiveness of the irrigation event in the soil salinity profile; and
5. To monitor the evolution of soil salinity during the crop vegetative stage in the study area and examine the effect of irrigation frequency and depth (either the beneath the furrow or beneath the ridge) on the soil salinity.

2. Materials and methods

2.1. Experiment

Data from Field 1, Field 2 and Field 3 experimental sites were used in this study (see the introduction chapter for its locations), soil characterization for the three fields was defined. The design of capacitance sensor installation was described in chapter 3. To achieve the objective 5 of this chapter, we add three more sensors beneath the ridge (Fig. 4.2).

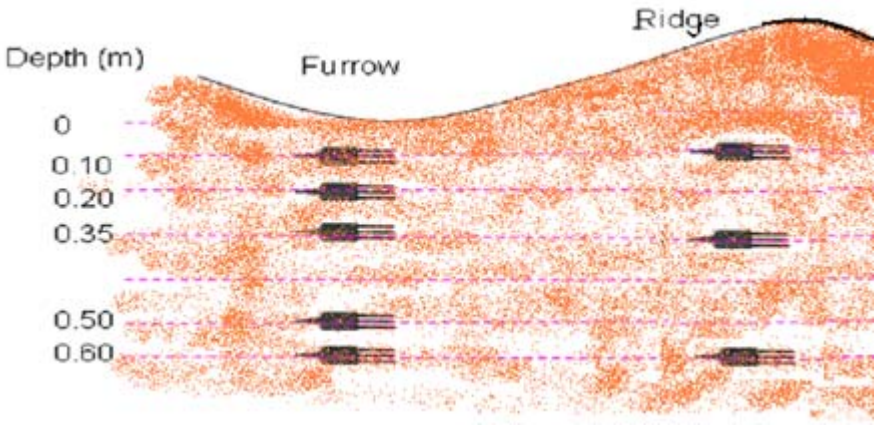

Fig. 4.2. Chart shows sensors distribution in the top 0.60 m soil profile

2.1.1. Capacitance sensor

In this study a capacitance soil sensors (5TE Decagon Devices, Inc., Pullman, WA) were used, they are a commercial capacitive sensors that simultaneously estimate θ , temperature and σ_b and use the Hilhorst (2000) model to convert σ_b to σ_P.

2.2. Deriving Hilhorst (2000) model

The theory behind capacitance soil sensors readings are based on independently measuring both components of the composite permittivity of a material. When an electric field passes through a material (such as soil) some of the energy in the field is transmitted, some is reflected, some is stored and finally some is absorbed and converted into heat. The extent to which each of these occurs within a particular material is determined by its dielectric properties. These are quantified by a parameter called the relative electrical permittivity (ε) of a material which characterises its response to the polarising effect of an applied electric field. The relative permittivity of a dielectric material is defined as:

$$\varepsilon = \varepsilon^{'} - j\varepsilon^{''} \tag{5}$$

where $j = \sqrt{-1}$ is an imaginary number. $\varepsilon^{'}$ and $\varepsilon^{''}$ are the real and imaginary parts of dielectric permittivity; the real part of ε′ represents the stored energy, known as the dielectric constant and provides a surrogate measure of soil water content. The

imaginary part (ε″), accounts for the total energy absorption or energy loss. The energy losses include dielectric loss ($\varepsilon_d^{"}$) and loss by ionic conduction:

$$\varepsilon^{"} = \varepsilon_d^{"} + \left(\frac{\sigma_i}{2\pi f \varepsilon_0} \right) \tag{6}$$

where f is the effective frequency (Hz) of the applied electric field, ε_0 is the permittivity for free space (ε_0=8.854*10^{-12} F m^{-1}), σ_i is the specific ionic conductivity of the material.

For extracted pore water, the imaginary part of the complex permittivity of the pore water is $\varepsilon_p^{"}$. In soil science it is not customary to use $\varepsilon_p^{"}$. It is more practical to use the conductivity of the pore water, σ_P, (Hilhorst, 2000) which can be defined as:

$$\sigma_p = 2\pi . f \varepsilon_0 \varepsilon_p^{"} = 2\pi f \varepsilon_0 \left(\varepsilon_{dp}^{"} + \frac{\sigma_{ip}}{2\pi f} \right) \tag{7}$$

where σ_{ip} represents the ionic conductivity of the extracted pore water. The relaxation frequency of water is 17GHz at 20ºC (Kaatze and Uhlendorf, 1981). The operation frequency for most dielectric or conductivity sensors is <1 GHz (our sensors is 70 MHz). At frequencies which are low with respect to the relaxation frequency of water, $\varepsilon_p^{"}$ is negligible and Eq. 7 can be reduced to:

$$\sigma_P \approx \sigma_{ip} \tag{8}$$

The complex permittivity of the pore water (ε_p) is equal to that of pure water. The real part of the complex permittivity of the water is $\varepsilon_p^{'}$ = 80.3 at 20ºC with temperature coefficient of about -0.37ºC^{-1} (Kaatze and Uhlendorf, 1981). By analogy with Eq. 5 the approximation of ε_p can be written:

$$\varepsilon_p \approx \varepsilon_p^{'} - j \frac{\sigma_p}{2\pi . f} \tag{9}$$

The complex permittivity of the bulk soil (ε_b) is proportional to both ε_p and a function of θ, $g(\theta)$. This $g(\theta)$ function includes soil type and frequency dependency.

For dry soil, there is no water to facilitate ionic conduction; that is, the conductivity of the bulk soil $\sigma_b \approx 0$. We can write ε_b as:

$$\varepsilon_b = \varepsilon_{\sigma_b=0} + \varepsilon_p g(\theta) \tag{10}$$

where $\varepsilon_{\sigma_b=0} \neq 0$ is the permittivity of dry soil; $\varepsilon_{\sigma_b=0}$ appears as offset to ε_b. Also $\varepsilon_{\sigma_b=0}$ is the extrapolated intercept with y axis from a linear part of the $\varepsilon_b^{'}$ vs. σ_b. With this and Eq 8 substituted in Eq 10 ε_b can be written as:

$$\varepsilon_b = \varepsilon_{\sigma_b=0}^{'} + \varepsilon_p^{'} g(\theta) - j\frac{\sigma_p}{2\pi f \varepsilon_0} g(\theta) \tag{11}$$

The working principle of the capacitance sensors (5TE, Decagon Devices, Inc., Pullman, WA) is based on considering that a dielectric material acts as a lossy medium between its two screws (such as soil between the probe parallel prongs), so that the electromagnetic wave impedance, Z (Ω), across the soil may be expressed as:

$$Y = j\omega\varepsilon_0\varepsilon_b k \tag{12}$$

where Y is the reciprocal of the impedance Z, $\omega = 2\pi f$ is the angular frequency (rad s^{-1}), ε is the soil permittivity, and k (m) is a geometric factor determined by the distance between the prongs and the area in contact with the soil, such that contact problems between the soil and the sensor´s screws will be reflected in this factor. A lossy capacitor can be represented by a capacitance, C, connected in parallel to an electrical resistance with a conductance, G. C represent the energy storage and is related to $\varepsilon_b^{'}$, G represent the energy loss and is related to σ_b (Regalado et al., 2007). Y may be written in terms of C and G as:

$$Y = G + j\omega C \tag{13}$$

From Eq 9 and 10, and with 4 to 11 Hilhorst (2000) was able to build up the relationship between σ_p from measurements of, σ_b, ε_p and ε_b as follows:

$$\sigma_p = \frac{\varepsilon_p * \sigma_b}{\varepsilon_b - \varepsilon_{\sigma_b=0}} \tag{14}$$

2.3. Kalman Filter

The purpose of the Kalman Filter is to provide an estimate of the unobservable state vector based on model information and measurement information, balancing out the errors of both. It is a sequential algorithm for minimising the state error variance.

Our study used the Hilhorst (2000) model to present results from the application of the Kalman filter statistical estimation technique to continuous soil state (σ_p and $\varepsilon_{\sigma b=0}$) determination, from capacitance soil sensor determinations. A Kalman filter soil state model is used to merge available soil physics data with data from capacitance sensors (ε_b). The model makes continuous estimates of soil status and weights ε_b observations according to input and model-propagated error covariances, in order to obtain suitable σ_p and $\varepsilon_{\sigma b=0}$ for the study area.

The state-space model has three parts, σ_p and $\varepsilon_{\sigma b=0}$ states, ε_b observations, and a Kalman filter that updates the state by assimilating observations into the dynamic soil state estimate. The dynamic model propagates the soil profile status estimate forward in time under time-varying atmospheric boundary conditions. When observations of ε_b are available, the Kalman filter uses the propagated state estimate and a record of the propagation steps to adjust the state, in proportion to the difference between the observed and the predicted value. The ratio of proportionality (the Kalman gain) is calculated from a propagated model state error covariance matrix and an estimate of ε_b measurement error. Together, these models produce continuous estimates of σ_p and $\varepsilon_{\sigma b=0}$ states and their error covariances.

2.4. Time-varying Dynamic linear Model

The Dynamic Linear Model (DLM) is presented as a special case of a general state space model, being linear and Gaussian. For dynamic linear models, estimation and forecasting can be recursively obtained by the well-known Kalman filter. Estimating unknown parameters in a DLM requires numerical techniques, but the Kalman filter can be used in this case as a building block for evaluating the likelihood function or for simulating the unobservable states.

The R (R Development Core Team 2012) package dlm (Petris, 2010) provides an integrated environment for Bayesian inference using DLM, and the package includes functions for Kalman filtering and smoothing, as well as maximum likelihood estimation.

2.5. Model identification

A time-varying DLM can be modelled as

Observation equation → $y_t = \alpha_t + x_t\beta_t + v_t$ $\quad v_t - \mathcal{N}(0, V_t)$ (15)

State equation → $\alpha_t = \alpha_{t-1} + w_{\alpha,t}$, $\beta_t = \beta_{t-1} + w_{\beta,t}$ $\quad w_{d,t} - \mathcal{N}(0, w_{\alpha,t})$ (16)

$w_{\beta,t} - \mathcal{N}(0, w_{\beta,t})$

here y_t is an m- dimensional vector, representing the observation at time t; in our study it represents ε_b observations. x_t is an m.m-dimensional matrix of covariates. While α_t and $\beta_t$are unobservable m-dimensional vectors presenting the state of the system at time t, in our study they represent $\varepsilon_{\sigma b=0}$ and σ_p, respectively. v_t , $w_{\alpha,t}$ and $w_{\beta,t}$ are the Gaussian white-noise errors. The only parameters of the model are the observations and evolution variancesV_t, $w_{\alpha,t}$ and $w_{\beta,t}$. These are usually estimated from available data using maximum likelihood or Bayesian techniques.

2.5.1. Seasonality

When the model has a seasonal component, it is usual to include a Dynamic Linear Model (DLM) to describe this component. In the state –space expression, the seasonal component may have a stochastic error that allows changes for the seasonal pattern over time.

So Eq. 15 may have a seasonal component (S_t) and may be written as:

$$y_t = \alpha_t + x_t\beta_t + S_t + v_t \qquad (17)$$

2.5.2. A transfer function model: influences of soil water, soil temperature and irrigation management on soil salinity in loamy sand soil.

We used techniques of time series analysis according to the methodology described in chapter 3 to accomplish this objective, but here we developed the transfer function model to include two inputs (soil water content and soil temperature), in order to obtain the output (soil salinity). In brief, time series analysis of soil salinity was made in three steps.

The first one involved applying the Box-Jenkins method (Box et al., 1994) in order to identify an appropriate univariate model for the time series of soil salinity , soil water and soil temperature at 0.10 m depth. This study used the seasonal autoregressive integrated moving average (ARIMA) $(p, d, q) \times (P, D, Q)_S$ model, where p, q are the orders of the regular autoregressive and moving average factors, and P, Q are the seasonal autoregressive and moving average factors, respectively; d and D are the orders of differencing for the regular and seasonal parts, respectively; sub-index S denotes the seasonal period (24 hours in this study).

The second step was evaluating the effects of irrigation time by including it in the soil salinity, soil water content and soil temperature models as intervention analysis and searching for the presence of outliers in the univariate series.

The third step was identifying the appropriate transfer function approach by modelling the linear system, using the soil water content and soil temperature time series at 0.10 m depth as inputs, while the outputs were the soil salinity time series at 0.10 m depth and the average soil salinity in the top 0.60 m of the soil profile.

The first and second steps were explained in details in chapter 3 (Materials and Methods); the third step consists of a transfer function (multiple input-single output).

Observations and predictions of two time series (input X_{1t} and X_{2t}) may be used to estimate the outcome of another time series (output G_t) by modelling the linear system with a relatively small number of parameters. The model takes the form:

$$G_t = \frac{A_1(B)}{C_1(B)} X_{1,t-b_1} + \frac{A_2(B)}{C_2(B)} X_{2,t-b2} + a_t$$

where $A(B)$ and *C(B)* are polynomials of the *s* and *r* orders, respectively:

$$A(B) = (A_0 - A_1 B - A_2 B^2 - \ldots - A_s B^s)$$
$$C(B) = (1 - C_1 B - C_2 B^2 - \ldots - C_r B^r)$$

where $A_0, A_1, A_2, \ldots, A_s$ and $C_1, C_2, \ldots, C_r$ are the parameters of the model, *b* is the latent parameter, *B* is the backshift operator, and a_t is a disturbance (noise).

$A(B)/C(B)$ is called the transfer function of the system. The procedure for building a transfer function model involves three steps: a) identification, b) estimation and c) model checking. By using a univariate model for input input X_{1t} and X_{2t} with white noise residuals, the same filter can be applied to the output series G_t (pre-whitening). Cross-correlation of the two residuals allows us to identify the transfer function form.

In this study, the transfer function approach was applied by choosing the soil water and soil temperature observations at 0.10 m as primary series (X_{1t} and X_{2t}), while the output series (G_t) was chosen from the observations of soil salinity time series at 0.10 m depth and the average soil salinity in the top 0.60 m of the soil profile. Average soil salinity in the top 0.60 m of the soil profile was calculated with the formula that Wu et al. (1997)[3].

[3] $W_{AVG} = \left[\frac{1}{2}(D_1 - D_0)\theta_1 + \sum_{i=1}^{n-1} \frac{1}{2}(D_{i+1} - D_{i-1})\theta_i + \frac{1}{2}(Z_n - Z_{n-1})\theta_n \right] / (D_n - D_0)$
where *D* is depth downward (m), and θ_i is volumetric water content at depth D_i

2.6. Data analysis and statistics: Effects of irrigation management applied on soil salinity

We will attain this objective by analysing the effect of irrigation frequency applied in the study area (Field 1: lettuce; Field 2: lettuce; Field 3: artichoke) on soil salinity, the null hypothesis is that**:** irrigation frequency according to the farmer's normal management practice does not affect soil salinity behavior, depending on soil depth and position (beneath the furrow or beneath the ridge). The alternative hypothesis is that**:** irrigation frequency according to the farmer's normal management practice affect soil salinity behavior, depending on soil depth and position (beneath the furrow or beneath the ridge).

For this analysis we collected 30 measurements of soil salinity after three days for each irrigation event. All data were subjected to analysis of variance (ANOVA) procedures using R (R Development Core Team 2012). Appropriate standard errors of the means (S.E.) were calculated. Tukey's studentized range test (HSD) was applied to separate measured parameters of soil salinity exposed to irrigation frequency for each depth.

3. Results and discussion

3.1. Soil characterization

Table 4.1 shows the soil characterization of the three study fields beneath the furrow and ridge at various depths. It shows that the soil particles for clay, silt and sand have little variations in the root zone. The organic matter in study fields is representatative of the area.

Table 4.1. Soil characterization for Field 1, Field 2 and Field 3

Position	Furrow						Ridge			
Depth	0.10 m		0.35 m		0.65m		0.15 m		0.80 m	
Field	Field 1	Field 2&3	Field 1	Field 2&3	Field 1	Field 2&3	Field 1	Field 2&3	Field 1	Field 2&3
Clay (<0.002 mm diameter) %	16.6	35.29	13.12	39.23	22.3	37.23	17.71	32.48	21.55	37.43
Silt (0.05 a 0.002 mm diametre) %	54.89	52.16	55.25	49.34	61.16	51.24	56.34	53.52	59.64	50.92
Sand (2 a 0.05 mm diameter) %	28.51	12.55	31.63	11.42	16.54	11.52	25.96	14	18.81	11.64
USDA Textural Name	silty loam	silty clay loam	silty loam	silty clay loam	silty loam	silty clay loam	silty loam	silty clay loam	silty loam	silty clay loam
Organic matter %	2.38	3.38	1.28	1.6	1.31	0.98	3.97	3.31	1.45	0.91

3.2. Time-varying Linear Dynamic Model (LDM)

In the beginning, the offset value was derived using the method of Persson (2002), by rearranging the Hilhorst (2000) model as follows:

$$\varepsilon_b = \varepsilon_p / \sigma_p * \sigma_b + \varepsilon_{\sigma_b=0} \tag{18}$$

By using hourly field measurements of ε_b and σ_b (1318 observations for each one, Field 1). Table 4.2 shows the relationship ε_b-σ_b. The offset of this relationship is 4.97 and the slope is $1/\sigma_p$= 0.33, so σ_p=5 d S m^{-1} is the average for the all the observations. By applying Durbin–Watson test to see if there is an autocorrelation between the residuals of that regression, Table 4.3 shows that there is an extremely strong and positive autocorrelation, which indicates that the result of that regression is not valid. Moreover, the linear model does not take the evolution of the unobservable variable over time into account. For this reason, it is reasonable to think that σ_p evolves with a stochastic component.

Table 4.2. linear regression ε_b - σ_b

	Estimate	Std. Error	t value	Pr(>|t|)
(offset)	4.978923	0.088208	56.45	<2e-16 ***
1/ σ_p	0.354256	0.002546	139.15	<2e-16 ***
Significant: *P < 0.05, **P < 0.01, ***P < 0.001.				

Table 4.3. Durbin–Watson test to the linear regression ε_b - σ_b

lag	Autocorrelation	D-W Statistic	p-value
1	0.9524539	0.09079999	0

The known parameters for the Hilhorst (2000) model are ε_b, σ_b and ε_p; they are simultaneously and hourly measured by capacitance sensors; while σ_b could be directly obtained from the data logger, ε_b and ε_p were calculated as follows:

$$\varepsilon_b = \frac{\varepsilon_{raw}}{50}$$

$$\varepsilon_p = 80.3 - 0.37\,(T_{soil} - 20)$$

where ε_{raw} represents the raw soil water content counts, and T_{soil} is the soil temperature measured by the sensor directly.

Fig. 4.3 shows the evolution of soil dielectric constant ε_b, water dielectric constant ε_p and soil bulk electrical conductivity σ_b; it also shows that the irrigation events have a significant effect on σ_b and ε_b.

Equation 18 can be modified to the time-varying DLM into observation and unobservable (state) models as follows:

The observation equation (from Eq. 17):

$$(\boldsymbol{\varepsilon_b})_t = (\varepsilon_{\sigma_b=0})_t + (\varepsilon_p * \sigma_b)_t(\frac{1}{\sigma_p})_t + \boldsymbol{s_t} + \boldsymbol{v_t} \qquad v_t - \mathcal{N}(0, {\sigma_v}^2) \qquad (19)$$

The state equation (from Eq. 16):

$$\begin{cases} (\varepsilon_{\sigma_b=0})_{\boldsymbol{t}} = (\varepsilon_{\sigma_b=0})_{\boldsymbol{t-1}} \\ (\frac{\mathbf{1}}{\sigma_p})_{\boldsymbol{t}} = (\frac{\mathbf{1}}{\sigma_p})_{\boldsymbol{t-1}} + w_t \qquad w_t - \mathcal{N}(0, (\sigma_w)_t^2) \\ \boldsymbol{s_t} + \boldsymbol{s_{t-1}} + \boldsymbol{s_{t-2}} \ldots\ldots + \boldsymbol{s_{t-23}} = \mathbf{0} \end{cases} \tag{20}$$

$\boldsymbol{s_t}$ is the seasonal component (every 24 hours). ${\sigma_v}^2$, q and K are the parameters of the model. In equation 19, we added a stochastic component to the Hilhorst (2000) model (the Gaussian white-noise error and the seasonality component (order= 24 hours)). In equation 20, we considered that the offset and the seasonal pattern are constant and that the slope $1/\sigma_p$ changes over time.

As we see in chapter 2, the irrigation events have significant effect on the behaviour of soil water content and should be captured as outliers to improve the model. Fig. 4.3 shows that irrigation events have also a significant effect on the behaviour of ε_b. We increase the state variance $(\sigma_w)_t^2$ by a constant factor (k>1) to capture the time of irrigation event as an outlier where:

$$(\sigma_w)_t^2 \begin{cases} q & if\ t \neq 103, 654, 770, 1112 \\ Kq & if\ t = 103, 654, 770, 1112 \end{cases} \qquad K > 1$$

where 103, 654, 770 and 1112 hours are the irrigation moments from the time of planting. This change in the model gives better estimates of the irrigation time effects on the state values. Once we estimate the parameters, we apply the Kalman filter to get the offset $\varepsilon_{\sigma_b=0}$ and the slope $\frac{\mathbf{1}}{\sigma_p}$.

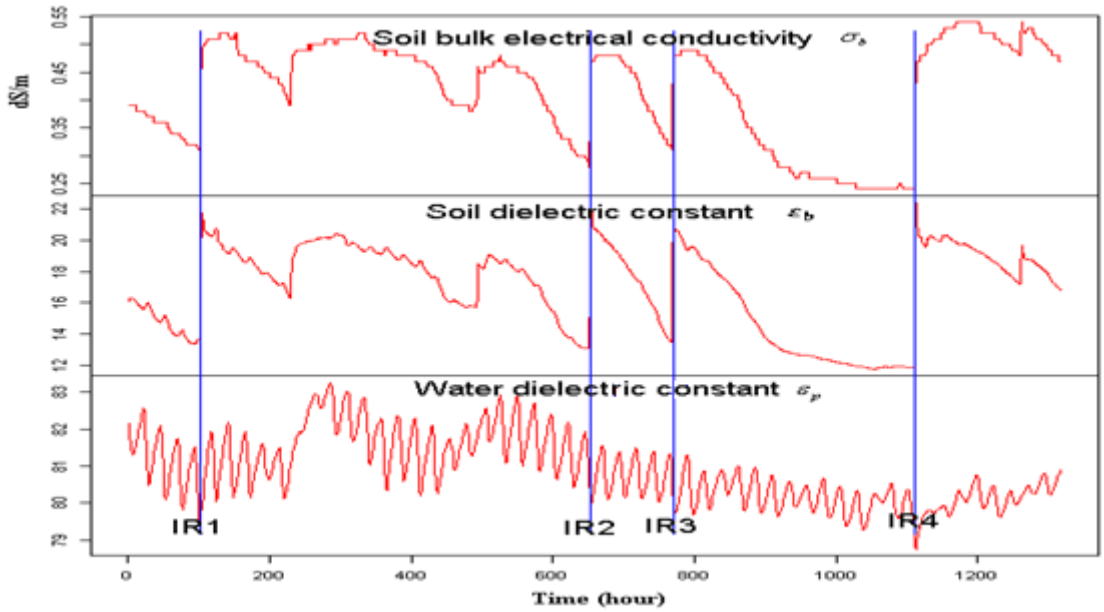

Fig. 4.3. Known variables for the Hilhorst model ε_b (σ_b, εb, *and* εp); IR1, IR2, IR3 and IR4 are the times of the irrigation events. Field 1, Lettuce**.**

3.3. DLM validation

Fig. 4.4 shows the observed and predicted time series of soil dielectric constant ε_b at 0.10 m depth (Field 1, lettuce, furrow). The predicted and observed values agreed reasonably after 1318 observations. The mean absolute error of variance forecasts between prediction and measurement for the time series never exceeded 0.02 (Fig. 4.5).

Fig. 4.6 shows the values of electrical conductivity of soil pore water (σ_p) and offset $\varepsilon_{\sigma b=0}$ by applying the time –varying DLM to the data from Field 1 at 0.10 m depth (lettuce crop). At this depth, the offset is 3.8 and σ_p was varying over time; the figure shows a clear decrease in σ_p at the time of irrigation, which may have been expected since irrigation leaches the salts downward.

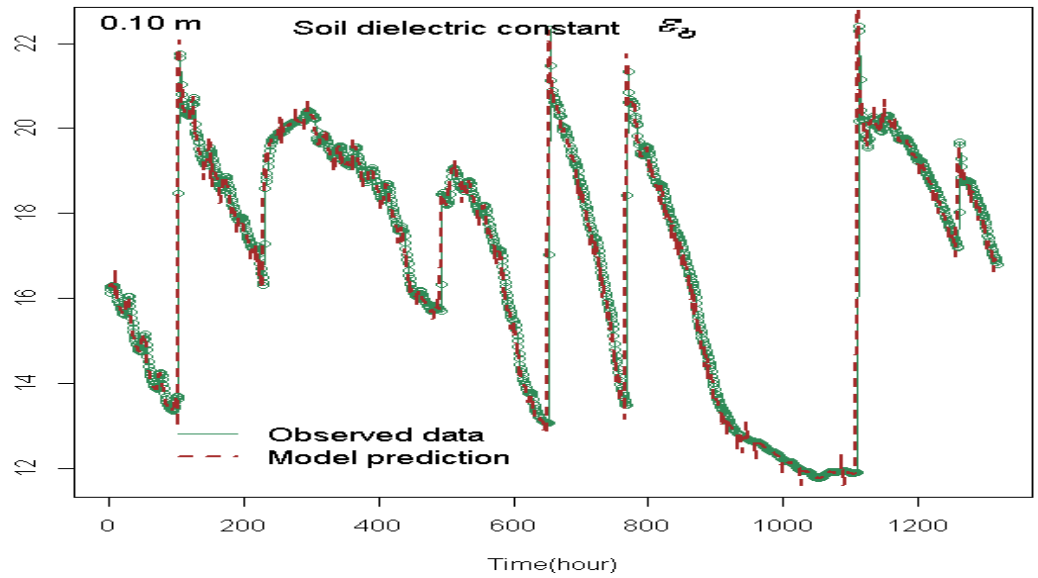

Fig. 4.4. Observed and predicted data of soil dielectric constant at 0.20 m depth (Field 1, furrow, lettuce).

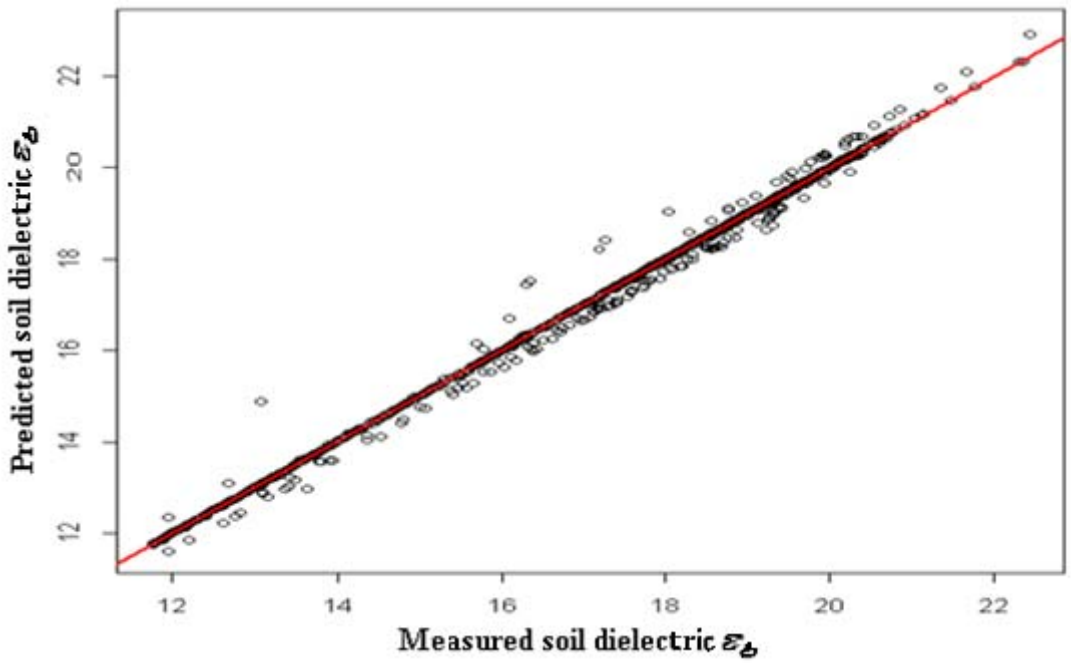

Fig. 4.5. Measured versus predicted soil dielectric constant.

3.4. Field estimation of $\varepsilon_{\sigma b=0}$ and σ_p

By applying the time –varying LDM to the observed data at the various depths (field conditions), we were able to estimate the constant value of $\varepsilon_{\sigma b=0}$ and the evolution of σ_p over time (within the range of 3.8 to 8.5). Fig. 4.7 shows the values of σ_p and $\varepsilon_{\sigma b=0}$ for 0.20 m and 0.60 m depths, respectively. The questions now were, what causes the

differences between the offset values of different depths, and are they statistically significant? To investigate these questions, many studies found that calibration measurements of electromagnetic EM induction for prediction of σ_b are affected by soil texture, water content, and soil temperature (McKenzie et al., 1989; Slavich and Petterson, 1990). Yuanshi et al. (2003) showed that ε_b changes when soil compaction and temperature vary.

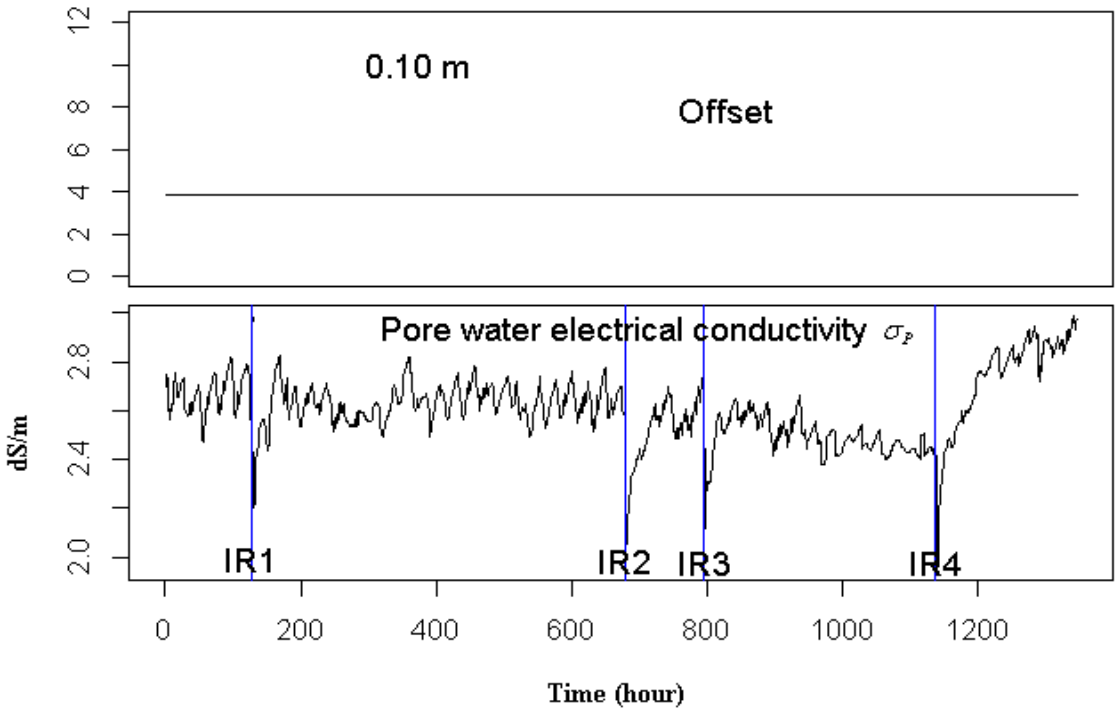

Fig. 4.6. Estimation of the unobservable data ($\varepsilon_{\sigma b=0}$ and σ_p) by applying the Time-varying DLM to data from Field 1 (lettuce, furrow, 0.10 m depth).

In this study, the value of the $\varepsilon_{\sigma b=0}$ was derived from the ε_b observations, and since temperature affects ε_b, we can consider the null hypothesis which stated that: the soil temperature has no effect on the $\varepsilon_{\sigma b=0}$ value. The alternative hypothesis stated that: the soil temperature has an effect on the $\varepsilon_{\sigma b=0}$ value.

For this analysis we took 30 measurements of soil temperature three days after one irrigation event. All data were subjected to analysis of variance (ANOVA) procedures using R (R Development Core Team 2012). Table 4.4 shows that the univariate ANOVA produced statistically significant results, so the soil temperature had an effect on the values of offset and this could be the reason for the difference found in offset values at different depths.

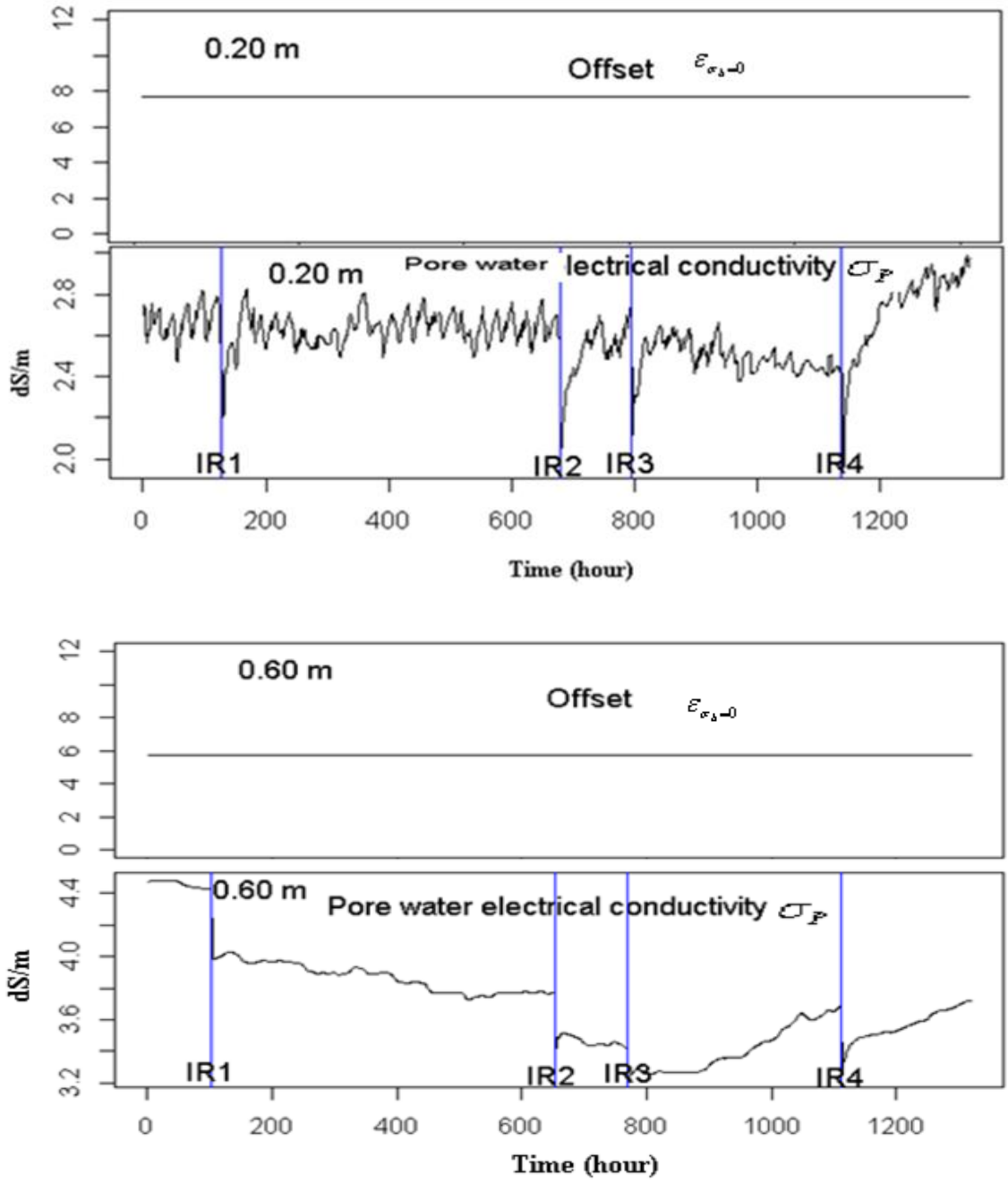

Fig. 4.7. Estimation of the unobservable data ($\varepsilon_{\sigma b=0}$ and σ_p) by applying the Time-varying DLM to data from Field 1 (lettuce, furrow, 0.20 m and 0.60 m depth).

Malicki et al. (1994) and Malicki and Walczak (1999) included sand content in % by weights in their empirical σ_b - σ_p - $\varepsilon_{\sigma b=0}$ model. Table 4.1 shows that there is a different sand content (%) at each depth in Field 1, but this study could not conclude that the sand content has an effect on the value of $\boldsymbol{\varepsilon_{\sigma b=0}}$ because more data would be required to statistically confirm this effect.

Table 4.4. Effect of the mean soil temperature (ºC) on the offset at various depths

	Depth				
Main factors	0.10 m	020 m	0.35 m	0.50 m	0.60 m
Mean soil temperature ºC					
18.14	3.8				
16.25					5.8
16.94				7.1	
18.04		7.8			
17.36			8.2		
significance	*	*	*	*	*

Significant: *P < 0.05, **P < 0.01, ***P < 0.001.

Due to the fact that most soils are heterogeneous, this could support the need to adapt an offset for each depth.

3.5. Influences of soil water, soil temperature and irrigation management on soil salinity in loamy sand soil.

Fig. 4.8 shows the variation of soil water content, soil temperature, and soil salinity content at 0.10 m depths with time. Irrigation events that were applied on days 4.29, 27.20, 32.04 and 46.33, and precipitation occurring on days 9.33, 20.50 and 52.54 had significant effects on soil salinity fluctuations; soil salinity decreased with each irrigation event and rainfall. Fig. 4.8 also shows that the soil temperature increased at the moment of irrigation due to the fact that the temperature of water irrigation is higher than the soil temperature before irrigation.

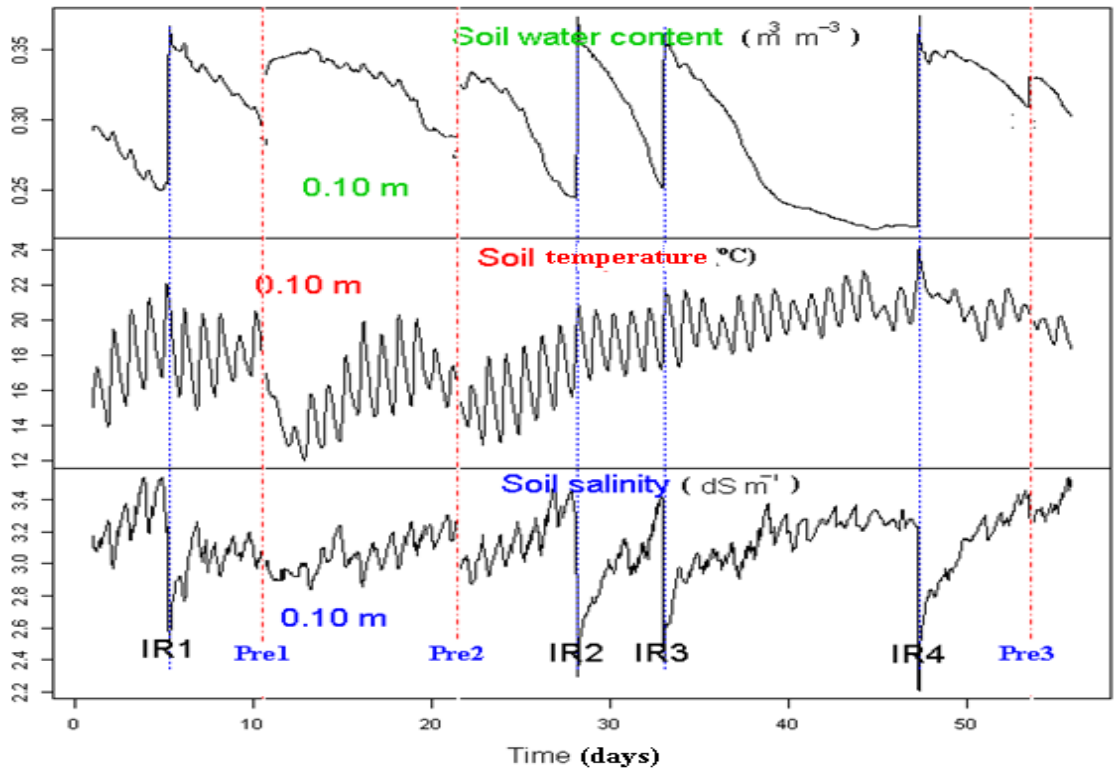

Fig. 4.8. Variation of soil water content, soil temperature and soil salinity at 0.10 m depth with time IR1, IR2, IR3 and IR4 are the irrigation events applied on days 4.29, 27.20, 32.04 and 46.33. Pre1, Pre2, and Pre3 are the precipitation event on days 9.33, 20.50 and 52.54.

The opposite occurred with precipitation: Fig 4.8 shows that soil temperature decreased at precipitation times; acknowledgement of these fluctuations will help in modelling soil salinity as a function of soil water content and soil temperature, as we will explain below. Later, we developed the ARIMA model for the soil salinity time series at 0.10 m depth and completed it by including the irrigation event as an intervention analysis and the precipitation as outlier detections.

3.5.1. Univariate modelling of soil salinity time series at 0.10 m depth.

Fig. 4.9 shows the time series of soil salinity at 0.10 m depth for the first four days of planting. The time series displays a strong seasonality every 24 hours.

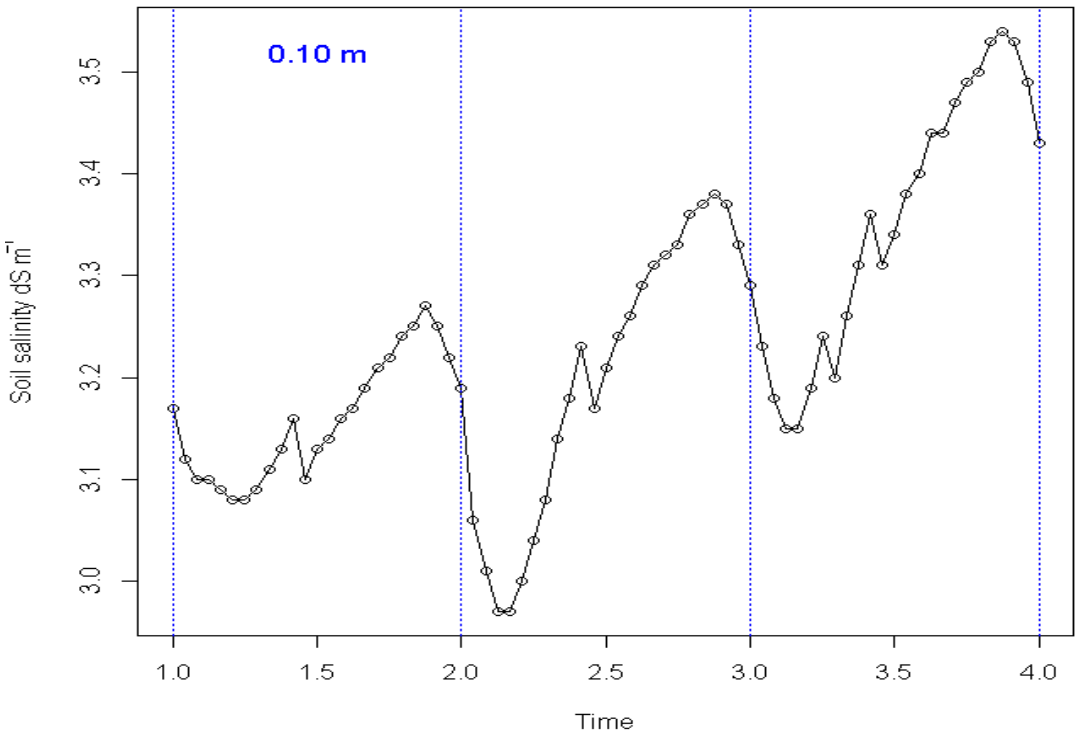

Fig. 4.9 Time series of soil salinity at 0.10 m depth (m^3m^{-3}) for the first 4 days of planting at 0.10 m depth.

The ACF of the original time series of soil salinity at 0.10 m depth converges very slowly, indicating that the time series is non-stationary (Fig. 4.10A). To obtain a stationary time series, the original series were differentiated (first order-difference and seasonal first order difference). No trend in variance is observed in this series, so there is no need to apply a logarithmic transformation.

The ACF and PACF of differentiated time series indicated that the series was approximately AR (3) for the regular component, and MA (1) for the seasonal component, because the ACF (Fig. 4.10 B) showed that only the correlation at the first three and at the 24^{th} lags of ACF were significant.

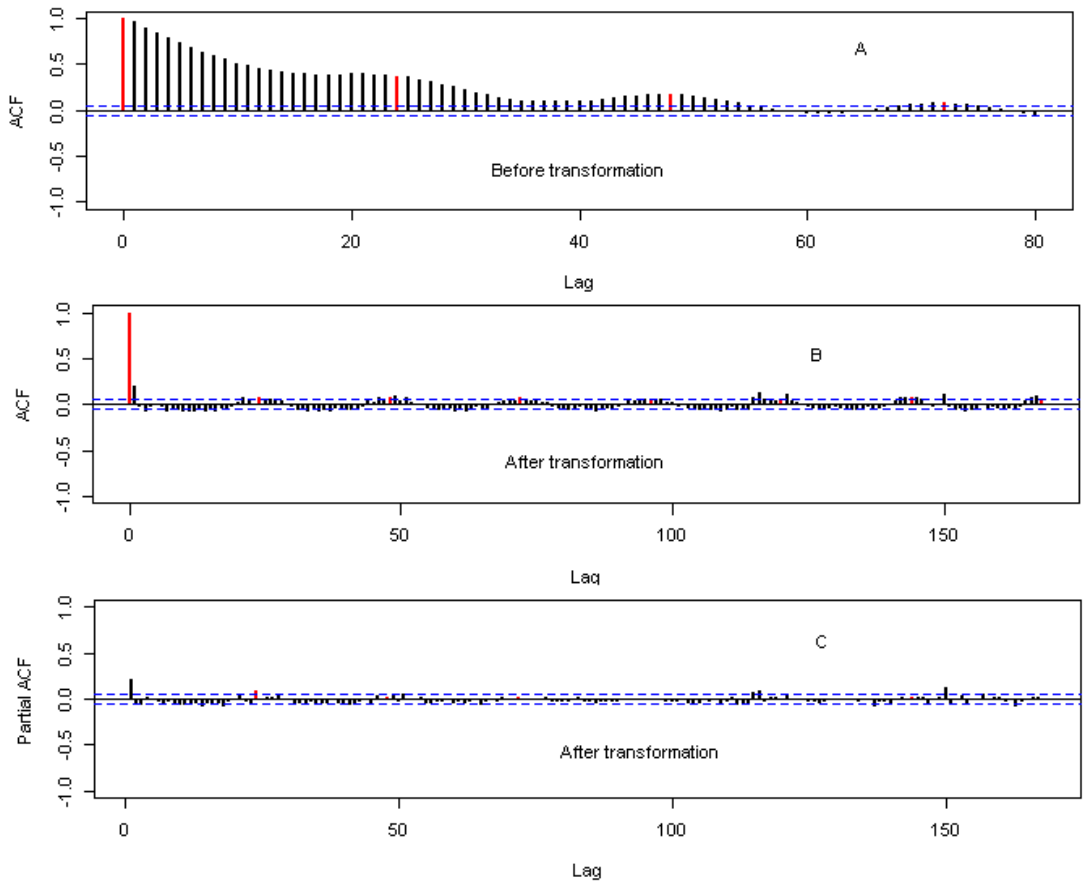

Fig. 4.10. (A) Autocorrelation function (ACF) of the original data, (B) autocorrelation function, and (C) partial autocorrelation function (PACF) of the transformed time series of soil salinity at 0.10 m depth. The ACF of the original data indicates that the series is not stationary. The dashed line represents 2 x standard errors.

The ARIMA *(p, d, q) (P, D, Q)$_S$* model of time series of soil salinity at 0.10 m depth was ARIMA (3, 1, 0) (1, 0, 0)$_{24}$. In usual notation the model is given by:

$$(1-\phi_1 B-\phi_2 B^2-\phi_3 B_3^{\ 3})(1-B)(1-B^{24})X_t=(1+\theta_{24}B^{24})a_t \qquad (20)$$

where a_t is an independent, identically distributed white noise term with zero mean and variance = 2.8.10^{-7}, ϕ_1 = 0.2088, ϕ_2 = -0.0468 , and ϕ_3 = -0.0883 are AR parameters. The θ_{24} = 0.99 parameter of the seasonal AR. We checked the serial correlation in the residuals of a fitted model (20) to verify if model (20) closely represented the observed time series of soil salinity. By using the Ljung –Box statistic test of model residuals, Fig 4.11 shows that model residuals are correlated and that the model is not valid.

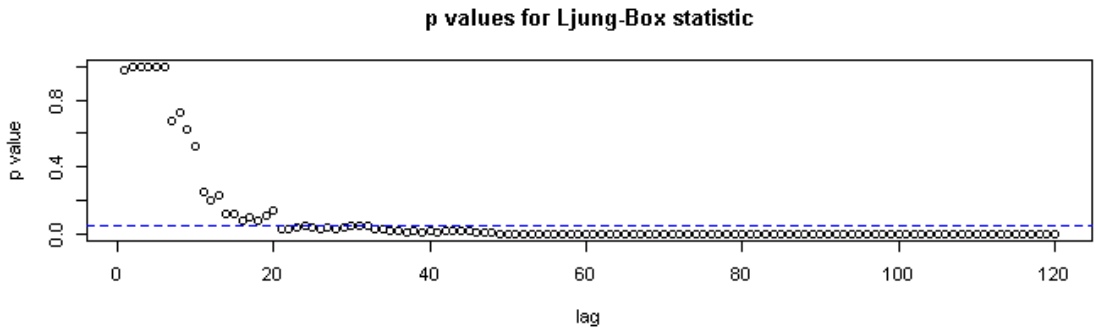

Fig. 4.11. The Ljung-Box statistic of the model ARIMA (2,1,0)(1,0,0) residuals.

Therefore, it is inadequate and needs to be improved in structure. An exploratory method, which is well-established in other fields, is a seasonal-trend decomposition based on locally-weighted regression (loess), widely known as "STL" (Cleveland et al., 1990; Hafen et al., 2009). The STL method is straightforward to use; it allows for flexibility in specifying the amount of variation in the trend and seasonal components of time-series; and it produces robust estimates that are not distorted by transient outliers (Cleveland et al., 1990). Fig. 4.12 shows that the large outliers of the remainder (random) are backed to the irrigation event. Since the timing of the irrigation event is previously known, the model could be completed with intervention analysis (irrigation event) and outlier detection (model 20), making it invertible and thus reducing its residual variance (Wei, 1989).

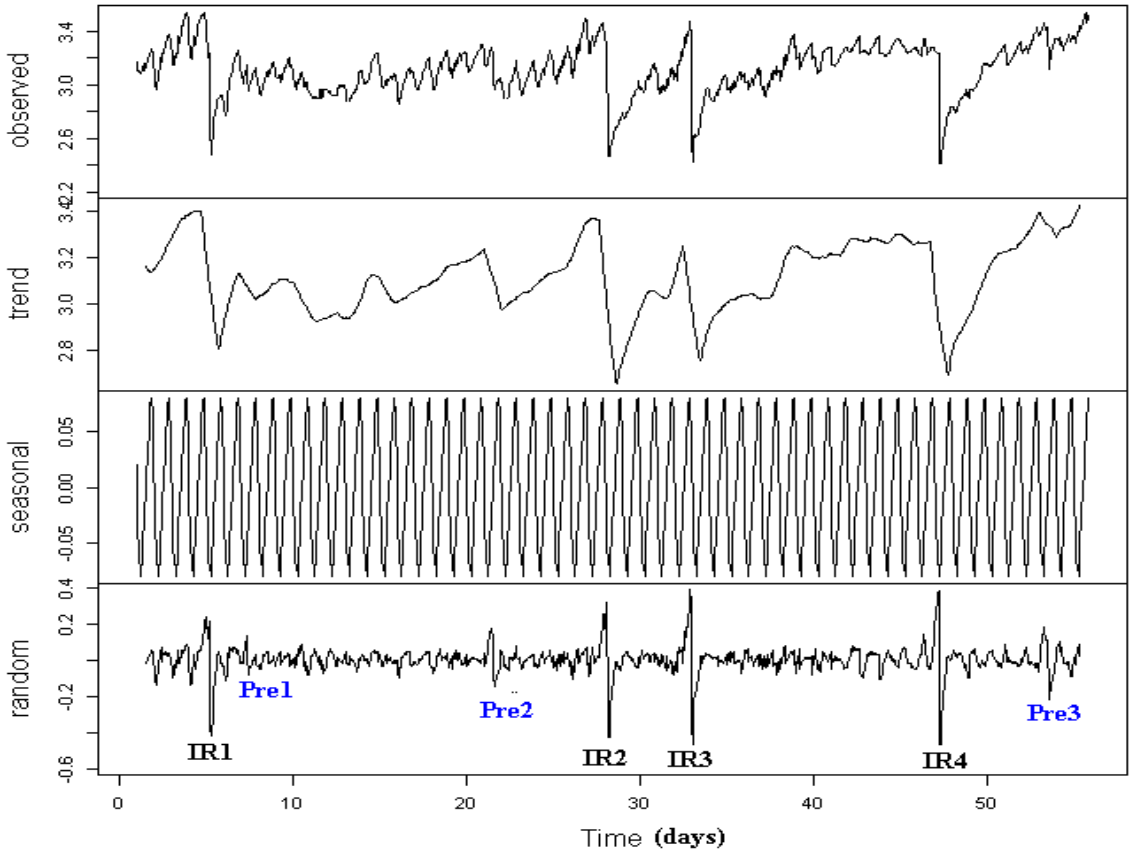

Fig. 4. 12 Decomposition plot of soil salinity at 0.10 m depth affected by the intervention variable (irrigation event in our case) and irregular variables (such as precipitation) over 55 days, STL method. This plot assists evaluation of the trend, seasonality and remainder (random) against the raw data. The graph (observed) represents the hourly time series of soil salinity affected by irrigation and irregular events like precipitation. The graph (trend) is the fitted trend. The graph (seasonal) is the seasonal pattern per 24 hours. The graph (random) represents the remainder after the trend and the seasonal pattern have been fitted to the time-series values. The sum of the trend, the seasonal pattern and the random equals exactly the time-series. IR is the time of irrigation event, and Pre is the precipitation time. The large peaks of the remainder correspond to the irrigation time which must be taken into account when building up ARIMA model on the series.

3.5.2. Outlier and intervention analysis in the ARIMA model for time series of soil salinity at 0.10 m depth: the effectiveness of the irrigation event on soil salinity.

Intervention analysis and automatic outlier detection were applied to the previous ARIMA (3, 1, 0) $(1, 0, 0)_{24}$ model to improve it and to assess the effect of irrigation events on soil salinity at 0.10 m depth (for more information about intervention analysis and outlier detection see Materials and Methods, chapter 3). With Grubb's test (Eq. 7,

chapter 3) 15 outliers were detected (Table 4.5) for the time series of soil water content at 0.10 m depth.

Table 4.5. Outlier Detection and parameter estimation for time series of soil salinity at 0.10 m

Observation time (hour)	type	ω
103	AO 0.18505831	7.968661
106	TC 0.12443606	4.554197
153	AO 0.09745569	4.564459
494	TC -0.17091216	6.035187
653	AO 0.29954989	12.203030
654	AO -0.11073225	5.145772
770	TC -0.23075883	7.883772
919	TC -0.11041299	4.181763
962	TC -0.10900883	4.183170
1001	TC -0.11738130	4.326400
1029	TC -0.10927677	4.165889
1089	TC 0.11360351	4.215289
1112	TC -0.28581633	9.320497
1113	TC -0.14613830	5.213316
1262	TC -0.20726519	7.219790

Including the outlier detection and intervention analysis, the observed value of time series of soil water content at 0.10 m depth can be described according to Eq. 8 (chapter 3) as:

$$X_t = \omega_r (S_{4.29}^{(t)} + S_{27.20}^{(t)} + S_{32.04}^{(t)} + S_{46.33}^{(t)}) + \sum_{i=1}^{23} \omega_i P_{T_i}^{(TC)} + \sum_{j=1}^{5} \omega_j P_{T_j}^{(AO)} + Z_t \quad (21)$$

Xt is the observed time series, *Zt* is the time series free of outliers, and ω_r =-0.7592 represents the permanent change in the mean level after the irrigation event, which characterizes the effectiveness of the irrigation event on the soil salinity. In this study, the flow rate and cut-off time for the four applied irrigations were almost equal. Therefore, we used an average coefficient for ω_r to estimate the weight of the peak caused by four irrigation events. The part $(S_{4.29}^{(t)} + S_{27.20}^{(t)} + S_{32.04}^{(t)} + S_{46.33}^{(t)})$ represents the step indicator at four irrigation times T_r (days 4.29, 27.20, 32.04, and 46.33). The part $\sum_{i=1}^{23} \omega_i P_{T_i}^{(TC)} + \sum_{j=1}^{5} \omega_j P_{T_j}^{(AO)}$ represents the effects of the 15 detected outliers.

By applying the Box-Jenkins approach to the time series of soil salinity Z_{t_t} obtained from Eq. (21), the ARIMA (3, 1, 0) $(0, 1, 1)_{24}$ model was determined. The model, in usual notation, is given by:

$$(1-\phi_1 B-\phi_2 B^2-\phi_3 B^3)(1-B)(1-B^{24})Z_t=(1+\Theta_{24}B^{24})a_t \qquad (22)$$

The model (22) is free of outliers, it is invertible, and the ACF and PACF of residuals at all lags are non-significant. Fig. 4.13 shows that the model (22) residuals are non -significant. Table 4.6 shows the comparison between the two models (20 and 22) in terms of statistical parameters.

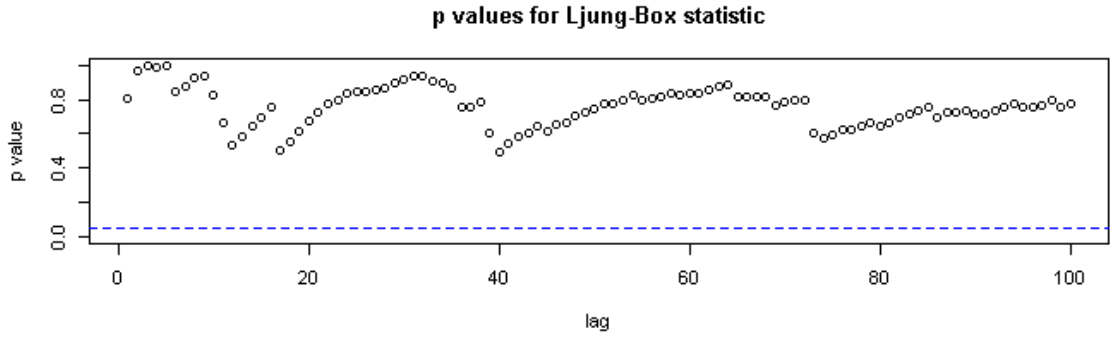

Fig. 4.13. The Ljung-Box statistics of the model ARIMA (3,1,0) (0,1,1) residuals

Table 4.6. Comparison of the two models for soil salinity at 0.10 m depth in terms of statistical parameters (one based on observed data X_t and the second based on outlier-free data Z_t)

Model	ϕ_1	ϕ_2	ϕ_3	θ_{24}	σ^2
Model based on observed data X_t (20)	-0.0114	-0.0684			$1.377.10^{-4}$
Model based on Outlier free data Z_t (22)	-0.0467	-0.0108	0.0273	-0.9226	$7.431.10^{-5}$

After modelling *σp*, the next step is to model the soil waer and soil temperatue time series at 0.10 m depth. Following the same steps to model *σp*, table 4.7 shows the ARIMA soil water and soil temperatue models. While the effect of irrigation event on soil water and soil temperatue time series at 0.10 was 0.0843 and 0.2882 respectively.

Table 4.7. models of soil water content (θ) and soil temperature (t) at 0.10 m

Model	ϕ_1	ϕ_2	ϕ_3	Θ1	θ_{24}	σ^2
Soil water	-0.0361	-0.0192				$1.056.10^{-5}$
Soil temperature	1.5510	-0.6414	0.0273	-0.877	-0.882	$1.833.10^{-5}$

3.5.3. Transfer function approach

The cross-correlation between the pre-whitened primary time series of soil water content and soil temperature at 0.10 m depth, and the target soil salinity time series at 0.10 m depth and average soil salinity in the top 0.60 m soil profile, showed that the primary series affects the target series, but the target series cannot in turn have a bearing upon the primary series. Fig. 4.12 proofs that the present value of soil water and content and soil temperature at 0.10 m has a significant effect on the present value of soil salinity at 0.10 m depth and average soil salinity in the top 0.60 m of the soil profile.

Models for predicting soil salinity from the soil water content and soil temperature at 0.10 m depths were identified (Table 4.8). The coefficients of X_t in the equations of Table 4.8 show that the present values of soil water content and soil temperature at 0.10 m have effects of -7.82, -0.050 on salinity at 0.10 m dpeth, respectively. Also, the present values of soil water content and soil temperature at 0.10 m have effects of -1.68, -0.004 on the present value of average soil salinity in the top 0.60 m soil profile, respectively.

3.5.4. Forecasting

Fig. 4.13 shows the model calibration and prediction for average soil salinity in the top of 0.60 m depth of soil profile and soil salinity at 0.10 m depth. The first 659 observations of each time series were used for model identification. The calibrated model represented the values before these 659 observations very well for each depth. The predicted and observed values after the 659 observation agreed reasonably. The relative difference between predicted and observed values was sometimes large. The absolute difference between the prediction and measurement never exceeded 0.27dSm^{-1}.

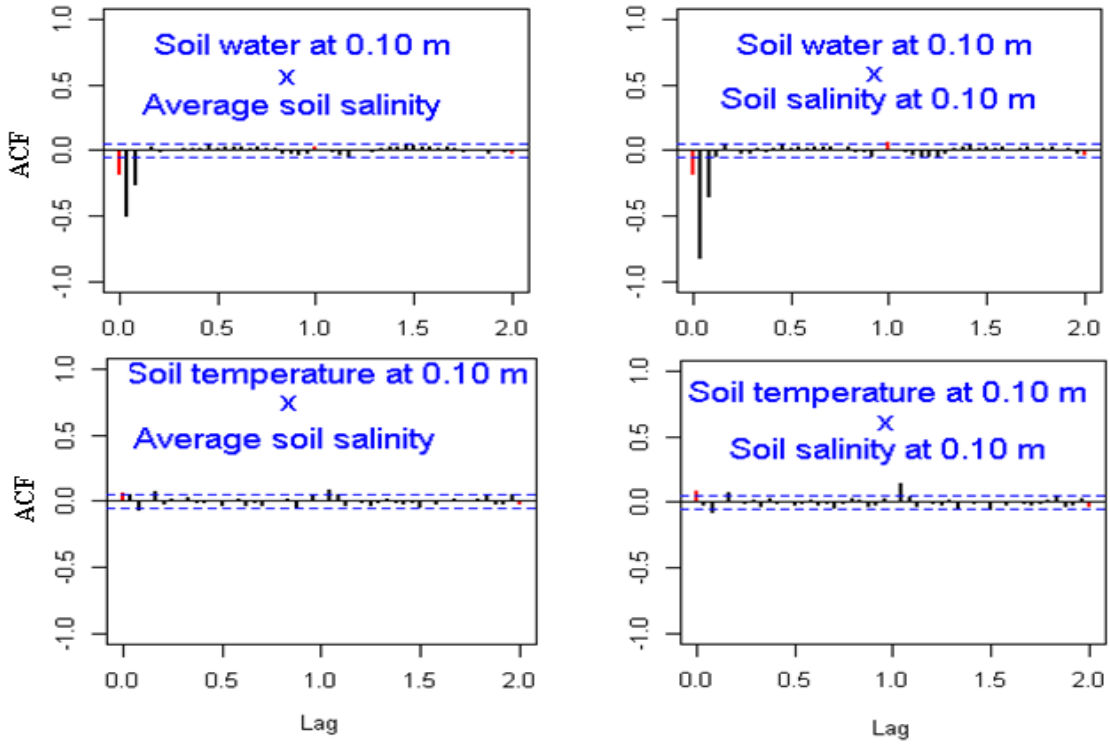

Fig. 4.12. Cross-correlation function for soil water content and soil temperature hourly time series at 0.10 m and soil salinity at 0.10 m depth , soil water content and soil temperature 0.10 and soil salinity in the top 0.60 m of soil profile, respectively. Dashed lines indicate 95% confident limits.

Table 4.8. Time series transfer function model for soil salinity at 0.10 m depth and in the top of 0.60 m of the soil profile.

Soil water content $X_{1,t}$, soil temperature $X_{2,t}$ at 0.10 m and soil salinity Y_t at 0.10 m:

$$Y_t = \frac{(-7.8242 + 1.4053B - 0.2606B^2 + 0.7234B^3)X_{1,t} + (-0.0508 + 0.0153B)X_{2,t} + a_t}{(1-B)(1+0.680B^{24})(1+0.1597B+0.1266B^2+0.0502B^3)}$$

$$a_t \sim N(0,\ 6.489\ .8\ 10^{-5})$$

Soil water content $X_{1,t}$, soil temperature $X_{2,t}$ at 0.10 m and average soil salinity Y_t

$$Y_t = \frac{(-1.6855 - 0.0548B + 0.4975B^2 + 0.0717B^3)X_{1,t} + (0.004 - 0.0111)X_{2,t} + a_t}{(1-B)(1-0.0358B^{24})(1-0.0627+0.0209B^2-0.1754B^3)}$$

$$a_t \sim N(0,\ 2.684\ \ 10^{-5})$$

Using the transfer function model presented in table 4.8, Fig. 4.14 shows an example of prediction of soil salinity (at 0.10 m and in the top 0.60 m soil profile) for two days, as a function of soil water content and soil temperature at 0.10 m. The observed values of soil salinity correspond to 55 days, and the prediction is for the 56th and 57th day. It includes the effect of the next irrigation if the farmer chooses to irrigate on the 56.5th day.

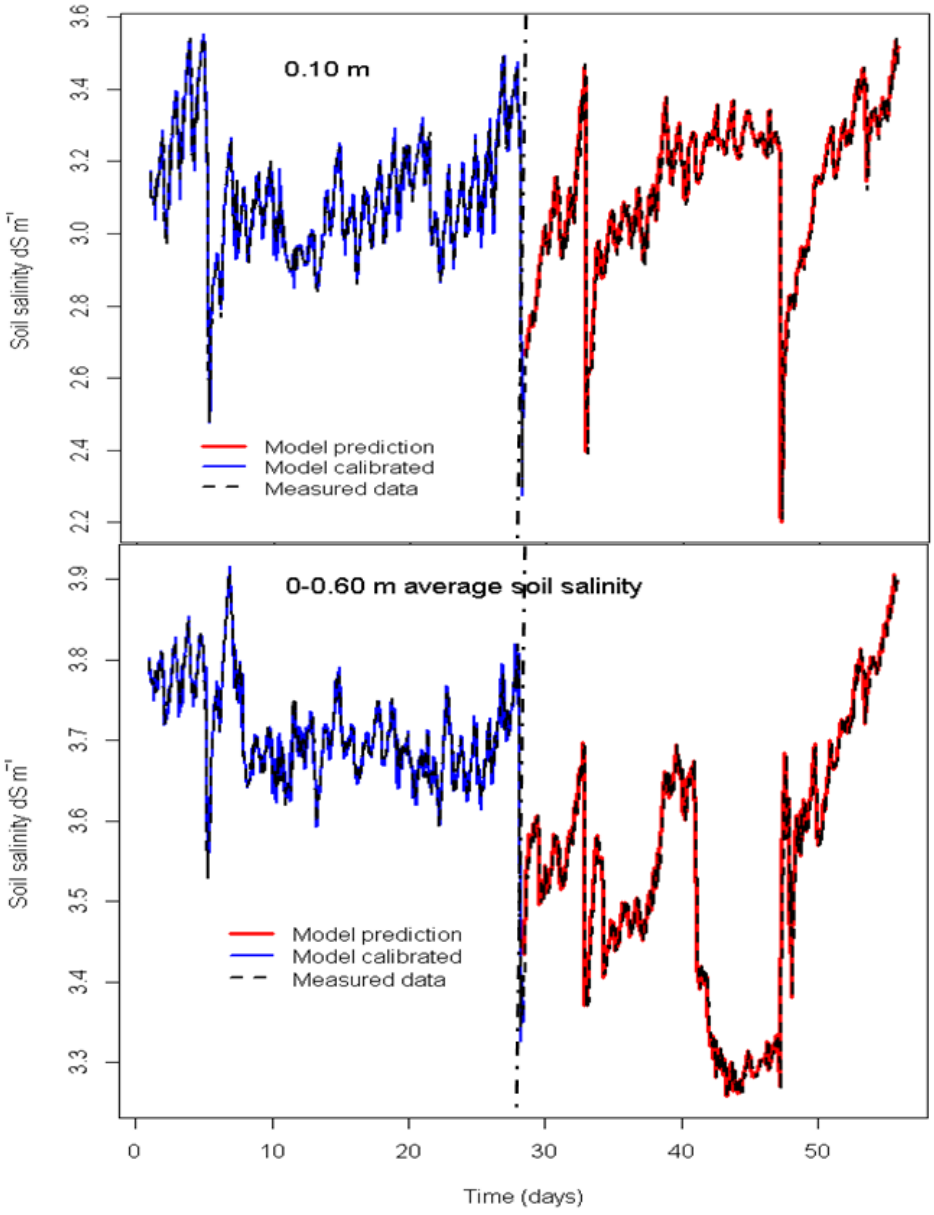

Fig. 4.13. Measured and predicted soil salinity versus time at 0.10 m depth and in the top 0.60 m of soil profile. Prediction was based on the identified transfer function models for each one. The curve before the vertical dashed line refers to model calibration and after the vertical dashed line to model prediction**.**

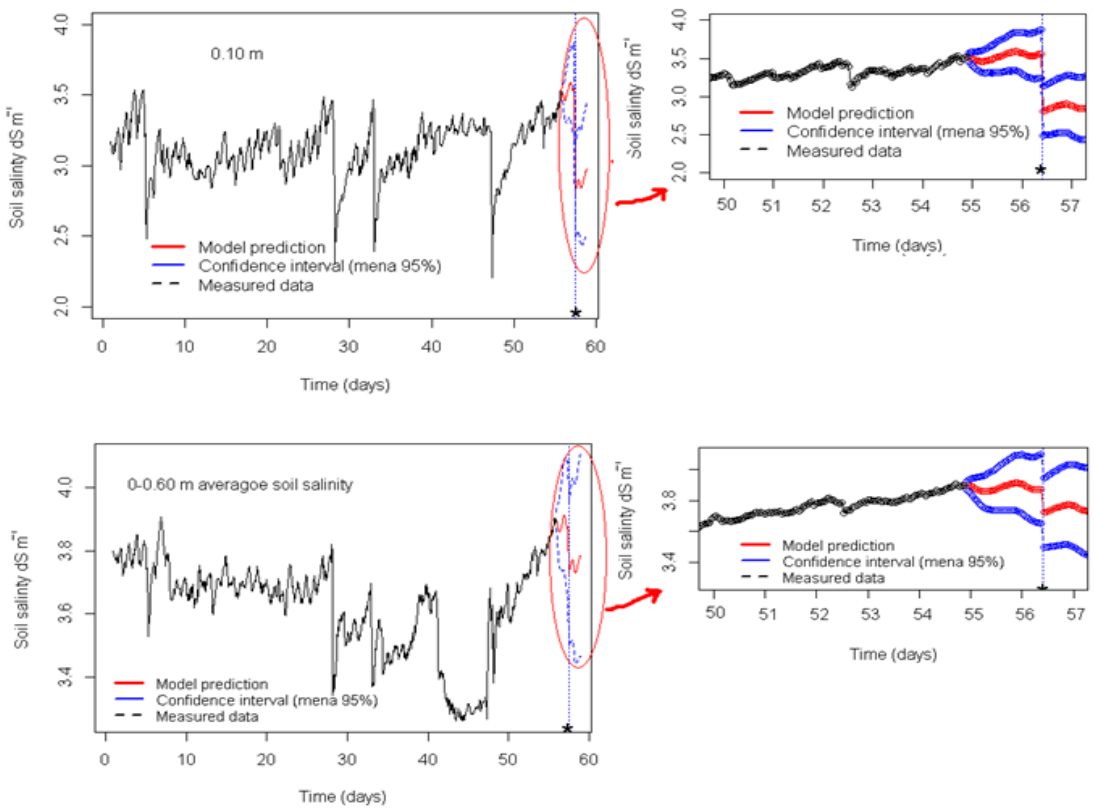

Fig. 4. 14. Prediction models for soil salinity at 0.10 m depth and average soil salinity in the top 0.60 m of soil profile. Prediction was based on the indentified transfer function. We have observed data for 55 days, the model predicts the 56th and 57th day taking into account the effect of next irrigation if the farmer choose to irrigate on 56.5th day (* is the irrigation time at 56.5th day).

3.6. Effects of irrigation management applied on soil salinity

Fig 4.15 and Fig 4.16 show how irrigation quickly reduces the salinity in the crop root zone (the top 0.60 m soil profile responds fast to irrigation envents). Table 4.9 and 4.10 presents the primary statistical results associated with the repeated measurement analysis of the soil salinity data (Field 1, lettuce, and Field 3, artichoke). The univariate ANOVA models with the position, depth and irrigation frequency for Field 1 (lettuce) and Field 3 (artichoke) had statistically significant resutls. There is an interaction between those factors. Fig. 4.17 and Fig. 4.18 show how the average soil salinity changed with irrigation frequency at different depths (beneath the furrow and the ridge in the case of Field 1, Fig 4.17). Based on the multivariate tests in tables 4.8 and 4.9, the patterns shown in Fig. 4.17 and Fig. 4.18 can be considered statistically distinct.

Table 4.9. Effect of irrigation frequency , and position (furrow, ridge) on mean of soil salinity (dS m^{-1}) at various depth Field 1, Lettuce.

	Depth							
Main factors	0.10 m		0.20 m	0.35 m		0.50 m	0.60 m	
Irrigation (IR)	Furrow	Ridge	Furrow	Furrow	Ridge	Furrow	Furrow	Ridge
Irrig1	2.84	1.82	4.7	3.90	4.74	3.33	4.07	5.40
Irrig2	2.68	2.00	4.90	3.40	4.13	3.16	3.55	5.16
Irrig3	2.78	1.78	4.80	3.50	3.9	3.09	3.31	5.14
Irrig4	2.70	1.40	5.20	3.38	3.80	3.01	3.48	NA
significance	*	*	*	*	*	*	*	*

	Depth				
	0.10 m	0.20 m	0.35 m	0.50 m	0.60 m
Position (POS)					
Ridge	1.76		4.16		5.23
Furrow	2.75	4.90	3.54	3.10	3.60
Significance	***		***		***

	Depth				
	0.10 m	020 m	0.35 m	0.50 m	0.60 m
Interaction					
IR X POS	***	***	***	***	***

Significant *P < 0.05, **P < 0.01, ***P < 0.001.

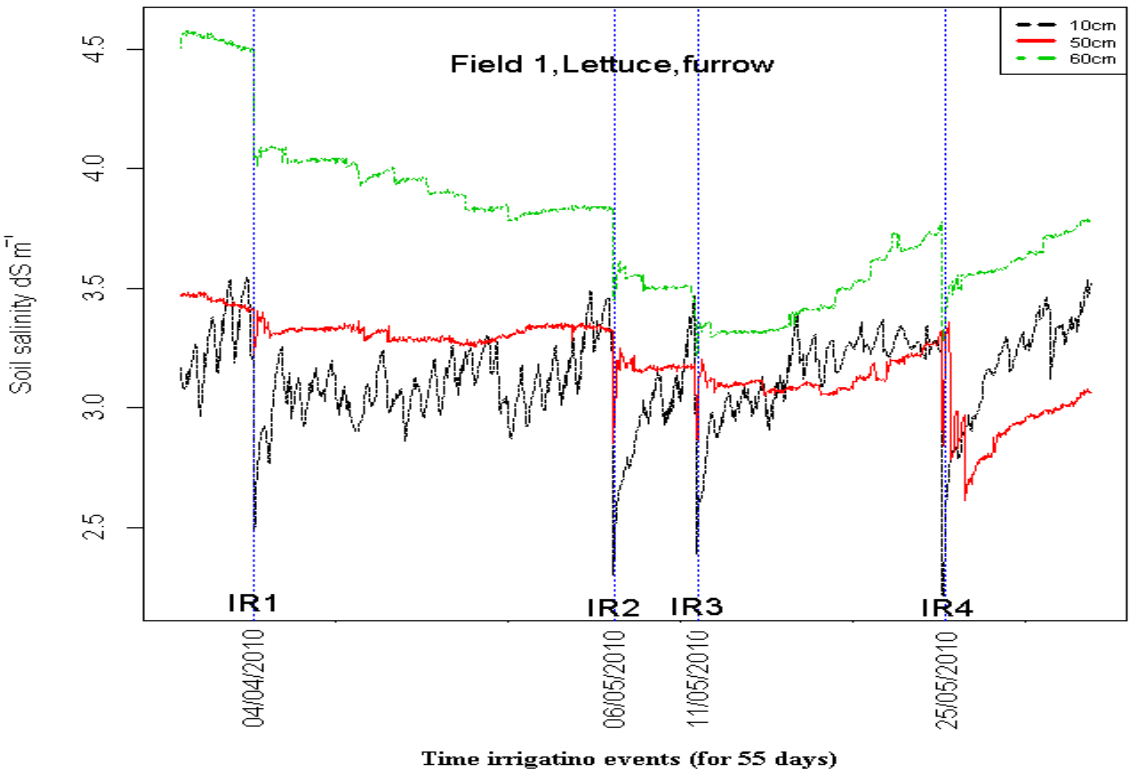

Figure 4.15. Effects of irrigation events on the salinity at various depths within the root zone of lettuce crop, Field 1 (4 irrigation events for 55 days, under the furrow).

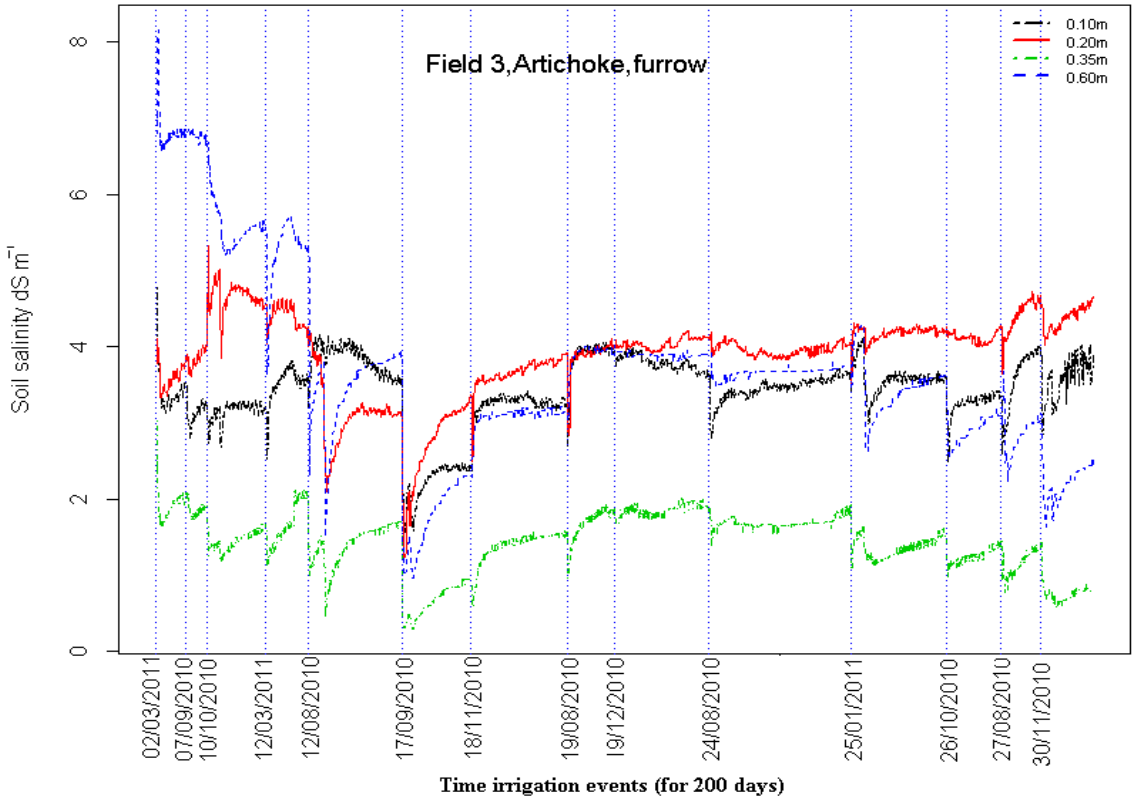

Figure 4.16 .Effects of irrigation events in the salinity at various depth within the root zone of artichoke crop, Field 3. (14 irrigation events for 200 days, under the furrow).

In field 2, lettuce, the univariate ANOVA models with the position, depth and irrigation frequency had also statistically significant results. Fig. 4.19 shows that the the average soil salinity changed with irrigation frequency across the depths beneath the furrow. Table 4.11 indicates that the comparison between Field 1 and Field 2 in terms of the mean of soil salinity for each depth is statistically significant results and Fig 4.20 shows that the irrigation water quality may be the main reason for these differences. Field 2 was irrigated from the Canal de la Infanta (water quality about 2 dS m^{-1}) while Field 1 was irrigated from the Canal de la Dreta (water quality about 1 dS m^{-1}). Soil salinity in Field 3 (in the root zone) was lower than in Field 2 because the farmer in Field 3 uses more irrigation events and also mix the water which came from Canal de la Infanta with water extracted from his well.

Table 4.10. Effect of irrigation frequency and depth on mean of soil salinity (dS m^{-1}) , Field 3, artichoke,

	Depth			
Main factors Irrigation (IR)	0.10m	0.20m	0.35m	0.60m
irrig1	3.27	3.21	3.06	3.24
irrig2	3.57	3.99	1.93	3.25
irrig3	3.97	3.93	3.08	3.52
irrig4	3.66	3.25	3.57	3.91
irrig5	4.25	4.78	4.54	3.47
irrig6	2.30	3.54	3.91	4.01
irrig7	3.99	4.07	4.39	4.22
irrig8	1.91	1.87	1.25	1.39
irrig9	1.5	1.36	0.41	1.28
irrig10	1.66	1.86	1.61	1.35
irrig11	1.07	0.62	6.79	6.75
irrig12	4.27	5.29	5.40	3.55
irrig13	1.18	3.10	3.97	3.89
irrig14	3.68	3.23	2.74	1.99
significance	***	***	***	***
Interaction IR*Depth	***			

significant; *P < 0.05, **P < 0.01, ***P < 0.001

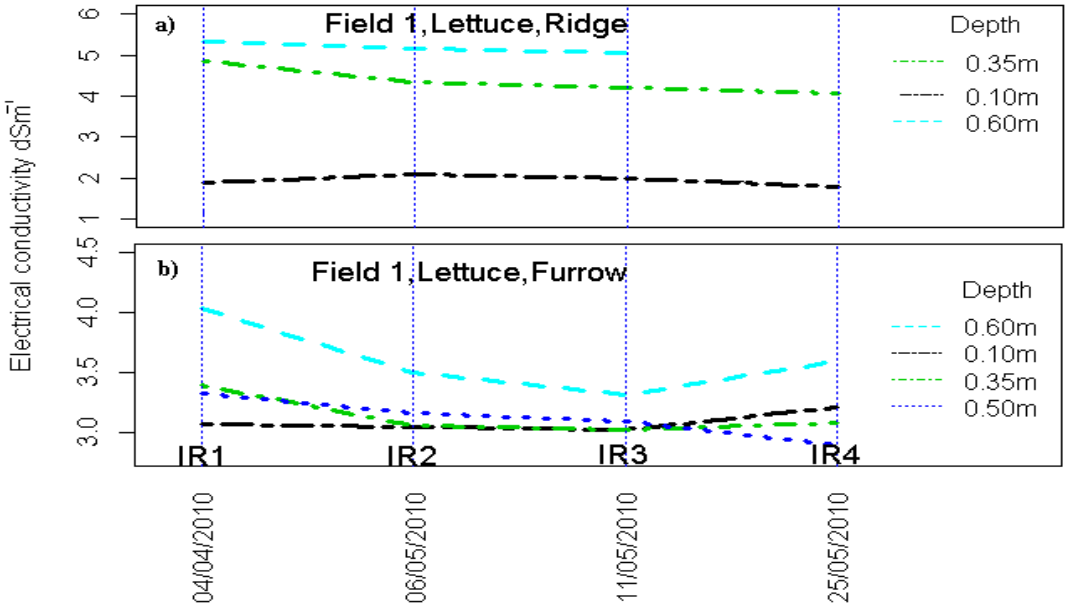

Figure 4.17. Average soil salinity interaction plot for irrigation frequency as related to depth, IR: irrigation event (1, 2, 3 and 4), a) beneath the ridge and b) beneath the furrow, Filed 1, lettuce

Table 4.11. Effect of water quality and depth on the mean of soil salinity (dS m^{-1}), Field 1 and 2, lettuce.

	Field	
Main factor	Field 1 (water quality 1dS m^{-1})	Field 2 (water quality 2ds m^{-1})
Depth		
0.10 m	3.092257	3.406583
0.20 m	5.187310	6.953250
0.35 m	3.141300	5.370667
0.50 m	3.123313	8.796500
0.60 m	3.612595	8.928667
Significance	***	***
Interaction Field *Depth	***	

significant; *P < 0.05, **P < 0.01, ***P < 0.001

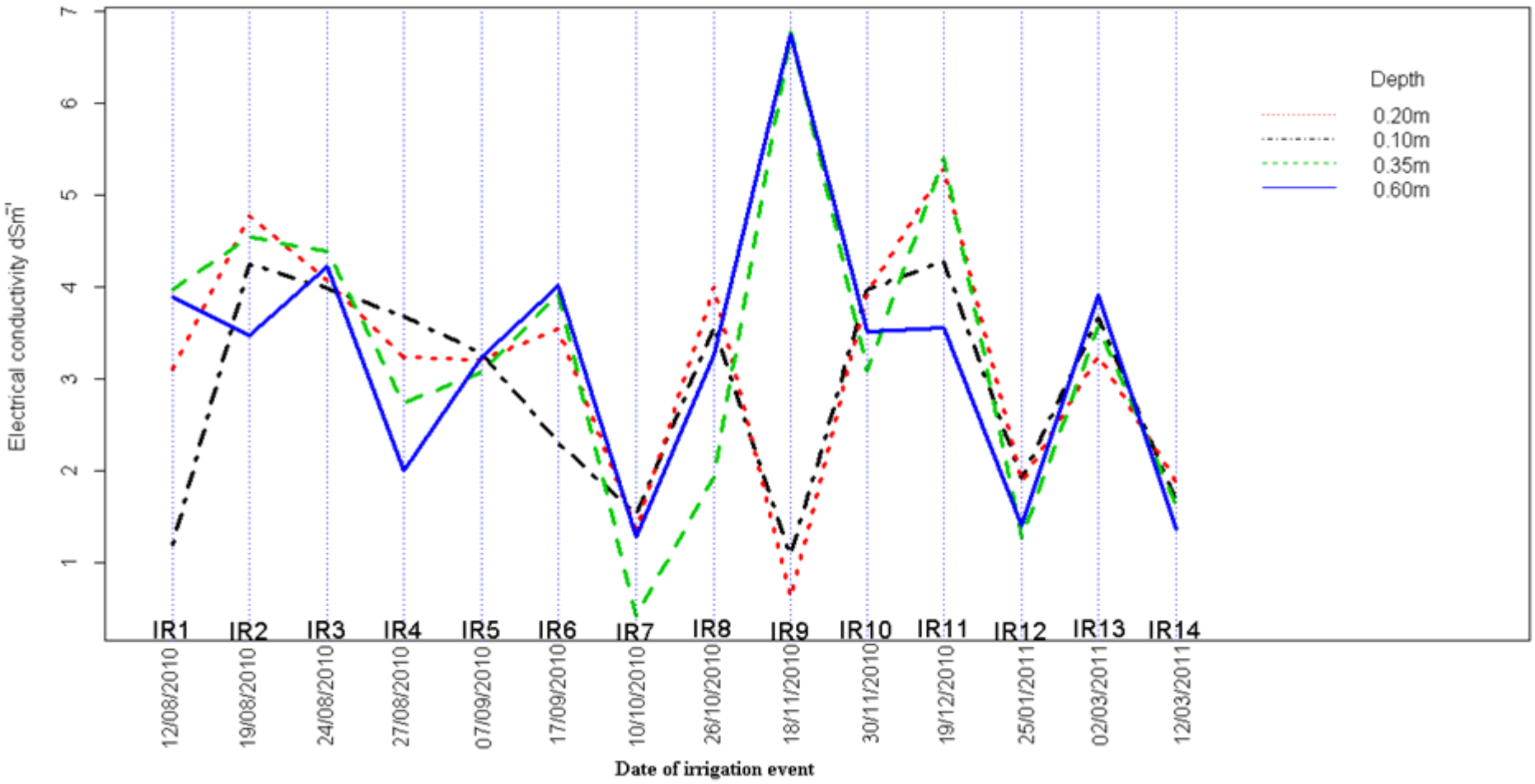

Fig. 4.18**.** Average soil salinity interaction plot for irrigation frequency as related to depth, IR: irrigation event (1, 2,.., 14), Field 3, artichoke.

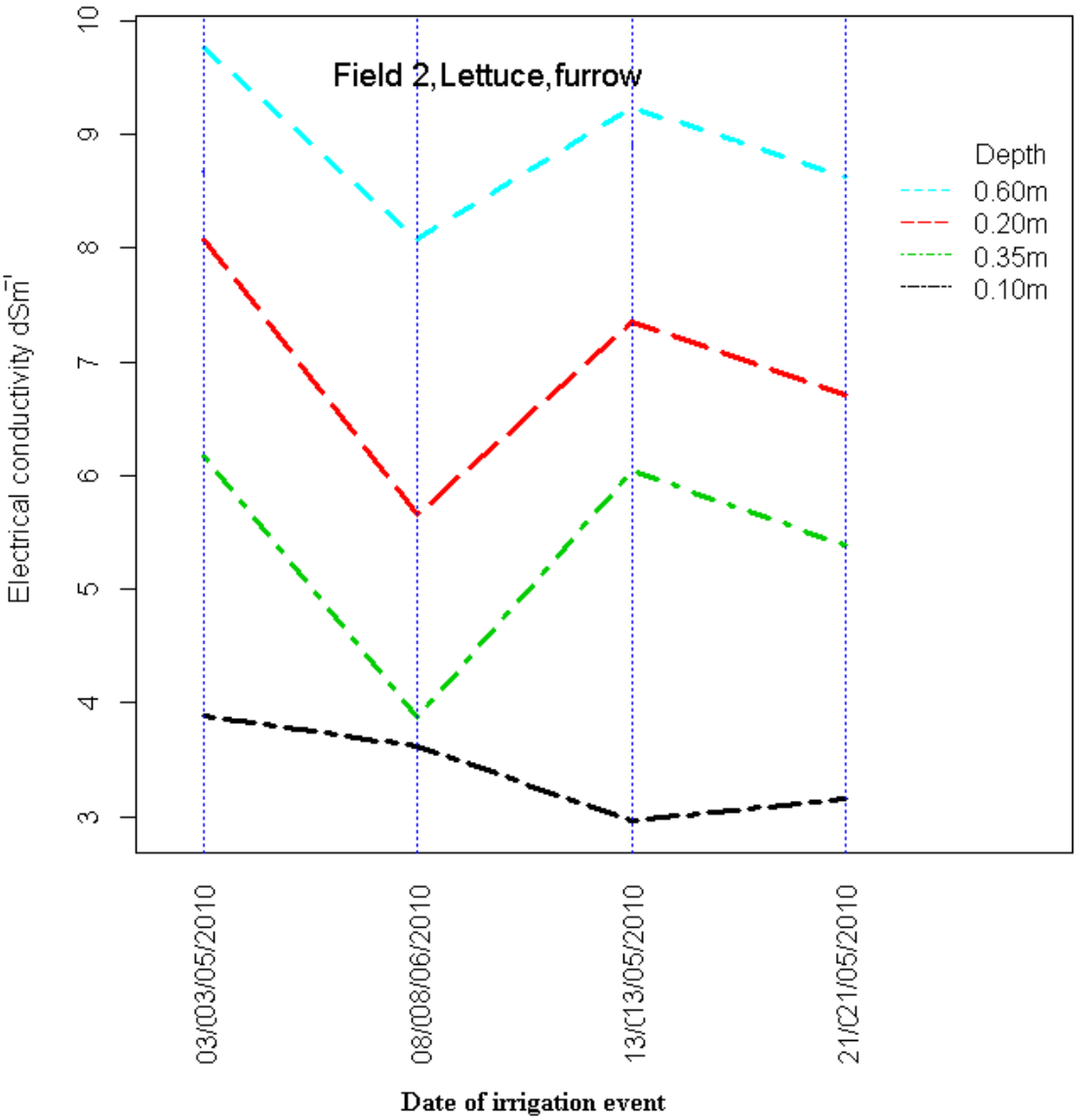

Fig. 4.19. Average soil salinity interaction plot for irrigation frequency as related to depth, beneath the furrow, Filed 2, lettuce.

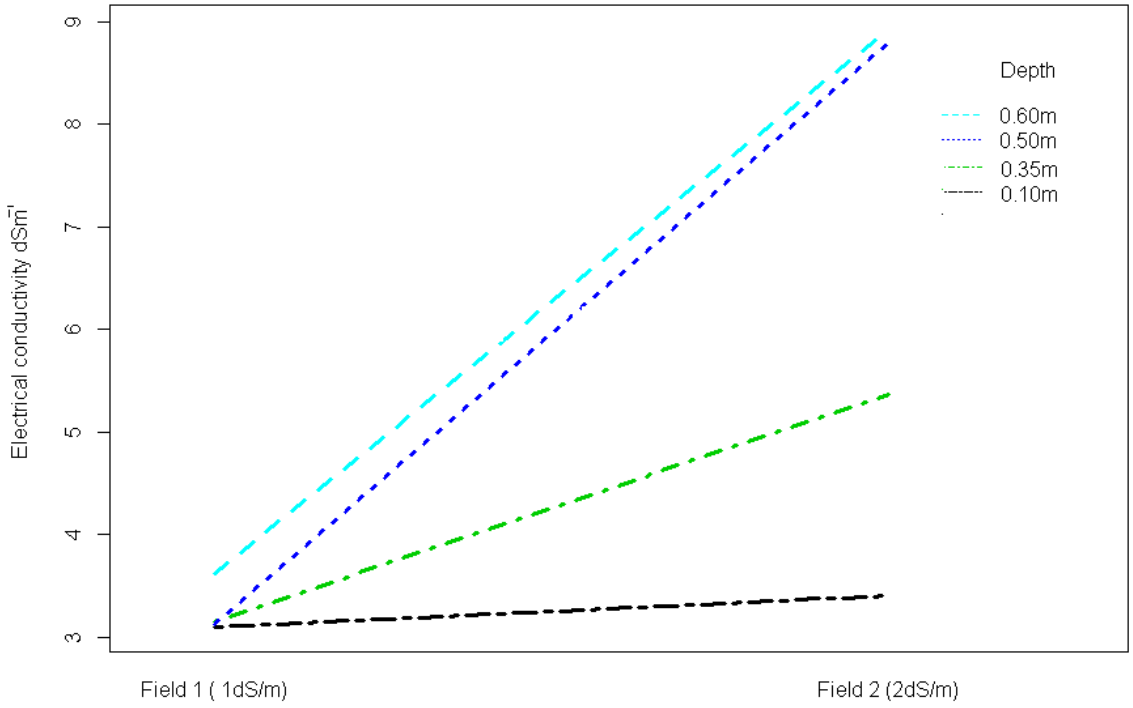

Fig. 4.20. Average soil salinity interaction plot for Field 1 and 2 as related to depth (beneath the furrow, lettuce crop), the affect of water quality in the soil profile at various depths is the main reason for this difference.

In General, in this study, the mean soil salinity significantly changed with depth and irrigation frequency, and we can see that at the end of crop's vegetative stage the farmers left the field with less soil salinity, for each depth, than at the beginning of crop's vegetative stage (Fig 4.17, Fig 4.18 and Fig. 4.19).

4. Conclusions

Several models have been studied to assess the σ_p from ε_b -σ_b relationship (Rhoades et al., 1976; Muallem and Friedman, 1991; Malicki and Walczak, 1999). Lately, Hilhorst (2000) presented a theoretical model describing a linear relationship between σ_b and ε_b in moist soil. By using this linear relationship, Hilhorst (2000) found that measurements of the σ_p can be made in a wide range of soil types without soil-specific calibrations. In this present study, applying the ε_b - σ_b linear relationship on the field condition data gotten from capacitance sensors, the autocorrelation between the

residuals of that regression were extremely strong positive. By including a stochastic component to the linear model and rearranged it to a Time- varying Dynamic Linear Model (DLM) and using kalman filtering and smoothing, we are enabled to derive an accurate offset of the relationship ε_b - σ_b and estimate the evolution of σ_p over time. It was shown that the offset varies for each depth in the same soil profile. A reason for this might be to the changes in soil temperature through soil profile. Once σ_p was estimated, by using transfer function model, prediction of soil salinity by measuring soil water conentent and soil temperatre were logical. Also, the next irrigation time and its effect on soil salinity at the depth of interest were correctly estimated.

Irrigation frequency according to the farmer's normal management practice had statistically significant effects on soil salinity behavior, depending on soil depth and position. For each depth, farmers left the field with less soil salinity than at the beginning of the crop's vegetative stage. Moreover, irrigation water quality had a significant effect on soil salinity at the root zone in the three fields.

5. References

Arquedas-Rodriguez, F. R., 2009. Calibrating capacitance sensors to estimate water content, matric potential, and electrical conductivity in soilless substrates. University of Maryland, MS Thesis. 118p.

Ben-Gal, A., Ityel, E., Dudley, L., Cohen, S., Yermiyahu, U., Presnov, E., Zigmond, L., Shani, U., 2008. Effect of irrigation water salinity on transpiration and on leaching requirements: a case study for bell peppers. Agricultural Water Management 95 , 587–597.

Beven, K., Germann, P., 1982. Macropores and water flow in soils. Water Resource Reseearch 18, 1311–1325.

Bouksila, F. Persson, M., Berndtsson, R. Bahri, A., 2008. Soil water content and salinity determination using different dielectric methods in saline gypsiferous soil. Hydrological Science Jouranl 53, 253-265.

Box, G.E.P., Jenkins, G.M., Reinsel, G.C., 1994. Time Series Analysis: Forecasting and Control. Englewood Cliffs, New Jersey.

Cleveland, R.B., Cleveland, W.S., McRae, J.E., Terpenning, I., 1990. STL: a seasonaltrend decomposition procedure based on loess. Journal of Official Statistics 6, 3–73.

Fortin, J.G., Anctil, F., Parent, L., Bolinder, M.A., 2010.Aneural network experiment on the site-specific simulation of potato tuber growth in Eastern Canada. Comput. Electron. Agric. 73, 126–132.

Ghassemi, F., Jakema, A. J., Nix, H. A., 1995. Salinization of land and water resources. University of New South Wales Press, Sydney, Aust., 526 pp.

Green, T.R., Salas, J.D., Martinez, A., Erskine, R.H., 2007. Relating crop yield to topographic attributes using spatial analysis neural networks and regression. Geoderma 139, 23–37.

Hafen, R., Anderson, D., Cleveland, W., Maciejewski, R., Ebert, D., Abusalah, A., Yakout, M., Ouzzani, M., Grannis, S., 2009. Syndromic surveillance: STL for modeling, visualizing, and monitoring disease counts. BMC Medical Informatics and Decision Making 9, 21.

Hajrasuliha, S., Baniabbassi, N., Metthey, J., Nilsen, D. R., 1980. Spatial variablility of soil sampling for salinity studies in southwest Iran. Irrigation Science 1, 197-208.

Hilhorst, M. A., 2000. A pore water conductivity sensor. Soil Science Society of America Journal 64, 1922-1925.

Huang, Y., Lan, Y., Thomson, S.J., Fang, A., Hoffmann, W.C., Lacey, R.E., 2010. Development of soft computing and applications in agricultural and biological engineering. Comput. Electron. Agric. 71, 107–127.

John, M., Pannell, D.J., Kingwell, R., 2005. Climate change and the economics of farm management in the face of land degradation: Dryland salinity in Western Australia. Paper presented at International Policy Forum on Greenhouse Gas Management, Victoria, British Columbia, April 28-29 2005.

Kaatze, U., Uhlendorf, V., 1981. The dielectric properties of water at microwave frequencies. Zeitschrift für Physikalische Chemie., Neue Folge, Bd 126, 151-165.

Khazaei, J., Naghavi, M.R., Jahansouz, M.R., Salimi-Khorshidi, G., 2008. Yield estimation and clustering of chickpea genotypes using soft computing techniques. Agron. J. 100, 1077–1087.

Maas, E. V., 1986. Salt tolerance of plants. Appplied Agriculture Research 1, 12-26.

Maas, E.V., Hoffman, G.J., 1977. Crop salt tolerance - current assessment. J. Irrigation and Drainage Division, ASCE 103 (IRI): 115-134. Proceeding Paper 12993.

Mahmut, C., Cevat, K., 2003. Spatial and temporal changes of soil salinity in cotton field irrigated with low-quality water. Journal of Hydrology 272, 238-249.

Malicki, M. A. & Walczak, R. T. (1999) Fvalualimj soil salinity status from bulk electrical conductivity and permittivity. Science Society of America Journal 50. 505-514.

Malicki, M. A. Walczak, R. T., Koch, S., Flühler, H.,1994. Determining Soil Salinity from Simultaneous Readings of its Electrical Conductivity and Permittivity using TDR. Proceedings of the Symposium on Time Domain Reflectometry in Environmental, Infrastructure, and Mining Applications, Evanston, Illinois, Sept 7-9, U.S. Bureau of Mines, Special Publication SP 19-94, NTIS PB95-105789, pp. 328-336.

McKenzie, R. C., Chomistek, W., Clark, N. F., 1989. Conversion of electromagnetic inductance readings to saturated paste extract values in soils for different temperature, texture, and moisture conditions. Canadian Journal of Soil Science 69, 25– 32.

Mualem. Y., Friedman, S. P.,1991. Theoretical prediction of electrical conductivity in saturated and unsaturated soil. Water Resource Research 27, 2771 -2777.

Munns, R., 2002. Comparative physiology of salt and water stress. Plant, Cell and Environment 25, 239-250.

Park, S.J., Hwang, C.S., Vlek, P.L.G., 2005. Comparison of adaptive techniques to predict crop yield response under varying soil and land management conditions. Agric. Syst. 85, 59–81.

Persson, M., 2002. Evaluating the linear dielectric constant –electrical conductivity model using time domain reflectometry Hydrological Science Journal 47, 269-278.

Petris, G., 2010. dlm: Bayesian and Likelihood Analysis of Dynamic Linear Models. R package version 1.1-1, URL http://CRAN.R-project.org/package=dlm.

R Development Core Team, 2012. R: A Language and Environment for Statistical Computing. R Foundation for Statistical Computing, Vienna, Austria, ISBN 3-900051-07-0, URL: http://www.R-project.org/.

Regalado, C.M., Ritter, A., Rodriguez-Gonzalez, R.M., 2007. Performance of the commercial WET capacitance sensor as compared with time domain reflectometry in volcanic soils. Vadose Zone Journal 6, 1539-1663.

Regasamy, P., 2006. World salinization with emphasis on Australia. Journal of Experimental Botany 57, 1017-1023.

Rhoades, J.D., Lesch, S.M., LeMert, R.D., Alves, W.J., 1997. Assessing irrigation/drainage/salinity management using spatially referenced salinity measurements. Agricultural Water Management 35, 147–165.

Rhoades, J.D., Manteghi, N.A., Shouse, P.J., Alves, W.J., 1989. Soil electricalconductivity and soil-salinity - new formulations and calibrations. Soil Science Society of America Journal 53, 433-439.

Rhoades, J.D., Raats, P.A.C., Prather, R.J., 1976. Effects of liquid-phase electricalconductivity, water-content, and surface conductivity on bulk soil electricalconductivity. Soil Science Society of America Journal 40, 651-655.

Sarangi, A., Man Singh, A. K., Bhattacharya, A. K., singh, A. K., 2006. Subsurface drainage performance study using SALTMOD and ANN models. Agricultural Water Management 84, 240-148.

Scoggins, H.L., van Iersel, M.W., 2006. In Situ Probes for Measurement of Electrical Conductivity of soilless substrates: Effects of Temperature and Substrate Moisture Content. HortScience 40, 210-214.

Shouse, P.J., Goldberg, S., Skaggs, T. H., Soppe, R. W. O., Ayars, J. E., 2010.Changes in spatial and temporal variability of SAR affected by shallow groundwater management of an irrigated field, California. Agricultural Water Management 97, 673-680.

Slavich, P. G., Peterson, G. H., 1993. Estimating the electrical conductivity of saturated paste extracts from 1:5 soil-water suspensions and texture. Australian Journal of Soil Research 31, 73-81.

Szabolcs, I., 1994. Soils and salinisation. In Handbook of Plant and Crop Stress. Ed. Pessarakli, M. Marcel Dekker, New York, pp. 3-11.

Thiruchelvam, S., Pathmarajah. S., 1999. Economic feasibility of controlling salinity problems in the Mahaweli H area, A research paper presented at the monthly seminar, IWMI (formally IIMI), March, 1999, Colombo, Sri Lank.

United States Salinity Laboratory Staff., 1954. Diagnosis and improvement of saline and alkali soils. US Department of Agriculture, Agricultural Handbook No. 60. Washington: US Goverment Printer.

Van Genuchten, M. TH., 1991.Recent progress in modelling water flow and chemical transport in the unsaturated zone. IAHS Publication.

Wei, W.W.S., 1989. Time Series Analysis: Univariate and Multivariate Methods. Person Addison-Wesley, New York.

White, R. E., 1985. The influence of macropores on the transport of dissolved matter through soil. Advances in Soil Sciences 1, 95-120.

Xiaoming, L. I., Jingsong, Y.,Meixian, L. I. U., Guangming, L. I. U., Mei, Y. U., 2012. Spatio-Temporal Changes of Soil Salinity in Arid Areas of South Xinjiang Using Electromagnetic Induction. Journal of Integrative Agriculture 11, 1365-1376.

Yuanshi, G., Qiaohong, C., Zongjia, S., 2003. The effects of soil bulk density, clay content and temperature on soil water content measurement using time-domain reflectometry. Hydrological Process 17, 3601-3614.

Zhang, J.Q., Zhang, L.X., Zhang, M.H., Watson, C., 2009. Prediction of soybean growth and development using artificial neural network and statistical models. Acta Agron. Sin. 35 (2), 341–347.

Zou, P., Yang, J., Fu, J., Liu, G., Li, D., 2010. Artificial neural network and time series models for predicting soil salt and water content. Agricultural Water Management 97 (12), 2009–2019.

5. Conclusions

Conclusion

This dissertation has evaluated furrow irrigation in the Parc Agrari del Baix de Llobregat area, according to the farmer's normal management practice. Soil water content and soil salinity were assessed temporally and spatially using capacitance sensors for evaluating the appropriateness of related management practices.

The purpose of the current study was the determination of the performance indicators of the furrow irrigation system and the study of the evolution of soil water content and soil salinity in the root zone. Such study allows us to determine the tools that could maintain and improve the agricultural sustainability of the study area. The more significant findings that emerge from this study are:

- The adaptation of the ARIMA model to the variable interval irrigation system for predicting soil moisture. In the case of variable interval irrigation, predicting the soil water content time series cannot be properly explained by the ARIMA model and its underlying normality assumption. In this research we completed the ARIMA model with intervention analysis and outlier detection to predict the soil water content in variable interval irrigation.
- The obtained ARIMA model was capable to determine precisely the next irrigation time.
- The effect of irrigation event on soil moisture was estimated reasonably.
- The soil moisture at greater depths was forecasted well from one single shallow depth by using transfer function model. The relative difference between predicted and observed values was sometimes large; it increased as the distance of separation between the primary and target increased. The absolute difference between the prediction and measurement never exceeded 0.03 m^3 m^{-3}.
- We built an advanced process to study the relationship between soil dielectric constant (ε_b) and bulk electrical conductivity (σ_b) by including a stochastic component to the linear relationship between them. The current study enables us to derive an accurate offset form this relationship to estimate pore electrical conductivity (σ_p) by using Time-varying Dynamic Linear Model (DLM). It was shown that the offset, $\varepsilon_{\sigma b=0,}$ varies for each depth in the same soil profile. A reason for this might be to the changes in soil temperature through soil profile.

- The soil salinity at the shallow depth and in the top 0.60 m of the soil profile was predicted well from measuring soil water content and soil temperature at the shallow depth by using (mulitpe input-single output) transfer function model.
- We show that the cutoff time (t_{co}) plays a significant role in evaluating furrow irrigation system to save irrigation water in the study area. 40 % and 43% of the applied water would have been saved in the Field 1 and Field 2 respectively, if the irrigation was stopped as soon as the soil water deficit was fully recharged taking into account the amount of water needed for salt leaching.
- Irrigation frequency according to the farmer's normal management practice had statistically significant effects on soil salinity behavior, depending on soil depth and position. For each depth, farmers left the field with less soil salinity than at the beginning of the crop's vegetative cycle. Moreover, irrigation water quality had a significant effect on soil salinity at the root zone in the three studied fields.

Taken together, these results we can draw out the following **suggestions**:

- From field conditions data, the study discovered that the offset of the linear relationship between soil dielectric constant and bulk electrical conductivity was varied in the same soil profile and was related to soil temperature. However, we recommend additional measurements in different soil types to validate this model.
- The study used the ARIMA model and completed it with intervention analysis and outlier detection for the data of Field 1, lettuce crop, the irrigation dose for four irrigation events were almost the same, we used one average mean level to depict the effectiveness of an irrigation moment on the time series of soil water content. In the case of variable irrigation doses, the study suggests studying the effect of each irrigation event and includes their effects separately in the model.
- Programming the ARIMA model and connect it to a device designed to aid in irrigation scheduling by visually indicating current soil water statues and determine the next time irrigation, so these types of low-cost sensors could expand to be used by normal framer users.

List of figures

Chapte 1

Chapte 2

Chapte 3

Chapte 4

List of Tables

Chapte 2

Chapte 3

Chapte 4

Dissertation Highlights

The research enables the ARIMA model to be applied on variable interval irrigation for predicting soil moisture and soil salinity.

The obtained ARIMA model was capable to determine precisely the next irrigation time.

The effect of irrigation event on soil moisture was estimated reasonably.

The soil moisture at greater depths was forecasted well from one single shallow depth.

The research showed an advanced progress to study the relationship between soil dielectric constant and soil bulk electrical conductivity and derive an accurate offset to convert bulk EC to pore water EC.

The soil salinity at greater depth was predicted well form measuring soil moisture and soil temperature at shallow depth.

30% and 43% of the applied water would have been saved in two fields of study area, if irrigation stopped as soon as soil water deficit was fully recharged taking into account the amount of water needed for salt leaching.

In the study area, farmers left the field with less soil salinity than at the beginning of the crop's vegetative cycle. Moreover, irrigation water quality had a significant effect on soil salinity at the root zone in the three studied fields.